Studies on the Development of a Nanosensor for Organophosphorus Neurotoxin Monitoring

By

Muhammad Musaddiq Shah

Reg. No. 74-FBAS/PHDBT/F-16

Department of Biological Sciences

Faculty of Basic and Applied Sciences

International Islamic University, Islamabad, Pakistan

(2016-2022)

Nanosensors

Organophosphorus compounds - Toxicology

Neurotoxins - Analysis

Biosensors.

Organophosphorus compounds - Detection

Studies on the Development of a Nanosensor for Organophosphorus Neurotoxin Monitoring

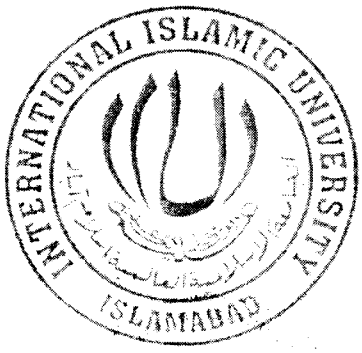

Researcher

Muhammad Musaddiq Shah

74-FBAS/PHDBT/F-16

Supervisor

Dr. Bashir Ahmad

Assistant Professor

Department of Biological Sciences

Faculty of Basic and Applied Sciences

International Islamic University, Islamabad, Pakistan

(2016-2022)

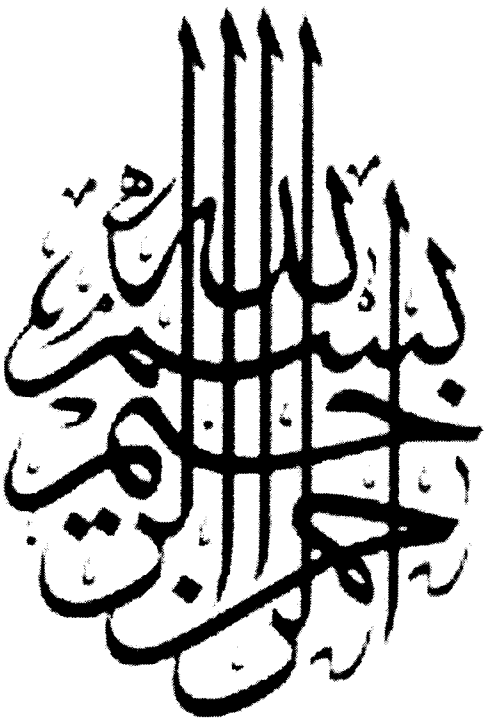

"In the name of ALLAH The Most Gracious and The Most Beneficial"

International Islamic University, Islamabad
Faculty of Basic & Applied Sciences
Department of Biological Sciences

Dated: 04-03-2022

FINAL APPROVAL

It is certified that we have read the final thesis entitled "Studies on the Development of a Nanosensor for Organophosphorus Neurotoxin Monitoring" submitted by **Mr. Muhammad Musaddiq Shah** and we judge that this thesis is of sufficient standard to warrant its acceptance by the International Islamic University, Islamabad for the Ph.D. degree in Biotechnology.

COMMITTEE

Supervisor
Dr. Bashir Ahmad
Assistant Professor
Department of Biological Sciences, FBAS
International Islamic University, Islamabad
Pakistan

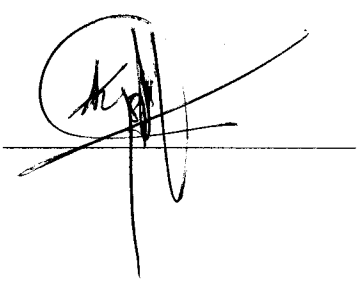

Internal Examiner
Dr. Asif Mir
Associate professor
Department of Biological Sciences, FBAS
International Islamic University, Islamabad
Pakistan

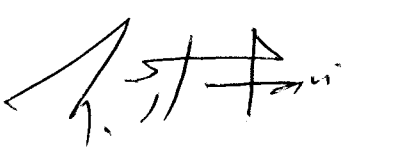

External Examiner-I
Dr. Muhammad Ishtiaq Ali
Professor
Department of Microbiology
Quaid I Azam University Islamabad, Pakistan

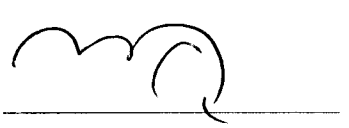

External Examiner-II
Dr. Mushtaq Ahmad
Professor
Department of Plant Sciences,
Quaid I Azam University Islamabad Pakistan

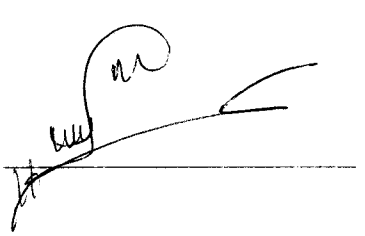

Chairman
Department of Biological Sciences,
Faculty of Basic and Applied Sciences
International Islamic University, Islamabad

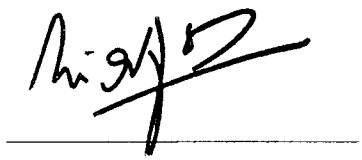

Dean
Prof. Dr. Muhammad Irfan Khan
Faculty of Basic and Applied Sciences
International Islamic University, Islamabad

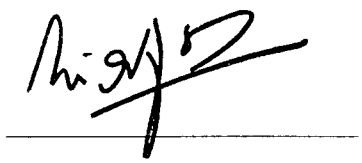

A thesis submitted to the Department of Biological Sciences, Faculty of Basic and Applied Sciences,

International Islamic University Islamabad, Pakistan

In partial fulfillment of the requirement for the degree of Doctor of Philosophy in Biotechnology

Dedicated

To

Parents, Siblings

&

Family

DECLARATION

I hereby solemnly declare that the present work in the following Doctoral thesis **"Studies on the Development of a Nanosensor for Organophosphorus Neurotoxin Monitoring"** is my own efforts, except where otherwise acknowledged, and that the thesis is my own composition. No part of the thesis has been previously presented for any other degree.

Dated: 4-3-2022

Muhammad Musaddiq Shah

ACKNOWLEDGEMENTS

First and foremost, I bow down before "**Almighty Allah**" with humbleness to express my deepest sense of gratitude to HIS blessing, mercy, wisdom, faithfulness and thus enabling me to accomplish this venture. Countless salutations upon the **Holy Prophet Hazrat Muhammad Mustafa (PBUH),** source of knowledge for enlightening with the essence of faith in Allah and guiding the mankind, the true path of life.

I would like to extend my deepest appreciation to those people, who helped me in one way or other in planning, executing the research work, and writing up this thesis manuscript. With an utmost degree of sincerity, I avail this opportunity to express my heartfelt thanks to my advisor, **Dr. Bashir Ahmad** Assistant Professor Department of Biological Sciences Faculty of Basic and Applied Sciences International Islamic University Islamabad, Pakistan for the supervision and guidance throughout the research work. The critical evaluation of the research work at different stages and valuable suggestions went a long way in bringing this research work to this stage. He has not only been a fathomless ocean of knowledge and wisdom to me but most of all his words of care and hands of blessing have been my pillar of strength and courage to complete this task. My fortune may not give anything more but has given me the opportunity to work under this great teacher and human being. **"Thank you, Sir,"**

I extend my profound gratitude to Honorable **Prof. Dr. Joseph Maria Kumar Irudayaraj** founder professor of bioengineering at the University of Illinois at Urbana Champaign (UIUC-USA), for providing me the delightful opportunity and the necessary research facilities to carry out the part of my research work under the IRSIP program.

I express my esteemed gratitude to **Prof. Dr. Muhammad Irfan Khan,** Head, Department of Biological Sciences and Dean Faculty of Basic and Applied Sciences International Islamic University Islamabad, Pakistan member for his worthy guidance and constant help.

I wish to take this valuable opportunity to express my gratitude to **Prof. Dr. Zafar Mehmood Khalid** ex. Head, Department of Biological Sciences Faculty of Basic and Applied Sciences International Islamic University Islamabad, Pakistan for his lucid guidance and constructive suggestions regarding my research work.

I would like to express my gratefulness to **Dr. Syed Imran Ali Bokhari** Assistant Professor Department of Biological Sciences Faculty of Basic and Applied Sciences International Islamic University Islamabad, Pakistan, for his thought-provoking

discussions, insightful interpretations, and continued courage during the course and research work.

I fall short of words to express my sincere gratitude to the faculty members of the Department of Biological Sciences Faculty of Basic and Applied Sciences International Islamic University Islamabad, **Dr. Asif Mir** Associate Professor, **Dr. Jabbar Khattak** Associate Professor, **Dr. Arshid Malik** Associate Professor, and **Dr. Imran Shabir** Assistant Professor for their moral support for completion of my research work.

I place on record my esteem affection and sincere thanks to my batch mates and lab fellows **Dr. Muhammad Faheem, Mr. Adnan Yousaf, Mr. Muhammad Riaz, Mr. Muhammad Imran, Mr. Faisal Saleh, and Mr.Ammir Ramzan** for their enjoyable company, help, moral and courageous support throughout the course of study. I am appreciative to my UIUC-USA lab fellows **Dr. Wen Ren, Dr. Muhammad Fayyaz, Ms.Mussarut Jabeen, Mr. Faizan Rashid, and Mr. Saeed Khan** for their valuable suggestions, cooperative behavior, and guidance during my IRSIP visit.

I found no theoretical gems from the ocean of words to express my heartfelt sense of gratitude; I bow my head before my mother and my father **Dr. S. M. Salahuddin** for their supreme sacrifice and eternal benediction in evolving my personality. Whose words of encouragement, care and good wishes always being spring of inspiration have made this work a great success.

Words fail to express my deep appreciation from the depth of my heart for my loving and caring wife and my brothers **Dr. Shahid Masood Shah, Dr. Mohsin Shah,** and sisters who provided me relentless encouragement, prayers, unmatched affection that made this reach work its fruitful destination. I thank every supportive hand that has not been mentioned by name but have given invaluable bits of help in their own way directly or indirectly with this study and soliciting good wishes for my future

Last but not least I am grateful to the **Higher Education Commission (HEC) of Pakistan** for granting me the International Research Support Initiative Program (IRSIP) award for UIUC-USA. Without this accolade, the accomplishment of this research work was hard to complete.

MUHAMMAD MUSADDIQ SHAH

Table of Contents

LIST OF TABLE

LIST OF FIGURES

ABBREVIATIONS

Sr. No	Abbreviation	Definition
1.	NPs	Nanoparticles
2.	AuNPs	Gold Nanoparticles
3.	C-AuNPs	Cysteamine Capped Gold Nanoparticles
4.	OP	Organophosphates
5.	AChE	Acetylcholinesterase
6.	ATCH	Acetylthiocholine
7.	ACh	Acetylcholine
8.	BChE	Butyrylcholinesterase
9.	DLS	Dynamic Light Scattering
10.	TEM	Transmission Electron Microscopy
11.	DF	Dark Field
12.	TMB	3,3,5,5-Tetramethylbenzadien
13.	GC	Gas chromatography
14.	CE	Capillary electrophoresis
15.	HPLC	High-performance liquid chromatography
16.	H_2O_2	Hydrogen peroxide
17.	SPR	Surface plasmon absorption
18.	PE	Parathion ethyl
19.	UV-vis	Utraviolet-visible
20.	HR-TEM	High-Resolution Transmission Electron Microscopy
21.	EDX	Energy Dispersive X-ray Analysis
22.	DNA	Deoxyribonucleic acids
23.	OPFRs	Organophosphate ester flame retardants
24.	GOx or GOD	Glucose oxidase
25.	STM	Scanning tunneling microscope
26.	AFM	Atomic force microscope
27.	TOAB	Tetrabutylammonium bromide
28.	$NaBH_4$	Sodium borohydride
29.	CTAB	Cetyltrimethylammonium bromide
30.	SOD	Superoxide dismutase
31.	AuNS	Gold nanostars
32.	LOD	Limit of detection
33.	nM	Nano Molar
34.	µM	Micro Molar
35.	MTB	Mycobacterium Tuberculosis
36.	pH	Power of Hydrogen Ions
37.	MoS_2	Molybdenum disulfide
38.	AA	Ascorbic acid

39.	AAP	Ascorbic acid 2-phosphate
40.	ABTS	2,20-azino-bis (3- ethylbenothiaoline-6-sulfonic acid)
41.	SMNC	Spleen mononuclear cells
42.	CQDS	Carbon quantum dots
43.	OPH	Organophosphorus hydrolase
44.	FRET	Fluorescence resonance energy transfer
45.	ppb	Parts per billions
46.	$mol \cdot L^{-1}$	Moles per litter
47.	SPR	Surface plasmon resonance
48.	$U \cdot mL^{-1}$	Unit per mL
49.	pM	Pico Molar
50.	ZP	Zeta potential
51.	$mmol \cdot L^{-1}$	Millimole per liter
52.	IE%	Inhibition efficiency
53.	AgNP	Silver Nanoparticles
54.	mV	Milli Volt
55.	FRET	Fluorescence resonance energy transfer
56.	MoO_3NPs	Molybdenum oxide nanoparticles
57.	SMNC	Spleen mononuclear cells
58.	SAB	Sodium acetate buffer
59.	DCP	Diethyl chlorophosphonate
60.	DNCP	Diethyl cyano phosphate
61.	PM	Paraoxon-methyl
62.	JI	Joseph Irudayaraj
63.	EDTA	Ethylene di-amine tetra acetic acid

Abstract

Cysteamine capped gold nanoparticles (C-AuNPs) were capitalized to develop a facile colorimetric biosensor for robust and sensitive detection of organophosphates (OPs). OPs are neurotoxic agents that have the potential to permanently block the active site of acetylcholinesterase (AChE), which is commercially applied as pesticides. AChE (EC 3.1.1.7), is a main functioning enzyme of the nervous system and the neurotransmitters. This enzyme manages the level of acetylcholine (ACh) by catalysing it into choline and acetate at the synapse, which leads to the culmination of neurotransmission in the nervous system of animals. C-AuNPs were synthesized using a standard protocol and characterized by the help of UV-Vis, Zeta sizer, Darkfield Imaging, Dynamic Light Scattering (DLS), and Transmission Electron Microscopy (TEM). C-AuNPs were utilized as a peroxidase mimic nanomaterial to directly oxidize 3, 3', 5, 5'-tetramethylbenzidine (TMB) into oxidized TMB. Tris-HCl buffer (pH 7.6) and sodium acetate buffer (pH 4.0) were capitalized as reaction mediums for the enzymatic and chromogenic reactions respectively. Acetylcholine chloride (ACh) was applied as a substrate for AChE to produce choline. Parathion ethyl (PE) was exploited as candidate OP as a neurotoxin agent to block the activity of AChE and suppress the production of choline. The detection assay was performed by the incubation of AChE with PE for 10 minutes at 37°C and then stepwise addition ACh, C-AuNPs, and TMB in buffer solution. The absorbance of the resultant reaction mixture was monitored at 300-800 nm for the different concentrations of PE. The wine-red color of the colloidal solution indicated the successful synthesis of C-AuNPs which was established by UV-Vis absorbance peak at 530 nm. A high surface charge of +39.4 ± 2.05 mV which was obtained with the help of zeta potential confirmed the resistance of these nanoparticles (NPs) against aggregation. Images obtained from the darkfield further sustained that the C-AuNPs have monodisperse in nature. The DLS results indicated that the average size of colloidal C-AuNPs was approximately 33 nm including the capping agent and solvent molecules present on the surface of these NPs. These C-AuNPs were additionally visualized through TEM and results obtained advocate that these NPs have a spherical morphology and the core size of these NPs was 13.24 nm. The monomers of C-AuNPs presented resilient catalytic activity (nanozyme) for the oxidization of TMB, revealed by the generation of blue color and supported by a sharp peak at 652 nm. AChE catalyzed acetylcholine chloride (ACh)

into choline, which induced the aggregation of C-AuNPs, causing the reduction of solution absorbance. Since the aggregated NPs lose their catalytic power and were incapable to catalyze the oxidization of TMB. Concurrently, the existence of PE in the system suppressed the enzymatic activity of AChE which prevented the aggregation of C-AuNPs, evident by the appearance of strong blue color and maximum sharp peak witnessed at 652nm. The detection limit and linear range of the proposed biosensor were 20 nM and 40-320 nM, respectively. The C-AuNPs have straightforward synthesis protocols, substantial catalytic power, and the C-AuNPs+TMB assay needs less incubation time, high sensitivity, and wider linear range, making the overall process simple, easy, and quick, which advocates robust nature as well as the novelty of the protocol. The results strongly recommend that the suggested sensor may provide an exceptional platform for on-field monitoring of organophosphates.

Introduction

Introduction

1.1 Overview

Nanosensors are sensing systems that comprise nanoscale elements including nanomaterial and are designed to detect the incidence of analytes (Yang & Duncan, 2021). Encapsulation of nanomaterial fabricates these sensing devices with the features like extraordinary efficiency, multiplex functionality, and enhanced flexibility (Vikesland, 2018). These platforms with a characteristic dimension at the nanometer scale are capable of conveying the responses in such a manner that output signals can be easily understood. The distinctive nature of nanomaterials makes them perfect and adaptable to be capitalized in different sensing devices including biosensors.

Biosensors are the prevailing and useful investigative stand-alone devices that are designed to monitor various targets such as biological molecules including DNA, RNA, proteins, amino acids, disease biomarkers, microbes, pollutants, contaminants, drugs, environmental toxins, agricultural chemicals, and so on with high precision and accuracy (Kaur & Prabhakar, 2017; Renneberg et al., 2007). These sensing devices possess biological elements which act as bioreceptor (e.g., enzymes, DNA, RNA, microorganism, tissue, or whole cells) which can recognize a specific analyte or target molecules (Erathodiyil & Ying, 2011; Zeng et al., 2016). These recognition measures are transduced at the detector elements into quantifiable and non-quantifiable signals. These output signs and signals are roughly proportional to the concentration of target agents (C. Pundir & Malik, 2019).

To develop an efficacious portable biosensor two factors, bioreceptor, and transducing agent should be carefully chosen. The selection of a bioreceptor is a critical factor in the fabrication of biosensors because it decides the usefulness and aptness of the designed sensor for on-site monitoring of the analyte (Sapsford et al., 2013). Likewise, the presence of an applicable transducing agent makes the whole sensing process free from expensive instrumentations so monitoring of an analyte can be done quickly without a technical expert. So, a biosensor is a simple analytical device that has the potential to provide an inexpensive, time-saving, scale-down, and label-free

detection process without lengthy protocols. All these features make biosensors potentially perfect for the on-site monitoring of analyte as well as point-of-care applications (Benito et al., 2016; Pilolli et al., 2013).

Out of different biosensing techniques, the colorimetric biosensors are the most adopted method for the development of senor, because these methods offer an extra useful option, that is visible change happened by the presence of target analyte. These visible variations can be judged by the unaided eye which rules out the requirements of sophisticated instruments (Bala et al., 2016; Fahimi-Kashani & Hormozi-Nezhad, 2016; Sun et al., 2018). The incorporation of nanozyme with colorimetric detection has added a few extra advantages in the monarchy of biosensor development for environmental, and clinical monitoring such as adaptability, disposable nature, and easiness in the process of fabrication (Liang & Yan, 2019; Z. Lin et al., 2020; Y. Meng et al., 2020).

Gold nanoparticles (AuNPs) have been intensively exploited in the field of biosensing due to surface plasmon resonance (Y. Zhang et al., 2014). Size, morphology, surface chemistry, composition as well as the degree of aggregation of AuNPs decide the wavelength of light absorbance of AuNPs and produce the different colors of AuNPs colloidal solution accordingly. Due to these unique features, AuNPs have been efficaciously applied in the colorimetric detection of numerous substances such as DNA, proteins, metallic ions, and toxins (Chai et al., 2010; H. Yin et al., 2014).

Nanotechnology is an advanced scientific discipline which deals with materials that have at least one measurement in nanoscale. This field of science is emerged intensively and have a prevailing role in everyday life, because of its enormous applications in different capacities including drug development, diagnostics, gene analysis, and development of better electronic devices, sensing, and communication system (Hulla et al., 2015). It is concerned with the various chemical structures of matter that possess sizes of a billionth (1×10^{-9}) of a meter (Saratale et al., 2018). It has opened a new research area for the synthesis, characterization, and applications of nanomaterials for the welfare of society (Saratale et al., 2018). Continuous progress

and development in nanotechnology have led the better and enriched nano-structures that can execute diverse functions including imaging, sensing, and targeting. By managing the size, shape, morphology, surface charge, and configuration of nanomaterials it is possible to manage and handle the physical as well as the chemical features of these materials in such a way that these can be applied in diverse applications including biosensors development with incredible sensitivity and implausible selectivity (Hulla et al., 2015).

The nanomaterials which can have enzymatic properties, are able to do the enzymatic hydrolysis itself, and possess the intrinsic enzyme mimic potentials, are termed nanozymes (Arias et al., 2020; Niu et al., 2016). 1st the time the nanozyme expression was coined to designate the gold nanoparticles having the competency of transphosphorylation (Manea et al., 2004). Wu and his colleagues elaborate on the details of different nanomaterials with their function's types of nanozymes such as peroxidase, oxidase, catalase, superoxide dismutase, hydrolase, and several other enzymes mimicking materials (J. Wu et al., 2019). To enhance the understanding of these nanomaterials, nanozymes are being grouped into two classes' oxidoreductase and hydrolase (Huang et al., 2019).

Protein-based natural enzymes possess substrate specificity and high activities that why these enzymes are commonly applied in diverse applications ranging from industry to medical fields. However, nanozymes have over advantages like low cost, mass production (X. Li et al., 2019), ease to synthesize, uncomplicated modification, high stability, long term storage, resistance to hard and rigid environments (Y. Meng et al., 2020; Song et al., 2019), and, most importantly, enzymatic potentials of nanozymes can be controlled by an external stimulus (Kotov, 2010; Liang & Yan, 2019). A lot of work has been done to discover the potentials of the nanozymes in diverse fields such as sensing (X. Li et al., 2019; Song et al., 2019) cancer diagnosis and bacteria detection (Huang et al., 2019) imaging (S. Singh, 2019a) therapeutics (X. Liu, Gao, Chandrawati, & Hosta-Rigau, 2019) electronics (Lien, Tseng, Huang, & Chang, 2014), and environmental applications (W.Chen et al., 2019). Due to their exceptional features, nanozymes have been recently applied extensively but the

catalytic mechanism and kinetics of these nanozymes are yet not thorough. So, to get the maximum potential of nanozymes more research is required to comprehend the non-enzymatic catalytic mechanisms, development of highly specific and efficient nanozymes as a better replacement of natural enzymes.

Agricultural yield has significantly upgraded by implementing innovative agricultural techniques. Healthier and viable seeds have been produced, advanced water management techniques have been developed and the usage of effective pesticides has enhanced pests control (Bassi, 2009). It is estimated that the practice of pesticides aids to secure approximately one-third of global crop production. The application of pesticides is a foremost factor for the enrichment of agricultural production in many countries such as the United States, China, India, and the United Kingdom.

Pesticides (are the general term applied as insecticides, herbicides, and fungicides) are broadly consumed in the agricultural industry to eradicate and reduce the presence of different classes of agricultural pests containing rodents, insects, fungi, weeds, etc. Based on the chemical configuration, pesticides have been divided into five major classes including organophosphorus, organochlorines, carbamates, pyrethrin, and pyrethroids. In common practices, pesticides are directly sprayed to the fields, plants, and soils but only 1% of pesticides reached the planned targets (Songa & Okonkwo, 2016). Besides, that sometimes accidental spills, underground storage tanks, and waste dumps may lead to the unintentional release of pesticides which may also create environmental issues. Pesticides have high toxicity and prolonged persistence in natural environments so pose long-term damages to the ecosystem and living beings. Resultantly, pollution due to abandoned usage of these pesticides has become a potential problem that needs to be addressed properly and thoroughly to save non-invasive species (P. Kumar et al., 2015).

So, detection of these chemicals with accuracy and reliability has attracted the attention of different research groups. Over the past decades, biosensors based on acetylcholinesterase have emerged as a sensitive, trustworthy, and reliable method for the onsite monitoring of pesticides. These sensors provide an alternative and

replacement for the classical analytical methods because these methods have very easy sample preparations, less or no production and usage of toxic chemicals, easy on-site testing, quick, and economical per sample analysis (Songa & Okonkwo, 2016).

Organophosphorus (OPs) is the major class of pesticides, extensively applied as agricultural pesticides due to low price, wide availability, and extraordinary affectivity in pest control. That is why these pesticides are the most widespread around the world and applied frequently as agricultural and household pest control agents for almost five decades. Some OPs such as sarin, tabun, soman, and venomous agent X (V.X) are being utilized as chemical warfare agents (Shimada et al., 2019). The residues and deposits of OPs that showed long persistence in the natural atmosphere induce the serious hazard to terrestrial and aquatic creatures (Xiong et al., 2018). According to U.S. Environmental Protection Agency reports, the OPs are incredibly poisonous compounds and branded in the utmost contaminated class "Class 1" (Songa & Okonkwo, 2016; Tiwari, Asthana, & Upadhyay, 2013).

OPs are esters of phosphoric acid possessing different combinations of oxygen, nitrogen, carbon, and sulfur. All OPs shared the backbone of the structure, at the center a phosphorus atom is present and an oxygen or sulphur atom is doubly bonded with this central phosphorous atom. Single bonded alkoxy substituents groups are also attached with this central phosphorus which already has a single bond with halogen (Carullo et al., 2015; Sulaiman et al., 2020). Most frequently applied OPs include paraoxon, chlorpyrifos, malathion, parathion, diazinon, methyl parathion, and fenitrothion. OPs pesticides kill the pests by upsetting the functionality of their essential enzymes such as Acetylcholinesterase (AChE) and butyrylcholinesterase (BChE). The existence of OPs takes to the malfunctioning of the central and peripheral nervous system by permanent hindering of the active site of AChE. AChE is a prime cholinesterase in the body and is responsible for catalyzing the hydrolysis of neurotransmitters. The AChE manages the level of acetylcholine (ACh) by catalyzing it into choline and acetate at the synapse, which leads to the termination of neurotransmission (C. S. Pundir & Chauhan, 2012). The formation of this choline

helps in the regeneration of acetylcholine, in this way the level of choline and acetylcholine remains in balance which best conducts transmission of a nerve impulse at its optimal pace.

The active site of AChE contains three essential amino acids such as histidine, serine, and aspartic acid (Dvir et al., 2010; Santoni et al., 2018). OPs block the enzyme irreversibly by establishing a covalent bond with the serine residue, leading to the phosphorylated enzyme, which leads to a non-functional form of AChE, incapable of catalyzing acetylcholine (Dvir et al., 2010). This malfunctioning state of AChE leads to the accumulation of ACh that consequences in the uninterrupted stimulation of the ACh receptors (Quinn, 1987). This accumulation of acetylcholine and cholinergic toxicity causes paralysis of muscular functions, respirational, myocardial abnormalities (C. S. Pundir & Chauhan, 2012), and sometimes death (Mulla et al., 2020; Rahman et al., 2020).

The toxic nature of OPs relies on different factors such as the extent of exposure, route of exposure, and the chemical structure of pesticides. Its toxicity is reported to cause cancer, vomiting, nausea, and dermatitis irritation in humans and a moderate level of toxicity in amphibians and fishes. The toxicity and lethality of OPs are due to their analogue features as a substrate of AChE; its restraining ability of AChE leads to the aggregation of the neurotransmitter acetylcholine (ACh). Oxime antidote was applied as a treatment of reactivation of AChE and atropine is used to eradicate the biochemical effects of ACh accumulation (Sidhu et al., 2019).

Due to the critical toxicity of the OPs (Eddleston et al., 2008), and the registered chronic effects (Fu et al., 2019), the OP residue confines in food, drinking water, and environmental samples are subject to regulation and control (Musarurwa & Tavengwa, 2020). So, quick detection and reliable quantification have become progressively essential. Although classical analytical methods such as gas chromatography (GC) (Rosch et al., 2019; Ying et al., 2009), liquid chromatography

(LC) (Lopez-Garcia, Romero-Gonzalez, & Frenich, 2019), high-performance liquid chromatography (HPLC) (Arias et al., 2020; Mahajan & Chatterjee, 2018), mass spectrometry (MS) (C.W. Lee et al., 2018), capillary electrophoresis (CE) (Cao, Hogan, & Moore, 2019), surface plasmon resonance(SPR) (Q. Li et al., 2019; Thepudom et al., 2018) have already been established for the determination of OPs in contaminated and filthy samples.

However conventional analytical approaches have been effectively applied and reliable enough to detect OPs with anticipated sensitivity and desired selectivity. But these methods present numerous shortcomings and limitations since these classical methods are time taking, lengthy protocols based, sample pre-treatment required, intricacy, sophisticated instrumentation based, trained and skilled personnel requirements are prerequisites. As these necessities can only be accessible in established test centres so these methods can only be applied in laboratories (Songa & Okonkwo, 2016). None of these approaches are appropriate for the on-field detection of these compounds with a fast, accurate, user-friendly, and cost-effective route, and no one fulfills the ASSURED criteria (Weerathunge et al., 2019). So, on-site deployable methods which can have features like sensitive, economical, rapid, and selective are the intensifying need of time. Different type of sensing systems has been reported and developed in the last decades to monitor these compounds with an attempt to fulfilled required needs and have all the desired features (Songa & Okonkwo, 2016).

These inadequacies create the need for the development of a method that can provide a quick, on-site, real-time, cost-effective, precise, and reliable sensing system for the monitoring of pesticides at trace levels. There is an escalating necessity for field-deployable analytical techniques having qualities such as simple, quick, sensitive, selective, low cost, reliable, portable, specific, detection of OPs at low concentrations. It is prime and foremost to have a detection system that detects these toxic and insalubrious compounds with consistent quantification. So, detection of these chemicals with accuracy and reliability has attracted the attention of different research groups. Over the past decades, biosensors based on nanomaterials have emerged as

sensitive and reliable systems for the onsite detection of pesticides. These sensors emerged as an alternative and replacement for the classical analytical methods because these methods have easy sample preparations, less or no production of chemicals, and limited requirements of precursors chemicals, making the on-site testing easy, quick, and economical per sample analysis (Songa & Okonkwo, 2016).

Biosensor-based detection of the neurotoxin's agents (OPs) have provided the simple, easy-to-use, quick, cost-effective, portable, specific, sensitive tool to detect these compounds without lengthy sample preparations (C. S. Pundir & Ch , 2012). Colorimetric methods are the most adopted biosensing metho ment of a biosensor. Oxidase mimicking nanomaterials like nano and surface amended cerium oxide nanoparticles have been appli OPs, and 3,3,5,5-Tetramethylbenzadien (TMB) system 17; ang et al., 2016). Pesticides are supplemented with chemicals that block the various enzymes of pests (Yan et al., 2015). So, an en r opens the gates to developing an efficient and applied dete stem se toxic chemicals. The unique features such as optical features, size-dependent electron density, magnetic properties, and sensing potential of gold nanoparticles attracted the research groups so much that 17% of enzyme-based OP sensors utilized these particles for the sensing of OPs (Xiong et al., 2018). TMB, nanomaterial, and hydrogen peroxide (H_2O_2) centred monitoring system is being previously exploited (T. Jiang et al., 2016; D. Zhang et al., 2015).

Detection and diagnosis of the problem are the initial steps to resolve any issue and move forward toward the solution. As mentioned above OPs are reported to have high acute toxicity and known chronic effects. The presence of these OPs in the food, drinking water, and environmental samples is needed to manage and regulate. So, to design a sensing system that detects these compounds robustly and quickly with reliable quantification without complex instruments is urgent to be addressed on a priority basis. So, an expanding need for on-site deployable methods enriched with features such as time-saving, sensitive, economical, and selective is urgent.

1.2 Motivation and goal

The foremost objective of the research elaborated in this study is to establish low-cost, very sensitive, and specific, C-AuNP-based colorimetric sensor platforms for the monitoring of neurotoxins such as the OP family. To achieve this objective, we put forward an instrument-free method for the detection of OPs by exploiting the enzyme-like characteristics of C-AuNPs. This enzyme-assisted approach can be applied to detect OPs with an extremely small nM detection limit. Critically, the color changes obtained in the proposed sensing system presence of analyte can be seen with the unassisted eye. Colorimetric detection assay based on C-AuNPs+TMB is inherently extremely sensitive due to the high extinction coefficients of the surface plasmon absorption bands of C-AuNPs, which are more than 1,000 times greater than those of organic dyes.

Herein, we took the advantage of the enzyme mimic potentials of C-AuNPs to establish a biosensor for quick and sensitive monitoring of parathion ethyl (PE) a candidate OP. This peroxidase-like activity of C-AuNPs was expolied to perceive the occurrence of PE in a the sample. The monomers of C-AuNPs demonstrated durable catalytic activity for the oxidization of TMB, leading to the appreance of blue color products. In the absence of the inhibitor (PE) acetylcholine chloride (ACh) will be hydrolyzed by AChE, causing to choline production. The presence of choline induces aggregation in the C-AuNPs and aggregated C-AuNPs could not catalyze the oxidization of TMB, the developed solution will be colorless. On the other hand, when PE will present in the system, PE would block the enzymatic capabilities of AChE, which reasons the destruction of choline production and tempted less aggregation of C-AuNPs. So, this non-aggregated and monodisperse C-AuNPs catalyzed the oxidation of TMB and the blue-colored product was obtained. The strength of the bluish color of the oxidized product will be directly proportional to the concentration of the target PE and vice versa.

1.3 Scope of the dissertation

Chapter two delivers an overall literature review of the chronological contextual of biosensing, nanomaterials, AuNPs synthesis, and the existing application of AuNPs in

colorimetric monitoring, scope, and applications of AuNPs in biosensing. This chapter also reviews prevailing analytical and biosensing detection methods for the OPs family. Enzyme-based sensing systems including electrochemical, amperometric, potentiometric, thermal, piezometric, optical, fluorescence and surface plasmon resonance (SPR) systems which were constructed for the detection of the OP family are also reviewed. Nanozyme based detection protocols are also being discussed to judge the potentials of these nanomaterials in future sensing apparatus. Chapter three provides the details of material and steps which are adapted to conducted experiments starting to form the preliminary and optimization steps to the selectivity assay. In chapter four all the results which are obtained during the optimization and establishment of this sensing system are mentioned with the help of graphs and figures. Chapter five describes and provides the full discussion of all outcomes of all experiments which are being conducted for the establishment of a reliable protocol for the onsite detection of neurotoxins.

1.4 Aim and Objectives

Development of a colorimetric nano-sensor to detect PE (a candidate OP) to monitor indirectly the activity of AChE

- To synthesize, C-AuNPs by adopting chemical synthesis.
- To characterize the C-AuNPs with the help of appropriate techniques.
- To exploit nanozymic features of C-AuNPs.
- To optimize the enzymatic and chromogenic reactions in the presence and absence of AChE.
- To develop a sensing protocol for the monitoring of PE.

Review of Literature

Review of Literature

2.0 Sensors

Sensors are tools and devices that detect, monitor, and quantify any physical or chemical inputs and variations in pH, light, heat, motion, moisture, force, pressure, etc. The output signals which are generated in the response of these inputs are human-readable and displayed at the sensor location. In other words, we can say that sensors are the devices that can convert the physical or chemical inputs into electrical or optical outputs. These outputs can be understandable by humans or can be detected by electronic instruments Sensors are only sensitive to the chemical or physical quantity which is the subject of detection and insensitive toward all other parameters (Ensafi, 2019; Ensafi & Kazemzadeh, 1999). Photo-sensor is a practical example of a sensing system that generates the signals in the response of visible light, ultra-violet, or infrared light; another example of an applied sensor is an oxygen sensor in a car's emission control system that identifies the ratio of gasoline/oxygen with the help of a chemical reaction that generates a voltage.

2.1 Biosensors

The demand for sensitive and reliable monitoring machinery capable of immediate, swift, and precise analysis is progressively increasing across a range of fields, including disease diagnostics (Barizuddin et al., 2016) forensics (Yanez et al., 2014) environmental monitoring (Rodriguez et al., 2005) and drug designing (Yu et al., 2005). Biosensors are analytical devices that contain an integrated biological element such as enzyme, antibody, DNA, RNA, whole-cell, or microorganism. These elements not only act as a recognition agent but also assimilate with the transducing microsystem. The transducing system such as an electrode, optical detectors, and piezo crystal translates the biochemical response to appropriate optical and electrical signals (semi-quantitative or quantitative). These signals are roughly proportional to the target concentration, which is further decoded into a suitable readout (Songa et al., 2009).

The field of biosensing come into existence in 1962 when the electrode-based system for the detection of glucose was reported by Leland Clark, Jr. and Cham Lyons.

Leland Clark, Jr. is known today as the "father of biosensors" due to this remarkable development (Clark Jr & Lyons, 1962). Leland Clark, Jr. and Cham Lyons conducted the experiment to measure oxygenation of blood via reduction of oxygen with a platinum electrode. Initially, the sensor was not fully functional due to the adsorption of blood components on the surface of the electrode. To resolve this issue cellophane packaging of a cigarette packet was applied, which acts as a semipermeable membrane and only allowed the passage of low molecular weight substances mainly oxygen, and blocked other blood constituents and particles to reach the electrode. Clark added glucose oxidase (GOD) (EC number 1.1.3.4) to the sample solution to calibrate his sensor. He improved the sensor more by entrapping concentrated GOD with another semipermeable membrane in front of the electrode, after these successful modifications, the sensor could be reused multiple times (Renneberg et al., 2007).

2.2 Nanotechnology brief history

The prefix ''nano'' is derived from the Greek word for ''dwarf.'' On the metric scale, 1 nm equals one-billionth of a meter (10^{-9} or 0.000000001 m). Nanotechnology is the synthesis, understanding, and application of matter at the dimension between 1-100 nm. The size of atoms is smaller than 1 nm whereas the size of proteins is equal are greater than 1 nm (Tretter, 2006; Whitesides, 2003).

Richard P. Feynman was the 1st person who introduced the concept of nanotechnology in his lecture ''There's Plenty of Room at the Bottom" on 29th December 1959 delivered at the meeting of American Physical Society (Feynman, 2018). Later the term "nanotechnology" was defined by Professor of Tokyo University of Science Norio Taniguchi in 1974 (Silva et al., 2017). In 1986 K. Erick Drexler published a book on nontechnology explaining the basic concepts of nanotechnology introduced by Richard P. Feynman (Silva et al., 2017). In the 1980s the birth of cluster science, an invention of scanning tunnelling microscope (STM), and the successful design of atomic force microscope (AFM) in 1985 were major milestones that accelerate the research in nanotechnology. These developments lead to the discoveries of fullerenes (the third allotrope of Carbon) and carbon nanotubes after a few years (Iijima, 1991; Iijima & Ichihashi, 1993; Kroto et al., 1985). Since

then the research, development, and applications of nanotechnology have increased significantly and this discipline opens the horizons of research, development, and application.

Nanotechnology bridges the gaps among the different scientific fields such as physics, chemistry, material sciences, and engineering. That is why several nanomaterial, nanostructures, and nanoparticles are synthesis and applied in different fields due to their unique physicochemical properties. The prominent unique property which makes nanoparticles an attractive candidate is a surface to volume ratio. This feature brings major variances in both physical and chemical properties and enables improved interaction and enhanced efficiency of a nanomaterial as compared to their huge counterparts (Malaikozhundan et al., 2017). The larger surface area of nanoparticles makes them more interactive and effective agents' comparison with molecules with fewer surfaces to volume ratio. The synthesis of nanoparticles is a joint venture of nanotechnology and biotechnology and has received increasing attention because of the increasing need to develop harmless technologies in the synthesis of different kinds of materials (Buzea et al., 2007).

Continuous progress and development in nanotechnology have led the improved nanomaterials that can perform diverse functions such as imaging, sensing, and targeting. Generally, nanomaterials display certain features that could not be expected from their bulk molecules but result in enormously beneficial for diverse applications including biosensing. By controlling the size, shape, functionality, surface area combined with their unique optical, electronic, and magnetic behaviours make them exceptional candidates in the field of biosensing (Chinen et al., 2015; Sandeep et al., 2015). Their application in biosensing becomes favourable due to the possibility to combine them with biological recognition elements (Erathodiyil & Ying, 2011). Nanomaterials are useful for the improvement of composite nano-size materials in combination with biological articles such as enzymes, proteins, antibodies, peptides, DNA, RNA, aptamers, and carbohydrates. These composites not only process the functionalities of biomolecules but also exhibit the sensing characteristics of the nanomaterials (Gomez et al., 2018; Sapsford et al., 2013).

2.3 Nanoparticles

Nanomaterials that exist in fluid suspensions of nanoparticles protected with capping agents are known as colloidal nanoparticles. Colloidal metal nanoparticles have exhibited excessive potential in optical, electronic, and magnetic applications. Nanoparticle-based electro-analytical systems are particularly auspicious for the development of advanced chemical and biosensor-based monitoring platforms (Lohse & Murphy, 2012). Metallic nanoparticles have presented prodigious potential in optical and electromagnetic applications, that why nanoparticle-based analytical methods are getting intention in the assembly of biosensor-based detection systems (Lohse & Murphy, 2012).

Out of different metallic nanoparticles, AuNPs have some extraordinary and salient features like biocompatibility, chemical stability, easy functionalization, and oxidation resistance which make gold nanoparticles adoptable for extensive applications including catalysis (Thompson, 2007), chemical sensing (Saha et al., 2012), biological labelling (Dykman & Khlebtsov, 2011), electronics (Teranishi, 2003) and imaging (Popovtzer et al., 2008; Reuveni et al., 2011). Colloidal AuNPs also exhibit high surface area (Gadogbe et al., 2013), unusual surface chemistry for chemical amendments, (Homberger & Simon, 2010), permitting them to successfully catalyse the redox process for molecules of analytical interest, leading to lower detection limits. Inimitable features of AuNPs such as electrical conductivity, catalytic nature, and optical possessions of these NPs are essentially reliant on the morphology and nano-scale dimensions (Sajanlal et al., 2011).

2.3.1 Gold nanoparticles (AuNPs)

AuNPs in the field of biosensors are the most applied nanoparticles because of their unique features of these nanoparticles. The optical uniqueness of AuNPs has been known since early in human history. Lycurgus Cup from the 4th century AD placed in British Museum in London is the most well-known example. The accidental presence of nanosize metal crystals of Ag and Au make the cup glow with different color depending upon light frequency. It looks red in transmitted light and blue when reflected light falls on it.

Michael Faraday in 1857 first reported the chemical synthesis of gold colloid (Faraday, 1857). Since then, several diverse methods have been optimized for the synthesis of AuNPs by the chemical reduction of $HAuCl_4$ in the presence of capping agents. According to literature the most applied chemical method for the synthesis of AuNPs is the Turkevitch method developed in 1951 (Turkevich et al., 1951). In this method boiling $HAuCl_4$ is being reduced by the trisodium citrate ($Na_3C_6H_5O_7$) under vigorous stirring. The Au (III) salt is reduced to Au (I) and then Au (0) species are formed via a disproportionation reaction. These thermodynamically unstable Au (0) species act as a center of nucleation to form further reduced Au^+ ions. This step-by-step reduction resulted in well-dispersed AuNPs. In this method, trisodium citrate played a double role, acting as a reducing and capping agent (Turkevich et al., 1951). Later, in 1973 this method was modified to get AuNPs in the size range from 15-120 nm by fine-tuning the ratios of $HAuCl_4$, citrate, temperature, and solution pH (Frens, 1973; Herizchi et al., 2016).

The Brust-Schiffrin method is the second most used method reported in 1994, which provides a simple method that produced size-controlled, heat, and air-stable AuNPs. This method applied a bi-phase water-toluene system under ambient conditions to produce AuNPs having a diameter of 1-5nm. Tetrabutylammonium bromide (TOAB) was used as a phase transfer agent where the metal ions are reduced by sodium borohydride ($NaBH_4$), in the presence of a thiol as a capping ligand. The size of these AuNPs can be adjusted by optimizing the ratios of thiol molecules and gold salt. These AuNPs can be re-dispersed in many organic solvents and possess stability for a long time (Brust et al., 1994).

2.3.1.1 Non-spherical AuNPs

Non-spherical and diverse shaped gold nanoparticles such as rods (Busbee et al., 2003), stars (P. S. Kumar et al., 2007), cubes (F. Kim et al., 2004), shells (Aguirre et al., 2003) represent different plasmonic properties depending upon the shapes of these materials. By adopting seed-mediated growth methods substantial improvement has been achieved in the synthesis of non-spherical gold nanoparticles (Busbee et al., 2003; Millstone et al., 2005). Gold nanorods have been described to synthesize by

mixing the gold solution with cetyltrimethylammonium bromide (CTAB). As a mild reducing agent ascorbic acid was also added (Busbee et al., 2003). Gold nanostars (AuNS) are branched nanostructures possessing several protruding arms with a central core, are reported to be synthesized with the help of polyvinyl pyrrolidone, and dimethylformamide (P. S. Kumar et al., 2007).

Localized surface plasmon resonance is the main reason for the exclusive optical properties of AuNPs (X. Huang et al., 2007). When light illuminates a solution of dispersed metal nanoparticles, the electromagnetic frequency tempts resonant coherent oscillation of the free electrons. When the frequency of the incident light matches the frequency of electron oscillation, specific wavelengths of light are absorbed (Willets & Van Duyne, 2007). The oscillation frequency of AuNPs is usually in the visible region giving rise to a strong color associated with SPR related absorption. SPR of AuNPs is related to the diameter of AuNPs. Small AuNPs (~10-nm diameter) show red-orange color with an absorbance peak at 510 nm whereas an absorbance peak at 570 nm was observed for larger AuNPs (~100-nm diameter) display purple color (Ngumbi et al., 2018). The higher size of particles leads to having a wider peak due to loss of coherent electron motion which causes spectral redshift towards longer wavelengths and expansion of surface plasmon band.

2.3.1.2 AuNPs-based biosensors

AuNPs can be synthesized in different ways to produce different colors and radiate bright resonance light scattering of different wavelengths depending on the size, shape, morphology, and level of aggregation. By adopting and exploiting these features of AuNPs highly sensitive colorimetric sensing systems have been developed. Features like the extinction coefficient of AuNPs which is 1000 times better than organic dyes, large surface area, and easy surface modifications make the metallic nanoparticles right for sensing elements for colorimetric detection of diverse targets including environmental toxins, small molecules, microbes, DNA, inorganic ions, and metal ions (Lou et al., 2012; F. Xia et al., 2010; M. Zhang et al., 2011).

2.3.1.3 Factors governing AuNPs size and dispersion

The estimation of shape, size as well as nature (monodisperse or polydisperse) of AuNPs is crucial for the systemic synthesis of these NPs. Concentrated solutions of gold salt or low concentrations of citrate (as a reducing agent) often lead to aggregation of these NPs, however when citrate was used in higher concentrations smaller and monodisperse AuNPs were produced (C. Li et al., 2011). The ratio of gold salt to sodium citrate (reducing agent) and the rate of adsorption of sodium citrate (as a stabilizer) influenced the size and dimensions of the AuNPs (Tyagi et al., 2016). In general, mono-dispersion is seen in smaller-sized AuNPs, particularly nanoparticles less than the 20-nm diameter, whereas polydispersion is observed in particles with a diameter greater than 20 nm (C. Li et al., 2011). So size, shape, and nature of AuNPs depend on the different factors like the gold salt concentration, addition rate of precursors, and state of mixing in the reactor, (X. Ji et al., 2007).

The Turkevich method was modified by adding pre-mixed $HAuCl_4$/citrate to boiling water with trace amounts of $AgNO_3$ in the mixture to attain minute-sized and quasi-spherical shape nanomaterials production (Lu et al., 2008). The hydrodynamic size of the NPs in colloidal solution was estimated with the help of dynamic light scattering (DLS) to investigate the modulation of the intensity of scattered light that passes through the colloidal solution as a function of time. In comparison to DLS data with TEM images elaborate the aggregated state of the NPs (Souza et al., 2016). For a mono-dispersed colloidal solution of NPs the diameter obtained with DLS is higher than the TEM results because DLS data includes core size, capping agent as well as solvent layer attached to the surface of NPs but TEM provides the diameter of core NPs (Souza et al., 2016).

2.3.1.4 Applications of AuNPs in the field of biosensing

AuNPs are well-studied nanomaterial because of different methods of synthesis which leads to giving different size ranges, formats, easy functionalization, and unique plasmonic features at the nanoscale as well as high stability. All these features make AuNPs perfect for diverse applications including biosensing of diverse substances. Simple detection methods for H_2O_2 and glucose were established by exploiting the

intrinsic peroxidase-like activity of positively charged cysteamine capped gold nanoparticles (+) AuNPs. Peroxidase substrate 3, 3, 5, 5-tetramethylbenzidine (TMB) was capitalized and the color of the substrate is changed to blue in the presence of H_2O_2 and (+) AuNPs. This method was further capitalized for the sensing of glucose. (+) AuNPs can rival natural enzymes due to easy synthesis and high stability. These findings lead to the innovative applications of AuNPs in the fields of chemistry, biotechnology, and medicine (Jv et al., 2010).

An aptamer functionalized AuNPs were used in the progress of a colorimetric biosensor for the monitoring and detection of omethoate (an OP). OP pesticide-binding aptamer (OBA) "artificial antibody" was used as a recognition element to develop a highly sensitive assay for the detection of OP family members. The scientific understanding behind the development of the sensor was the single-stranded DNA, wrapped in gold nanoparticles, remain in the dispersed form under the influence of salt but when the candidate OP was added to the reaction mixture AuNPs get disconnected from the aptamer and color of the solution were being changed due to the aggregation of AuNPs. The assay showed linearity between 0.1-10 μM, with a low detection limit of 0.1 μM. Soil samples were quantified for omethoate with the help of this assay (P. Wang et al., 2016).

Detection of ethoprophos (an OP) was done by the development of a dual-sensing system i.e. colorimetric as well as fluorometric. A sensitive and selective assay was established by utilizing adenosine triphosphate and exploiting the aggregation property of rhodamine B modified gold nanoparticles. The linear range for this detection system was calculated in between 4.0-15.0 μM and LOD was detected as low as 37nM. To check the practical applications of this simple assay, tap water samples were tested for the ethoprophos detection, obtained results were highly reliable and consistent which confirms its on-site applications (X. Li et al., 2018). In another study, AuNPs/three-dimensional reduced graphene oxide (rGO) film was used for the development of an amperometric sensor by the immobilization of AChE on the electrode. The film was constructed by the advantage of AuNPs on 3D graphene. The synergic relationships of AuNPs and rGO played an outstanding role in the electrical

conductivity of the film. The linear relationship for this sensor was found to be in the range of 1.0×10^{-10}-1.0×10^{-6} $g\cdot L^{-1}$. The sensitivity of the sensor was tested for malathion and methyl parathion in the water sample and minimum detection was found up to 2.78×10^{-11} $g\cdot L^{-1}$and 2.17×10^{-11} $g\cdot L^{-1}$, respectively. This optimized AuNPs/rGO film can be utilized in different ways to immobilize other biological elements such as antibodies and DNA for the development of biosensing systems. The sensor showed reliability, precision, accuracy, repeatability, and reproducibility (Dong et al., 2019).

An easy to use as well as versatile photothermal biosensing method was developed for the detection of nucleic acid using a common thermometer. In this method, a thermometer was used as a single reader without the assistance of any other analytical device. DNA of mycobacterium tuberculosis (MTB) was used as a target to optimize the sensing of AuNP aggregation-induced photo-thermal biosensing method. LOD was as low as 0.28 nM which is 10 times lower than the LOD for many biosensing methods. The simplicity and economical nature of this method are obvious because no DNA amplification, as well as no DNA labeling, was required in this detection procedure. Moreover, this method can also be applied for the detection of all sorts of organisms and is not limited to nucleic acid detection (W. Zhou et al., 2020).

2.4 Nanozymes

The natural enzymes own some fundamental limitations including high-cost production, less stability, and sophisticated storage requirements. These limitations created the development and progress of various enzyme mimics ''Nanozymes'' (also known as ''artificial enzymes''). Nanozymes have emerged as the next generation of enzyme mimics since the unexpected discovery of magnetic Fe_3O_4 nanoparticles with peroxidase-like activities in 2007 (Gao et al., 2007). ''Nanozymes'' was defined as ''nanomaterials with enzyme-like characteristics'' in the first comprehensive review on nanozymes published in 2013 (Wei & Wang, 2013). Inspired by nature but advantageous over natural enzymes, nanozymes are generally low-cost production, stable, and mass-production can be achieved easily (J. Wu et al., 2019).

2.4.1 Metal-Nanozyme based biosensing

The biocompatibility and electronic characteristics of metal nanoparticles made them strong candidates to be used in diverse applications including catalysis, biosensing, imaging, fuel cell, and biomedicine (Cobley et al., 2011; Y. Xia et al., 2009). Intrinsic features of other metallic nanoparticles possess the activity of peroxidase, oxidase, catalase, superoxide dismutase (SOD), glucose oxidase (GOx or GOD), etc. (S.B. He et al., 2020; C. P. Liu et al., 2016; Mahmudunnabi et al., 2020; Pandey et al., 2020; You et al., 2017). Gold-based nanomaterials due to advantages over all different metallic nanomaterials have been applied even more extensively (Alle et al., 2021; Borghei et al., 2017; L. Hu et al., 2018; V. Kumar et al., 2018; C. Wang et al., 2016; Y. Wu et al., 2018).

Intrinsic peroxidase-like of activity of positively charged AuNPs was studied. Cysteamine was used in the synthesis of AuNPs possessing an average size of 34 nm. The presence of NH^{+3} on the surface of these AuNPs resulted in the surface charge +11.3 mV. The surface chemistry of these nanoparticles directly influenced the catalytic nature of the nanoparticles. Peroxidase-like catalytic activity was also influenced by the surface charge of nanoparticles. AuNPs which were synthesis by using citrate having the negative surface charge did not exhibit the strong peroxidase-like catalytic activity (Jv et al., 2010). Different research groups conducted a series of experiments to assess the effect of ligands and capping agents on the catalytic activity of nanomaterials (Akanda et al., 2021; Deng et al., 2017; X. Jiang et al., 2015; B. Liu, et al., 2016; G.L. Wang et al., 2015; Y. Wu et al., 2018; Q. Zhao et al., 2016).

The efficiency of nanozyme was also highly dependent on the pH of the working atmosphere (Gu et al., 2020; L. Hu et al., 2018; S. Li et al., 2020; Yanga Liu, 2018). It was found that AuNPs show optimal peroxidase activity at around a pH of 4.0 (acidic medium). Nanozyme cannot play well at higher pH especially at physiological values which limits their applications in biological systems. Heparin was introduced under natural conditions and significantly improves the peroxidase-like activity of AuNPs. This modification increases the electrostatic interaction between TMB and negatively charged AuNPs which induces enhanced catalytic activity (L. Hu et al., 2018).

Besides the peroxidase activity, it is also well documented that AuNPs also showed oxidase, catalase, SOD, and GOx like activities (Golchin et al., 2018; W. He et al., 2013; Zhan et al., 2019; H. Zhang & Yang, 2020; S. Zhu et al., 2019). The catalytic activity of AuNPs depended on and can be altered by the deposition of metal ions on the surface of AuNPs. The presence of Ag^{+}, Bi^{3+}, or Pb^{2+} on the surface of AuNPs induces strong peroxidase-like properties to AuNPs. On the other hand, the presence of Ag^{+}/Hg^{2+} makes the AuNPs oxidase mimic, and Hg^{2+}/Bi^{3+} makes the AuNPs catalase mimic. It is also reported that the enzyme mimics properties of AuNPs also depends on the oxidation state of AuNPs. Other metal nanoparticles including Pt, Pd, Ag, and Fe also possess enzyme mimic features (Cormode et al., 2018; Gao et al., 2020; Xueliang et al., 2021; S. Singh, 2019b). In an acidic medium, Pt-derived nanoparticles showed peroxidase activity. Under the influence of the alkaline medium, these Pt-NPs showed catalase mimic activity (Yi et al., 2014).

Catalytic and electrical properties of Molybdenum disulfide (MoS_2) were exploited in the development of nano-composite of AuNPs@MoS2-QDs. These gold nanoparticles decorated over MoS_2 quantum dots expressed the peroxidase activity and did the oxidation of TMB in the existence of H_2O_2. The nano-composite followed the Michaelis–Menten kinetics with a widespread range of pH and temperature. The method was further established to progress a portable kit for the detection of glucose in different body fluids. This designed enzyme mimetic colorimetric assay can be further applied to the clinical diagnoses field (Nirala & Prakash, 2018).

Molybdenum oxide nanoparticles (MoO_3NPs) showed the oxidase mimicking activity by catalyzing the oxidation of 2, 20-azino-bis (3- ethylbenothiaoline-6-sulfonic acid) (ABTS) to a green product. The catalytic mechanism of this oxidation process was studied by applying electron spin resonance and radical inhibition methods. The MoO_3 NPs catalyze dissolved O_2 and generate O_2 radical and this free radical reacts with the substrate. Ascorbic acid (AA) was produced by the hydrolysis of the ascorbic acid 2-phosphate (AAP) by acid phosphatase (ACP). Generation of AA causes to fade of the coloration process ABTS oxidation. With the help of oxidase mimicking features of MoO_3NPs and the ACP-catalysed hydrolysis of AAP, a simple

colorimetric method was established with a detection limit of 0.011 $U \cdot L^{-1}$. This sensing system was successfully applied for ACP detection as a diagnostic tool (Z. Lin et al., 2020).

Effects of different crystal structures α, β, and γ were studied for the physical and chemical properties of MnO_2 nanorods and concluded that different structures having the same morphology showed different catalytic activity. To test the catalytic activity of these MnO_2 nanorods, TMB was castoff as the substrate. It was found that the surface of β-MnO_2 was enriched with hydroxyls and relatively high concentration of Mn^{4+} ions made β-MnO_2 perfect to exhibit the highest catalytic activity in comparison with α- MnO_2 and γ- MnO_2. Using these β-MnO_2 nanorods, a β-MnO_2-TMB-GSH system was developed to detect the concentration of glutathione (GSH) in human serum samples by adopting a colorimetric biosensing method. The detection range for this method was (0.11–45 μM) and the LOD was as low as 0.1 μM. So, different crystal structures and surface physicochemical properties can be exploited for the development of different sensing systems for diverse field applications (Y. Meng et al., 2020). Platinum oxide nanoparticles (PtO_2) are shown intrinsic oxidase-like and peroxidase-like properties. Data obtained from X-ray diffraction (XRD) and X-ray photoelectron spectra indicate that the majority of these nanoparticles which are being synthesized by adopting the green method have Pt (IV) states. These nanoparticles induced the generation of reactive oxygen species (ROS) which was the main reason for its enzyme-like characters. By capitalizing on these enzyme-like properties of PtO_2 colorimetric method was established for the monitoring of glucose in human serum. This glucose-sensing protocol has the potential for applications in medical and food safety applications (Xueliang et al., 2021).

2.5 Organophosphates (OPs)

OPs are organic esters that are derivatives of thiol or amide. These compounds have orthophosphoric, phosphonic, or phosphoric acids with additional side chains of phenoxy, cyanide, and thiocyanate group (Shardendu et al., 2016; O Brien, 2016). OPs are the key constituents of pesticides, herbicides, insecticides, and nerve gas (Adeyinka et al., 2018). OPs consist of synthetic and non-synthetic compounds that

are enriched with C-P linkage. This C-P linkage makes it thermally and chemically inert which leads it to resist its thermal hydrolysis, photolytic deprivation, and chemical breakdown (Greaves & Letcher, 2017). Analyzing the basic structure of OPs reveals that terminal oxygen is connected with phosphorus by a double bond, i.e. a phosphoryl group, two lipophilic groups bonded to a phosphorous which is connected to halide member (V. Kumar et al., 2013; Perera & Dulmini, 2020).

Extensive applications of OPs in the diverse field including agriculture, horticultural, pest and vector control, plastic making, domestic and industrial usage, and as a warfare weapon has been reported (Adeyinka et al., 2018; Ballantyne & Marrs, 2017; Kaushal et al., 2021; P. Singh & Prasad, 2018). The universal usage of OPs rose to the amount of 5.0 million to 6.8 million from 2011 to 2015 (R. Wang et al., 2015). 40% usage of OPs is reported in the Asia-Pacific region, North America stood 2nd and consumption of OPs are at 3rd in European countries (Sidhu et al., 2019).

The polar nature of OPs makes it a good solute for water, the water-soluble form of OPs have easy distribution in nature, besides that dissolution, abrasion, and volatilization cause them to spread effortlessly into the environment (Balderacchi et al., 2013; A. Wang et al., 2014). This easy spread of OPs in nature leads to acute and chronic exposure which roots the different levels of toxicity in humans, animals, insects, and even plants (Sidhu et al.,, 2019). These OPs are analogous to the substrate of acetylcholine esterase (AChE) so able to block the active site of AChE which interrupts the normal neural as well as overall body functions of terrestrial and aquatic fauna (G.H. Lee & Choi, 2020; Muhammad et al., 2017). This inhibition of AChE is not only observed in target species such as insects or pests but also affects the non-target terrestrial and aquatic organisms, leading to abnormalities in the normal physiological functions such as respiratory, reproductive, nervous, hepatic, and renal disorders (Sidhu et al., 2019).

2.5.1 Toxic effects of OPs on animals

Critical and enduring exposure to the OPs can cause a varying level of toxicity in humans, animals, plants, and insects. The toxic effects of two OPs were studied on

freshwater gastropod *Planorbarius corneus*. Different concentrations of these toxic compounds were applied in single and binary studies. After 24 hr. exposure, a noticeable reduction in the level of glutathione disulphide (GSSG) and glutathione S transferase (GSH) was observed. The reduced level of these GSSG and GSH confirm the oxidative damage and oxidative stress on the tissues of *Planorbarius corneus* (Cacciatore et al., 2015). Two concentrations (1.09 and 2.18 $\mu L \cdot L^{-1}$) of quinalphos were applied for 20 days on *Cyprinus carpio* (European carp-Freshwater fish) to study the oxidative stress and antioxidant responses under the influence of this OP. The presence of quinalphos elevates the level of malondialdehyde and abnormal level of oxidative parameters such as superoxide dismutase, catalase, and GSH activity confirmed the toxic nature of quinalphos (Hemalatha et al., 2016). Different target organs such as the gills, brain, muscles, and kidneys of *Cyprinus carpio* were studied for the toxic effects of phorate on lactate dehydrogenase. In the 30 days study period obvious deleterious effects on the activity of lactate dehydrogenase were observed in all these organs of the fish (Lakshmaiah, 2016).

LC50 at different time intervals 24, 48, 72, and 96 hr. for the frog *Euphlyctis cyanophlyctis* studied and found to be 8.252, 7.254, 6.247, and 4.993 $mg \cdot L^{-1}$ respectively in the presence of chlorpyrifos. Mortality studies confirm the toxic effects on the treated frog as compared to control and declination in the frog populations were observed (Srivastav et al., 2017). The toxic nature of malathion was studied in nile tilapias (*Oreochromis niloticus*) and reported that the presence of malathion causes major alterations in the functions of the kidney (pyknosis), gills (hyperplasia, lamellar fusion), liver (narrowing of the lumen, blood sinusoids) and brain. Respiratory issues, impulsive swimming, and sudden death were also reported. The dose-dependent mortality rate was observed in experimental fishes (Subburaj et al., 2018).

A study was established to understand immunotoxicity mechanisms caused by diazinon. Spleen mononuclear cells (SMNC) of nile tilapia were subjected to study calcium flux in cells, apoptosis, senescence, and mitochondrial membrane potential under the influence of different concentrations of diazinon. After analyzing the results

is was obvious that diazinon significantly damages all these parameters which have the key roles in the regular working of immune cells. For this study, it was concluded that OP pesticides have negative effects on immune cell signalling and have immunotoxin effects (Diaz-Resendiz et al., 2019). Different hematological parameters like RBCs, WBCs, CT, PT, etc were taken into consideration under the influence of different doses of malathion. Four doses 25, 50, 75,100 $mg \cdot Kg^{-1}$ bodyweight of albino rats (male and female) were selected, and samples were taken after the treatment of 7 and 15 days. Obtained results confirm that the higher concentrations cause more fluctuation in these hematological parameters confirming that malathion has toxicological effects on the normal physiological functions of albino rats (C. Sharma, et al., 2020).

Besides the neurotoxic effect of these toxins various research groups also reported the genotoxic effects of OPs (Pinkas et al., 2015; L. Sun et al., 2016). OPs can lead to an increase in the potential disorders in endocrine, metabolic, neurological functions, leukemia, bladder cancer, psychiatric manifestations, and neuritis (Shardendu et al., 2016; Sidhu et al., 2019). The above described the toxic effects of OPs and the potential threat of accumulation of OPs in food resources and ultimately entering into the food chain and water supplies. More investigation and research work are required to assess the least exposure time and minimal concentration of these OPs which become lethal and cause damage to the functionality of different organ and organ systems.

2.6 Analytical methods for the sensing of OPs

The increased use of pesticides around the globe causes a significant deleterious effect on non-targeted populations including humans. Several analytical techniques s have been described for the detection of different members of the OP family. Some of these methods have been elaborated on in the coming sections.

The gas chromatography method was adopted for the detection of thirteen organophosphate pesticide residues extracted from Allium tuberosum (Chinese chive) by using acetonitrile. DB-1701 capillary column (30 m×0.32 mm×0.25 μm) was used

for the separation and a flame photometry detector was used for the detection of these toxic chemicals. At the injection pressure of 68.9 k·Pa and oven temperature ramp velocity of 5 °C min^{-1} thirteen OPs pesticides were separated from the plant matrix in half-hour. LOD of this method was from 0.01 to 0.03 $mg \cdot kg^{-1}$ and the relative standard deviation were found between 2.6%-10.7% (Ying et al., 2009). The novel and precise protocol were established to detect nine urinary metabolites of organophosphate ester flame retardants (OPFRs) by adopting solid-phase extraction and ultra-performance liquid chromatography coupled to tandem mass spectrometry (UPLC-MS/MS). The detection limit was found between 0.08-0.25 $ng \cdot mL^{-1}$. Out of all OPFR metabolites, only desbutyl-tris-(2-butoxy-ethyl) phosphate could not found in these 24 samples were collected from pregnant Canadian women participants which are a piece of evidence that the population was exposed to OPFRs (Kosarac et al., 2016).

Carbon quantum dots (CQDs) were capitalized for the detection of OPs with the help of fluorescence resonance energy transfer (FRET). The fluorescence emission of CQDs was decreased by the presence of AuNPs because both CQDs and AuNPs have maximum fluorescence emission at 520 nm, which leads to the overlap of absorption of these bands. Hydrolysis of acetylthiocholine (ATC) in the presence of BChE produces thiocholine which causes the aggregation in AuNPs resultantly FRET-quenched fluorescence is being recovered. In this way, a simple sensing fluorometric determination of paraoxon was established. So, a facile FRET-sensing platform for OPs with the help of tunable CQDs fluorescence emission was developed and can be applied for the sensing of OP for environmental and food safety applications (X. Wu et al., 2017).

HPLC–DAD-based analytical route for instantaneous monitoring of profenofos and fenthion was established. Both OPs pesticides are being applied frequently in agricultural practices. Dichloromethane was applied for the extraction of these pesticides from spiked water samples and 80-90% recovery was done. The mobile phase for this HPLC system contained 75% methanol and 25% water, an optimum flow rate of 0.8 $mL \cdot min^{-1}$, and a diode array detector was set at the wavelength of 210

nm. Within 20 min of HPLC run, significant separation of both pesticides was obtained. By this method, simultaneous detection of fenthion and profenofos were established with the detection limit of 0.0328 $mg \cdot L^{-1}$and 0.104 $mg \cdot L^{-1}$ respectively. Similarly, the limit of quantification for this system was 0.0995 $mg \cdot L^{-1}$ and 0.316 $mg \cdot L^{-1}$ for fenthion and profenofos respectively (Mahajan & Chatterjee, 2018).

Another study was conducted to develop a mass spectrometric method for the quick identification of OP compounds in gastric juice. Thermal desorption electrospray ionization and mass spectrometric analysis of the six OPs in the gastric juice were obtained within 30 sec. The detection limit of OPs is at the 10–100 ppb level. A very good linearity curve was obtained between the mass spectrometric signal intensities. The data obtained from the mass spectroscopic method was enough for providing sufficient toxicological information for medical management in medical emergencies (C.W. Lee et al., 2018). A novel eco-friendly gas chromatography-based detection system was established for the detection of eight pesticides. The developed method was validated by using parameters like linearity, precision, accuracy, and sensitivity. All the calibration curves were in upright linear relation within the test range, intra and inter-day testing were done to double-check the precision of the system. The outcomes of this system confirm that all eight pesticides were detected below the detectable limit in a single run. This method could be applied for the detection of pesticides present in fruits and vegetables (Wani et al., 2019).

2.7 Biosensors for the detection of OPs

Various kinds of biosensors have been developed for sensing different kinds of analytes, including enzyme-based biosensors, tissue-based biosensors, immunosensors, DNA biosensors, microbe-based biosensors, cell-based biosensors, etc. Among the reported sensors which are designed to detect the OPs, enzyme-based biosensors are common, easy to develop methods and under the scope of this dissertation so here only the details of different kinds of enzyme-based biosensors are elaborated

2.7.1 Enzymes based OPs biosensors

Enzyme-based biosensors used the enzyme in proximity with transducer elements which produces high and precise reactivity with their substrate. In these kinds of OP biosensors, enzymes are applied in two different ways. 1st method is known as an enzyme inhibition-based mechanism in which OP pesticides block the active site of enzymes like AChE or BChE which leads to a decrease in the enzymatic product. In the 2nd method, the hydrolytic ability of enzyme (e.g. OPH) was used to measure the presence of OPs compounds. Organophosphorus hydrolase (OPH) catalysis the hydrolysis of OPs compounds, the higher the concentration of OPs higher will be the catalytic activity. Enzyme-based biosensing of OP compounds is mostly adopted because the assay possesses a reckless response, high robustness, and easiness of immobilization of enzyme (Rassaei et al., 2011).

2.7.2 Enzyme inhibition-based OP biosensors

Enzyme inhibition-based OP biosensor based on the principle that when OPs compounds are present in the environment the enzymes (AChE or BChE) are blocked and could not convert their respective substrates (acetyl thiocholine, or acetylcholine or butyryl thiocholine, or butyryl choline) into thiocholine or choline and acetic acid/butyric acid. In the absence of OPs, generated thiocholine/choline undergoes oxidation/dimerization under the applied voltage (electrochemical sensor) but when OP compounds are present the current produced due to oxidation will decrease depending upon the concentration of OPs in the test sample (Rajangam et al., 2018).

2.7.3 Classification of enzyme inhibition-based OP biosensor

Enzyme inhibition-based biosensors can be classified based on physical and chemical interaction, matrices used for immobilization, and transducer applied but here the classification of OP biosensors based on the transducer is considered only. On this basis, we can divide the enzyme inhibition-based OP biosensor into the following four main types.

1. Electrochemical (Amperometric and Potentiometric)
2. Thermal
3. Piezoelectric
4. Optical (Fluorescence, Colorimetric, and Surface plasmon resonance (SPR)).

2.7.3.1 Electrochemical enzyme inhibition-based OP biosensor

Enzyme-based electrochemical sensors are easy to apply for field applications because these do not only possess a simple manufacturing process but also provide a compact and portable analytical device by providing the fact miniaturizing of the required instruments. These devices can be engineered to hold a high level of selectivity as well as sensitivity (Campas et al., 2009). These biosensors are well established and emerged as a portable alternative to detect OPs (Ovalle et al., 2009). Electro-active species which are being generated by biological entities such as enzymes (AChE or BChE) via electrochemical active transducer (electrode) are analyzed in electrochemical OP biosensors. In the case of amperometric biosensing redox reaction generated current is being monitored and in the potentiometric biosensor, the signals are monitored when the pH of the reaction medium is being altered (Andreescu & Marty, 2006).

2.7.3.2 Amperometric enzyme inhibition-based OP biosensor

The principle of amperometric sensing involves the measurement of the response of the indicator electrode under the influence of current. The redox reaction which is being catalyzed by the enzymes generates net current under a constant potential which is being applied between working and reference electrodes. The amount of this current is in direct relation to the concentration of electroactive species present in the given sample at a constant potential. Out of a large number of amperometric OP biosensors, the biosensors in which AChE is immobilized on o-phenylenediamine/carbon/cobalt pthalocyanin (CoPc) printed electrode showed the lowest LOD (1×10^{-11} μM) and linearity range (1.0×10^{-11} – 1.0×10^{-2} μM) for the detection of dichlorvos, parathion and azinphos. The entrapped enzyme showed stability up to 92 days and the incubation time for this sensing system was only 10 minutes (C. S. Pundir & Chauhan, 2012).

An amperometric biosensor was established by immobilizing BChE on the electrode which was already modified with prussian blue. LOD for paraoxon and chlorpyrifos-methyl oxon was 4.0 ppb and 1.0 ppb respectively (C. S. Pundir & Chauhan, 2012). In one study amperometric biosensor was constructed by cross-linking BChE onto a screen-printed electrode possessing prussian blue nanoparticles. Paraoxon was

detected with a LOD of 1 ppb and the detection system was found to be stable for up to 60 days. BChE showed much higher storage stability. These kinds of biosensors can be exploited for applications in the agro-food industry (Arduini et al., 2015). Amperometric enzyme inhibition-based OP biosensor systems showed very limited response time, high sensitivity, wide linear range, a very low limit of detection, the linearity of the calibration plot, and these kinds of the process can be managed by the electrode potential. But the specificity of these sensors is sometimes compromised due to the presence of interfering substances such as heavy metals and other toxins. The requirement for long incubation time is another limitation of these biosensors.

2.7.3.3 Potentiometric enzyme inhibition-based OP biosensor

The potentiometric enzyme inhibition-based biosensors worked on the principle of conversion of hydrogen ions (H+) into an electrical signal. These hydrogen ions are either generated or absorbed by the transducing element. The variation in the pH indicates the presence of an analyte in the test sample (Andreescu & Marty, 2006). BChE based potentiometric biosensor was developed with the help of glutaraldehyde for the detection of trichlorofon. The LOD of the system was 10^{-7} M and the response time of the system was very short (Reybier et al., 2002). A disposable highly sensitive screen-printed potentiometric biosensor using BChE was constructed for the detection of malathion in human serum. The LOD of this sensing system was 8×10^{-7} mol·L^{-1} and linear range of 10^{-6} to 10^{-2} mol·L^{-1} (Khaled et al., 2010). Reproducibility and enhanced LOD of these sensing systems make them suitable for the monitoring of OP residues in food and agricultural products. On the other side the high potential requirements and the problem of fouling which is being raised by the presence of thiol group limit the applications of these systems.

2.7.3.4 Thermal enzyme inhibition-based OP biosensor

In this kind of heat-sensitive sensing system, the heat which is being generated during the enzyme catalytic reaction is capitalized by the heat sensing transducer and being used for the development of OP biosensor. For example, malathion was detected via an AChE sensing system in which a decrease in the generation of heat was found to be directly proportional to the concentration of the analyte (C. Pundir & Malik, 2019).

Parathion was detected in onion, lettuce, and salad via a photothermal biosensing system. In this system cholinesterase (AChE/BChE) was cross-linked with glass beads and LOD was found to be 0.005–0.013 $mg \cdot kg^{-1}$ (Pogacnik & Franko, 2003). As all the biological reactions are exothermic so thermal OP biosensing provides a good option for the development of a specific biosensor. But when the heat is generated by the non-specific source or change in optimum pH and variation in the viscosity may generate an undesired signal which limits the development of this type of biosensor for commercial applications.

2.7.3.5 Piezoelectric enzyme inhibition-based OP biosensors

When piezometric crystals are partially or fully immersed in a liquid, the change in the mass of the crystal occurs. By adopting this basic principle of piezoelectric sensing approach, OP pesticide detection was reported by (N. Kim, Park, & Kim, 2007). The unique property of piezoelectric crystals has been exploited for the development of OP biosensors with the inference of biological components such as enzymes that are used for the coting of these crystals (Marrazza, 2014). Di-isopropyl fluorophosphate was also detected from river water samples (Halamek et al., 2005). An innovative sensing system was reported by immobilizing the BChE coupled with an inhibitor on the surface of piezoelectric quartz crystal. The LOD for di-isopropyl fluorophosphate for this competitive affinity assay was 10 $nmol \cdot L^{-1}$. The addition of EDTA dissolved the chelate complex which makes this sensing system applicable to the on-site monitoring of OPs (Makower et al., 2003). Very sensitive and highly selective quartz crystal microbalance sensors were established which showed very high analytical performance for the monitoring of parathion and paraoxon, respectively (Funari et al., 2013; Ozkutuk et al., 2013). Piezoelectric sensing systems proved to have a very simple mechanism, with real-time output and high sensitivity. On the other hand, these systems are slightly expensive and need a longer time to develop a stable and reliable baseline. Also, high molecular weight OP compounds cannot be detected with acceptable sensitivity. These imperfections make them impractical for daily applications.

2.7.3.6 Optical enzyme inhibition-based OP biosensor

Optical parameters such as absorbance, fluorescence, and chemiluminescence were measured by capitalizing transducers such as fiber optics and optoelectronic to detect the presence of analytes.

2.7.3.6.1 Fluorescence enzyme inhibition-based OP biosensor

These types of OP sensing systems are based on specific interaction that exists between the applied enzyme and target analyte. Optical signals like absorption or emission band are being generated by the chemical interaction of enzyme and analyte and the strength of these signals is directly proportional to the concentration of the analyte. Electrostatic interactions of AChE with poly-allylamine hydrochloride/CdTe quantum dots/glass were utilized for the development of an optical biosensor to monitor paraoxon and parathion. LOD was found to 1.05×10^{-5} μM and 4.47×10^{-6} μM and linearity range of 1.0×10^{-6} −1.0 μM and 1.0–0.1 μM for paraoxon and parathion respectively (C. S. Pundir & Chauhan, 2012). AChE was encapsulated onto a chromoionophore (N-Octadecanoyl-Nile blue) doped sol-gel to perform the optical detection of dichlorvos. LOD and linear range for this detection system were 2.26 μM and 2.26–31.67 μM respectively (C. S. Pundir & Chauhan, 2012).

Fluorescence-based detection of OP provides a very quick and extremely sensitive detection with 106 times lower LOD than other absorbance techniques (Andreescu & Marty, 2006). High extinction coefficients and symmetric emission spectra of quantum dots (as fluorescence reagents) add extra efficiency and size-tunable light emission for this kind of detection system. But these systems can produce false results if similar chemiluminescent emitting compounds are present in the test sample.

2.7.3.6.2 Surface plasmon resonance (SPR) based enzyme inhibition-based OP biosensors.

SPR biosensors detect the concentration of the analyte by analyzing the binding kinetics of the analyte and biological molecules such as enzymes. In the presence of analyte variation in the intensity of the SPR angle was observed. An SPR sensor was developed with the help of an alkanethiol self-assembled monolayer and immobilizing of AChE on an SPR chip for the monitoring of chlorpyriphos at a LOD of 52–58

$ng \cdot L^{-1}$ (Lin, Huang, & Liu, 2006; Mauriz et al., 2006). Optical sensors based on the SPR sensing system proved to have a very good consistency and reliability for even those analytes of very low molecular weight. With the help of these devices, real-time onsite monitoring can be done without the demand for any labeling molecules.

Table 2.1 Summarizes different methods that are devised for the monitoring of OP compounds

Sr. No	Method	Linear Range $ng{\cdot}mL^{-1}$	LOD $ng{\cdot}mL^{-1}$	Target Analyte	References
1	LC-MS	--	0.5	Glyphosate	(Okada et al., 2019)
2	Enzyme-linked immunosorbent assay	0.44-8.48	0.19	Parathion	(Z.L. Xu et al., 2012)
3	3QD based sensor	25-3000	18.0	Parathion-Methyl	(Yan et al., 2015)
4	Biosensor using MPH enzyme	0-26,312	1052.8	Parathion-Methyl	(Lan et al., 2012)
5	Fe_3O_4 imprinted polymers	15-2500	5.2	Parathion-Methyl	(S. Xu et al., 2014)
6	MIP-B-TiO2 NRs-Voltammetry	0.01-100	7.4×10^{-3}	Chlorpyrifos	(X. Sun et al., 2017)
7	Fluorometric and colorimetric	0.125–750	0.125	Carbaryl	(Yan et al., 2019)
8	AChE/AuNPs based system	0.01-1.0	2.78×10^{-5}	Malathion	(Dong et al., 2019)
9	RB-AuNPs based system	969.2–3632.5	8.965	Ethoprophos	(X. Li et al., 2018)
10	Aptamer-AuNPs	21.31-2130	2.1×10^{7}	Omethoate	(P. Wang et al., 2016)
11	Amperometric	0.2–45.0	0.001	Malathion	(Touloupakis et al., 2012)
12	Optical biosensor	2.75-68.8	1.38×10^{-3}	Paraoxon	(Khaksarinejad et al., 2015)
13	Electrochemical DNA aptasensor	37.363-3737.3	100.88	Profenofos	(Selvolini et al., 2018)
14	Cysteamine-stabilized gold nanoparticles	0.84×10^{-6} – 11.83×10^{-6}	9.94	Glyphosate	(Jinmin et al., 2013)
15	Electrochemical	6.92–55.4	4.82×10^{3}	Fenitrothion	(Soysal, 2019)
16	Multicolor sensor	40-5000	2.42	Parathion-methyl	(X.L. Yin et al., 2021)
17	Multicolor sensor	10-5000	0.95	Fenitrothion	(X.L. Yin et al., 2021)

18	SPE-GC–MS	1-50 2.5-30	0.018 0.067	Parathion methyl Fenthion	(Ozer et al., 2020)
19	UCNPs-MnO_2 aptasensor	0.1–5000	0.05	Carbendazim	(Ouyang et al., 2021)
20	Nano Gold-electrochemical biosensor	0.1 -1500	0.019- 0.077	Trichlorfon, Dichlorvos	(G. Zhao et al., 2021)
21	Fluorescence-MnO_2 Nanosheets	0.005–500	1.6×10^{-3}	DDVP	(Yuan et al., 2019)
22	Fluorescence	0.5–25	0.37	Aldicarb	(Ton et al., 2013)
23	Fluorescence sensor	0.005 to 25.0	0.0029	DDVP-dichlorvos	(X. Zhou, et al., 2021)
24	Colorimetric sensor	27-2842.11	24.4	Paraoxon methyl	(Bui & Abbas, 2015)
25	Colorimetric and fluorometric sensor	Not given	34500	DCP	(Gupta & Lee, 2017)
26	Colorimetric and fluorometric	0.0-195	9.13	DCNP	(Kundu et al., 2019)
27	RF-QDs/PRO-AuNPs	$0\text{-}4 \times 10^{8}$	18×10^{-6}	Paraoxon-methyl	(Yan et al., 2015)
28	MnO_2/CDs FRET	0.05– 5.0	0.015	Paraoxon	(Yan et al., 2018)
29	SiQDs/OPD/Ag+/AChE/ATC	10– 500	10	Paraoxon	(Jin et al., 2019)
30	CDs/DNTB/ATCh/AChE	1- 1000	0.4	Paraoxon	(H. Li, Yan, Lu, & Su, 2018)
31	TPCA/β-CD@AgNPs	100-2500	--	Malathion	(M. Wang et al., 2019)
32	Colorimetric detection	$1\text{-}5\times 10^{3}$	14.0	Malathion	(Faghiri, et al., 2021)
33	Colorimetric Gold Nanoparticles	100- 6000	34.0	Carbendazim	(Y Ma et al., 2017)
34	Colorimetric AgNPs	100–5000	10.0	Cartap	(M. Wu et al., 2018)
35	Colorimetric AgNPs	--	1.8×10^{4}	Malathion	(Dissanayake, et al., 2019)
36	Colorimetric AuNPs	--	1.39×10^{5}	Malathion	(Dissanayake et al., 2019)

37	Colorimetric Ag-Au	--	1.189×10^6	Malathion	(Dissanayake et al., 2019)
38	Fluorescence turn-on probe	100-10000	80	Thiodicarb	(Tseng et al., 2019)
39	Colorimetric sensing	--	350	Parathion	(S. Wu et al., 2017)
40	Fluorometric sensing	0.1-100	0.1	DDVP	(Yaqing et al., 2020)

Materials and Methods

Materials and Methods

The research work to complete the present study entitled "**Studies on the Development of a Nanosensor for Organophosphorus Neurotoxin Monitoring**" was performed in the Applied Microbiology and Biotechnology Laboratory (AMBL), Department of Biological Sciences, International Islamic University, Islamabad, Pakistan, and JI-Laboratory, Carle Cancer Centre, the University of Illinois Urbana-Champaign, USA.

The details of materials, experiments, methodologies employed, and techniques adopted have been elaborated as follows.

3.0 Experimental

All glassware used in the below-mentioned experiments was thoroughly cleaned with a freshly prepared 3:1solution of HNO_3/HCl, rinsed with water, and air-dried before use.

3.1 Materials and reagents

Analytical grade chemicals were consumed in this research work and used as received. Acetylcholinesterase (AChE, from *Electrophorus electricus*), acetylcholine chloride (ACh), $HAuCl_4.3H_2O$ (gold salt), and PE were purchased from Sigma Aldrich USA. TMB was obtained from MOSS Inc. USA.

Working solution (2.0 m $U \cdot mL^{-1}$) of AChE were obtained by diluting the stock solution of AChE possessing the concentration of (0.5 $U \cdot mL^{-1}$) using 20 mM Tris-HCl buffer (pH 7.5). Standard and working solutions of $HAuCl_4.3H_2O$, cysteamine, sodium borohydride ($NaBH_4$), and 4.0 $mmol \cdot L^{-1}$ working solution of ACh were prepared by using Milli Q water (18.25 MΩ · cm) in volumetric flasks. The working solution of TMB with the concentration of 0.4 $mmol \cdot L^{-1}$ was made in 100 mM sodium acetate buffer (pH 4.0) and 95% ethyl alcohol was capitalized to make these dilutions of PE (20, 40, 60, 80, 100, 200, 300, and 400nM). All of these solutions and dilutions were kept at 4 °C till further use.

3.2 Instrumentations

Nanodrop One UV-Vis Spectrophotometer (Thermo Scientific, Loughborough, U.K.) was used to perform absorption measurements. Surface charge density (Zeta

potential) and hydrodynamic size (DLS) were calculated with a zeta sizer (Malvern Zetasizer, Nano ZS-90, U.K.). CytoViva hyperspectral imaging system (CytoViva, Auburn, AL, USA) was employed to get darkfield microscopy of C-AuNPs, morphological studies (TEM) were conducted with the help of JEOL TEM 2100 LaB_6 thermionic gun TEM at Material Research Laboratory (MRL)-UIUC.

3.3 Synthesis of C-AuNPs

Cysteamine capped gold nanoparticles (C-AuNPs) were synthesis by adopting the methods of (S. Ren et al., 2015) with necessary modifications. Briefly, 40 mL of 1.42 mM solution of $HAuCl_4.3H_2O$ was sonicated for 5 minutes and mixed with 400 µL of cysteamine solution at a concentration of 213 mM, followed by continuous stirring at 500 rpm for 20 minutes in an amber flask. Then 10µL $NaBH_4$ solution concentration of 10 mM, was added and kept at constant stirring for 30 more minutes at room temperature. To remove the unreacted species and unbound cysteamine ligands from colloidal C-AuNPs, the solution was centrifuged at 12000 rpm for 20 minutes at room temperature, the supernatant was removed, and the pellet was re-suspended in Milli Q water (18.25 MΩ· cm). After the confirmation C-AuNPs through UV-Vis, the colloidal solution was kept at 4°C to avoid aggregation. The synthesized C-AuNPs were characterized by the help of UV-Vis, Zeta Potential, Darkfield, DLS, and TEM.

3.4 Characterization of C-AuNPs

3.4.1 UV-spectrophotometer analysis

The spectrophotometric analysis of synthesized nanoparticles was performed at a range of 200 to 800 nm at room temperature with the help of the Nanodrop One spectrophotometer. Baseline correction was done by using Milli Q water as a blank reference. 2.0 µL of the sample was placed on the micro-volume pedestal of the Nanodrop for the ultraviolet-visible (UV-Vis) absorbance measurements.

3.4.2 Zeta potential (ξ) and Dynamic light scattering (DLS) measurements

Zetasizer Nano ZS90 (Malvern) was used to measure the electrokinetic potential of the colloidal systems (zeta potential (ξ)) and average hydrodynamic diameters were determined by taking a mean of at least three measurements in series.

Zeta potential was performed by putting a sample colloidal solution to a zeta sizer cell (Malvern Folded Capillary Cells) that contains two gold-plated copper electrodes. The solvents were corrected for refractive index, dielectric constant, and viscosity. After a voltage was applied to the electrode, the particles had moved toward the electrode with the opposite charge. A Doppler technique was used to measure the particle velocity as a function of voltage. With DLS the measurement of the size was performed by filling a quartz cuvette with the sample that was corrected for viscosity and refractive index for Milli Q Water. Laser light was used to illuminate the sample and scattering in the beam of light was detected on the photon detector. It took about 2.0 minutes to optimize the measurement conditions and to stabilize the temperature of the sample around 25°C. For the hydrodynamic diameter, and zeta potential analysis approximately 5-10 runs of 20 cycles were measured for each sample, three replicates were measured, and their average values were reported.

3.4.3 Darkfield microscopy

To make a sample for darkfield analysis of C-AuNPs, a drop of the nanoparticle suspension was placed on a sterile glass slide and covered with the coverslip and placed at room temperature to settle down and dry. Then slides were studied under the magnification power of 40x. In the darkfield apparatus, a special disc was present which blocked the illumination so that only oblique rays could reach the sample under study. The light was directed with an angle so the light did not fall directly on the surface of the objective. In this way dark picture containing bright points was obtained due to the scattering of the light by the samples, representing the presence of the sample. Resultantly darkfield imaging produced the bright image of C-AuNPs against the dark background.

3.4.4 Transmission electron microscopy (TEM)

In TEM imaging a high-energy beam of electrons was being accelerated and a tinny section usually less than 100 nm of the sample was targeted. When a beam of the electrons interacts with the atoms of the sample the transmitted beam of scattered electrons was generated which was being detected by fluorescence on a phosphor screen or envisioned with a camera. The drop-casting method which is known as a

standard method for TEM sample preparation was adopted for the making TEM sample of C-AuNPs. The samples for TEM characterization were prepared by adding a drop of C-AuNPs colloidal solution on a carbon-coated copper grid. After 5.0 minutes the excess of the solution was absorbed with filter paper and the grid was left to dry at room temperature overnight. Higher magnifications were applied to visualize/measure the size and morphology of the C-AuNPs via JOEL TEM 2100 operated at 197kV. ImageJ software was used to draw a histogram of these C-AuNPs.

3.5 Absorbance variation (ΔA)

Relative absorbance ΔA ($\Delta A=A_0-A$) was applied during optimization steps, where A_0 was the absorbance at 652 nm in the absence of AChE and A was representing the absorbance at 652nm when the reaction was done in the presence of AChE.

3.6 Optimization of experimental conditions

Optimal experimental conditions for the enzymatic hydrolysis of ACh by AChE and the chromogenic reaction (oxidation) of TMB by C-AuNPs were needed to find before moving to core experiments. The factors involved in the enzymatic hydrolysis of ACh and the chromogenic reaction of TMB were optimized one by one. These include the optimum pH for enzymatic and chromogenic reactions, incubation time for the enzymatic reaction, and the respective concentration of ACh, TMB, and C-AuNPs. The absorbance variation (ΔA) at 652nm was applied to find out the best values for these factors.

3.6.1 Optimization of enzymatic hydrolysis

The preliminary experimentations were done to find the optimum conditions for the enzymatic reaction of AChE. Different experiments were done to find out the optimum pH, incubation time of the reaction, and optimum concentration of ACh which best fit-out for the reaction.

3.6.1.1 Optimization of Tris-HCl buffer pH

The pH is the prime factor to get optimum activity from the enzyme, so the selection of optimum pH was done as a prime step. Optimization of buffer pH for enzymatic hydrolysis of ACh by AChE was done by keeping the other conditions and concentrations constant including AChE (2.0 $mU \cdot mL^{-1}$), ACh (4.0 $mmol \cdot L^{-1}$) and incubation was done for 20 minutes at 37°C. Tris-HCl buffer was used as a reaction

medium, and a pH range from 7.2-8.4 was applied to find out the best pH for the reaction.

3.6.1.2 Optimization of incubation time

Another critical factor besides the pH of the reaction was the incubation time. To find out the optimum incubation time, AChE (2.0 $mU \cdot mL^{-1}$), ACh (4.0 $mmol \cdot L^{-1}$), incubation temp (37°C), and pH (7.6) of buffer were kept constant throughout this experiment. The reaction mixture was incubated for 10-60 minutes at 37°C with 10 minutes intervals and the best incubation time for the enzymatic hydrolysis was selected.

3.6.1.3 Optimization of substrate (ACh) concentration

To find out the optimum concentration of ACh different concentrations of ACh were added to the experiments. All other factors such as the concentration of AChE (2.0 $mU \cdot mL^{-1}$), incubation temp (37°C), Tris-HCl buffer (pH 7.6), incubation time (20 min) were kept constant. Minimum substrate concentration with the maximum product of choline was examined by selecting the range of concentrations from 2.0-10 $mmol \cdot L^{-1}$ of the substrate with an interval of 2 units.

3.6.2 Optimization process for the chromogenic reaction

The chromogenic reaction was done to inspect the enzyme-like nature of cysteamine capped gold nanoparticles (C-AuNPs). To acquire the optimum condition for this reaction, different experiments were done to find out the optimum pH for the reaction, the best concentration of TMB, and the concentration of C-AuNPs.

3.6.2.1 Optimization of pH of Sodium acetate buffer

Different solutions of sodium acetate buffer having pH (3.6, 3.8, 4.0, 4.2, 4.4, 4.6, and 4.8) were capitalized to determine the best pH for this reaction. Other factors for this chromogenic reaction including TMB concentration (0.4 $mmol \cdot L^{-1}$), and C-AuNPs concentration (100 pM) were kept constant. The absorbance variation (ΔA) was monitored at 652 nm against different pH.

3.6.2.2 Optimization of TMB concentration

The concentration range used for the optimization of TMB was 0.2, 0.4, 0.6, 0.8, and 1.0 ($mmol \cdot L^{-1}$), by keeping constant the buffer pH at 4.0 and 100 pM concentration of C-AuNPs.

3.6. 2.3 Optimization of C-AuNPs concentration

Dilutions were made with the help of Milli Q water to find out the effect of C-AuNPs concentration on the oxidation of TMB. The ranges of concentrations of C-AuNPs from 10-120 pM were used. During this optimization reaction pH of the buffer was kept at a 4.0 and 0.4 mmol·L^{-1} of TMB was added in each experiment.

3.7 AChE activity assay

The 50 µL of Tris-HCl buffer of pH 7.6 having a concentration of 100 mM, 25 µL of AChE (2.0 mU·mL^{-1}), and different concentrations of 25 µL ACh were mixed with a micropipette in 500 µL micro-centrifuge tube and incubated for 20 minutes at 37°C. Then 50 µL of sodium acetate buffer (pH 4.0) possessing the concentration of 100 mM, 25 µL of 0.4 mmol·L^{-1} TMB, 25 µL colloidal solution of C-AuNPs in the concentration of 100 pM, and 20 µL of the above reaction mixture were mixed comprehensively. Then UV-Vis spectrum of the resultant solution was measured. The reduction in absorption at 652 nm representing the aggregation effect of choline as an enzymatic product of AChE activity was measured.

3.8 Protocol for OP sensing

Parathion-ethyl (PE) was employed as a candidate OP as an AChE inhibitor. The OPs are neurotoxins, nerve agents, so all the experiments were performed under the fume hood with all necessary protective measurements. The 50 µL of Tris-HCl buffer (100 mM, pH 7.6), 25 µL of AChE (2.0 mU·mL^{-1}), and different concentrations of 25 µL of PE were mixed and incubated at 37°C for 10 minutes. Then 25 µL of ACh having the concentration of 4.0 mmol·L^{-1} was added into all samples, and solutions were incubated for further 20 minutes at 37°C. The chromogenic reaction was done by mixing 50 µL of sodium acetate buffer pH 4.0 (100 mM), 25 µL of 0.4 mmol·L^{-1} TMB, 25 µL of C-AuNPs, and 20 µL from of above solution was mixed with a micropipette. The UV-Vis spectrum of this consequential solution was taken and increased in the absorption at 652 nm directly linked with the concentration of PE.

3.9 Instantaneous oxidation of TMB by C-AuNPs

In 50 µL of sodium acetate buffer pH 4.0 (100 mM), 25 µL of 0.4 mmol·L^{-1} TMB was added then after the addition of 25 µL C-AuNPs having a concentration of 100 pM, the reaction was set to perform at room temperature and the resultant blue-colored product was analyzed from 200-800 nm via Nanodrop.

3.10 Oxidation of TMB under the different combinations of AChE and ACh

To find out the effect of different combinations of AChE and ACh on oxidation of TMB three different reaction mixtures were made by incubating the respective reactant by adopting optimized concentrations and conditions. In 1st reaction mixture equal volumes of C-AuNPs (100nm), TMB (0.4 mmol·L^{-1}), and ACh (4.0 mmol·L^{-1}) were mixed in 50 µL Tris-HCl buffer (pH 7.6). In 2nd reaction mixture, 50 µL of Tris-HCl buffer (100 mM, pH 7.6) and 25 µL of AChE having the concentration of 2.0 mU·mL^{-1} were added in the mixture of C-AuNPs (100nm) and TMB (0.4 mmol·L^{-1}). In another reaction, 50 µL of Tris-HCl buffer (100 mM, pH 7.6), 25 µL of AChE (2.0 mU·mL^{-1}) incubated with 25 µL of ACh (4.0 mmol·L^{-1}) for 20 minutes and then 25, 25 µL, of C-AuNPs (100 nM) and TMB (0.4 mmol·L^{-1}) were mixed. All three resultant products were analyzed on nanodrop for UV-Vis Spectra.

3.11 Aggregation of C-AuNPs under influence of choline

In 50 µL of Tris-HCl buffer (100 mM, pH 7.6), 25 µL of AChE (2.0 mU·mL^{-1}) and 25 µL of ACh were added, then the reaction mixture was incubated at 37°C for 20 minutes. After that 25 µL of colloidal solution of C-AuNPs (100 pM) and 20 µL of the above reaction product were mixed with a micropipette and the resultant product was analyzed via UV-Vis.

3.12 Oxidation of TMB under the influence of choline and PE

In the reaction mixture of 50 µL Tris-HCl buffer (100 mM, pH 7.6) and 25 µL of AChE (2.0 mU·mL^{-1}), 25 µL of ACh (4.0 mmol·L^{-1}) was mixed and incubated for 20 minutes at 37°C. The 50 µL of sodium acetate buffer pH 4.0 (100 mM), 25 µL of 0.4 mmol·L^{-1} TMB, 25 µL of C-AuNPs, and 20 µL from of above solutions were mixed

with a micropipette and the resultant product was examined to study the effect of choline on the oxidation of TMB. To analyze the effect of PE on the oxidation of TMB, 50 µL of Tris-HCl buffer (100 mM, pH 7.6), 25 µL of AChE (2.0 mU·mL^{-1}), and different concentrations of PE (25 µL) were mixed and incubated for 10 minutes at 37°C. Then 25 µL of ACh having the concentration of 4.0 mmol·L^{-1} was mixed into the reaction mixture and incubated for another 20 minutes. Then 50 µL of sodium acetate buffer pH 4.0 (100 mM), 25 µL of 0.4 mmol·L^{-1} TMB, 25 µL of C-AuNPs (100pM) and 20 µL of the above reaction mixture were mixed together in and the resultant product was investigated.

3.13 C-AuNPs aggregation and concentration of PE

Three concentrations of PE (0, 50, and 100 nM) were selected to inspect the influence of diverse concentrations of PE on the aggregation. 50 µL of Tris-HCl buffer (100 mM, pH 7.6), 25 µL of AChE (2.0 mU·mL^{-1}) were added, and these three concentrations of PE were mixed in different microcentrifuge tubes (500 µL) and incubated at 37 °C for 10 minutes. Then 25 µL of ACh (4.0 mmol·L^{-1}) was added to the reaction mixture and incubated for another 20 minutes. After the completion of reaction mixture were added in 25 µL of C-AuNPs concentration of 100pM and resultant product was analyzed for UV-Vis absorption.

3.14 C-AuNPs concentrations and oxidation of TMB

In 50 µL of sodium acetate buffer pH 4.0 (100 mM), 25 µL of 0.4 mmol·L^{-1} TMB were added than 25 µL of different dilutions of C-AuNPs (10, 30, 50, 60, 70, 80, 90, 100, 120 pM) were added to the reaction mixture and resultant product was evaluated at 652nm.

3.15 Detection of PE by the oxidation of TMB

To detect the presence of PE by the catalytic oxidation of C-AuNPs different concentrations (0, 20, 40, 60, 80, 100, 150, 200, 250, 300, 400 nM) of PE were employed. The 25 µL of above-mentioned concentrations were added in the solution of 50 µL of Tris-HCl buffer (100 mM, pH 7.6), 25 µL of AChE (2.0 mU·mL^{-1}) incubated for 10 minutes. After that 25 µL of ACh (4.0 mmol·L^{-1}) was added and the

reaction mixture was incubated for 20 more minutes. Then C-AuNPs (25 µL, 100 pM), and TMB (25 µL, 0.4 mmol L^{-1}) were added to this reaction mixture the resultant product was investigated for UV-Vis absorption.

3.16 The inhibition efficiency

The inhibition efficiency (IE%) of the AChE activity was used as an indicator to calculate the effect of PE on the activity of AChE. The formula which was utilized to calculate the IE% is described below acquired from (Caballero-Diaz, Benitez-Martinez, & Valcarcel, 2017; Korram et al., 2020).

$IE = (F\ (inhibitor) - F\ (no\ Inhibitor))/ (F_0 - F\ (no\ inhibitor)) \times 100\%$

Where

F refers to absorbance intensity at 652nm.

F (no inhibitor) = (AChE+ACh+ C-AuNPs +TMB)

F (inhibitor) = (AChE+PE+ACh+C-AuNPs +TMB)

F_0= (C-AuNPs+TMB)

Where F (no inhibitor), F (inhibitor), and F_0 are the absorbance intensities at 652nm in the UV-Vis spectra from the above-mentioned combinations.

3.17 Selectivity assay

To investigate the selectivity of the devise assay different recent environmental contaminants including cancer-causing and other potential chemical agents were applied. Members of Per- and polyfluoroalkyl substances (PFAS) family including perfluorooctanoic acid (PFOA), perfluorooctanesulfonic acid (PFOS), and GenX were exploited. Other chemicals such as Imidazole (anti-cancer agent), Cobalt (II) Chloride Hexahydrate ($CoCl_2.6H_2O$)-Toxic to the aquatic environment, Potassium osmate (VI) dihydrate ($K_2OsO_4.2H_2O$), Sodium periodate ($NaIO_4$), Manganese(II) sulfate monohydrate ($MnSO_4.H_2O$) and Cupric nitrate $Cu(NO_3)_2$ were capitalized to check the cross-reactivity of the assay. These toxins were added in the higher concentration (100 nM) in the assay elaborated in section 3.9 at the place of PE.

Results

Results

4.1 Synthesis of C-AuNPs

After the completion of all steps for the synthesis of C-AuNPs as explained in chapter 3 sections 3.4 under the heading of "Synthesis of C-AuNPs", the appearance of the wine-red colloidal solution indicates the successful formation of C-AuNPs. The maximum absorbance at 530 nm which is obtained by the UV-Vis spectroscopy confirmed the successful synthesis of C-AuNPs.

4.2 Characterization of cysteamine capped AuNPs

The characterization of the C-AuNPs, including optical (absorptivity), chemical (surface charge), and physical (shape, size) features, were considered to inspect and explore the different features of C-AuNPs.

4.2.1 UV-Visible Spectra

UV-Vis spectroscopy is frequently used for the initial quantitative investigation of colloidal nanoparticles. Spectroscopic analysis in the ultraviolet (UV) and visible (Vis) region is called electronic spectroscopy. In this region of the electromagnetic spectrum, the material when absorbs the photon they get excited and their electrons jump from lower energy orbitals to higher energy orbitals. The absorption or reflection in the visible region (380-700 nm) determines the color of the chemical substance. The UV-Vis absorbance spectra showed in Fig. 4.1 (a) displayed a characteristic peak at 530 nm for the C-AuNPs due to the strong surface plasmon resonance (SPR) of these nanoparticles, which confirmed the successful synthesis of C-AuNPs. The inset diagram is showing the color of the fresh synthesized C-AuNPs appeared wine red. The concentration of the C-AuNPs was calculated to be 7.15×10^{10} nanoparticles·mL^{-1} with the help of the method mentioned by (Haiss et al., 2007). After the initial confirmation of synthesis of C-AuNPs, the colloidal solution was stored at 4°C in an amber flask to avoid aggregation.

4.2.1.1 Stability of C-AuNPs

Long term stability and mono-dispersed nature of C-AuNPs colloidal solution kept at 4°C in an amber flask were evaluated. Colloidal solutions of C-AuNPs may get aggregated during storage because the capping layer of cysteamine may get defected

during synthesis due to slight variations in stirring time, darkness, and temperature. The presence of contamination in glassware and water also leads to induce the defect in the capping layer. The C-AuNPs are regularly monitored via UV-Vis and disposed-off if the stability of these C-AuNPs was considered not sufficient and possess defected layer of cysteamine. As indicated by Fig. 4.1 (b), no prominent variations in the SPR bands were appeared even after the 7^{th} days of synthesis of C-AuNPs confirm the stability of C-AuNPs.

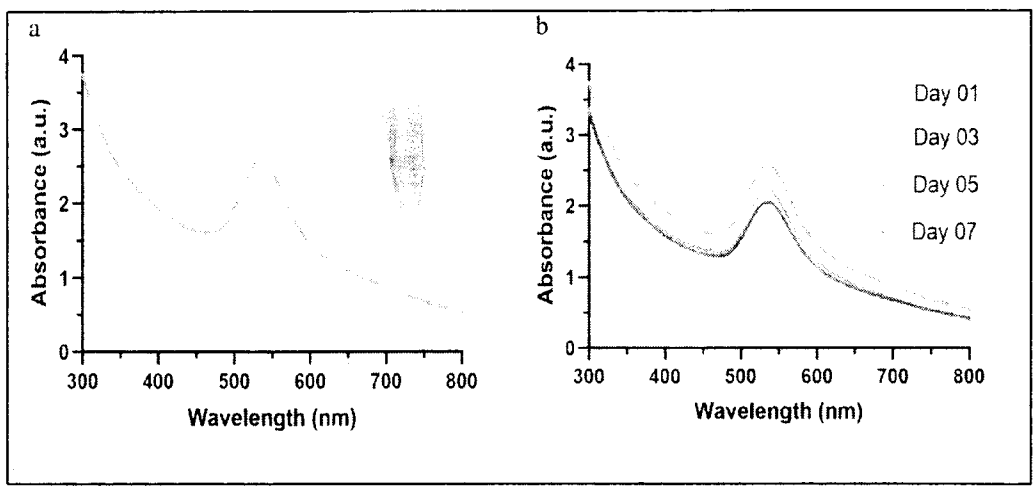

Figure 4.1 (a) UV-Vis of C-AuNPs indicating maximum peak at 530 nm. The inset diagram indicates the corresponding color of C-AuNPs. (b) UV-Vis was taken on different days confirming the stability of colloidal C-AuNPs.

4.2.2 Zeta-potential measurements

Time by time UV-Vis analysis indicated that these nanoparticles are stable (at 4 °C) and do not show any sign of aggregation. To further confirm the stability of these particles Zeta-potential of these nanoparticles was measured. It is a simple analysis that is a key indicator of the stability of colloidal suspensions. Higher values of ZP on both sides of zero indicate the stability of nanoparticles and ensure the resistance of aggregation of these particles. Results obtained from ZP measurements of C-AuNPs as shown in Fig. 4.2 specified the presence of a highly positive surface charge (+39.4 ± 2.05 mV-an average of 3 readings data). This high value not only refers to the monodisperse colloidal C-AuNPs but also designates the occurrence of amine groups on the external surface of these NPs. Cysteamine which is enriched with amino groups was added as a capping agent in the synthesis, and this high positive ZP value

confirms the presence of cysteamine as a capping agent. Appendix 1 contains the detailed figures of ZP.

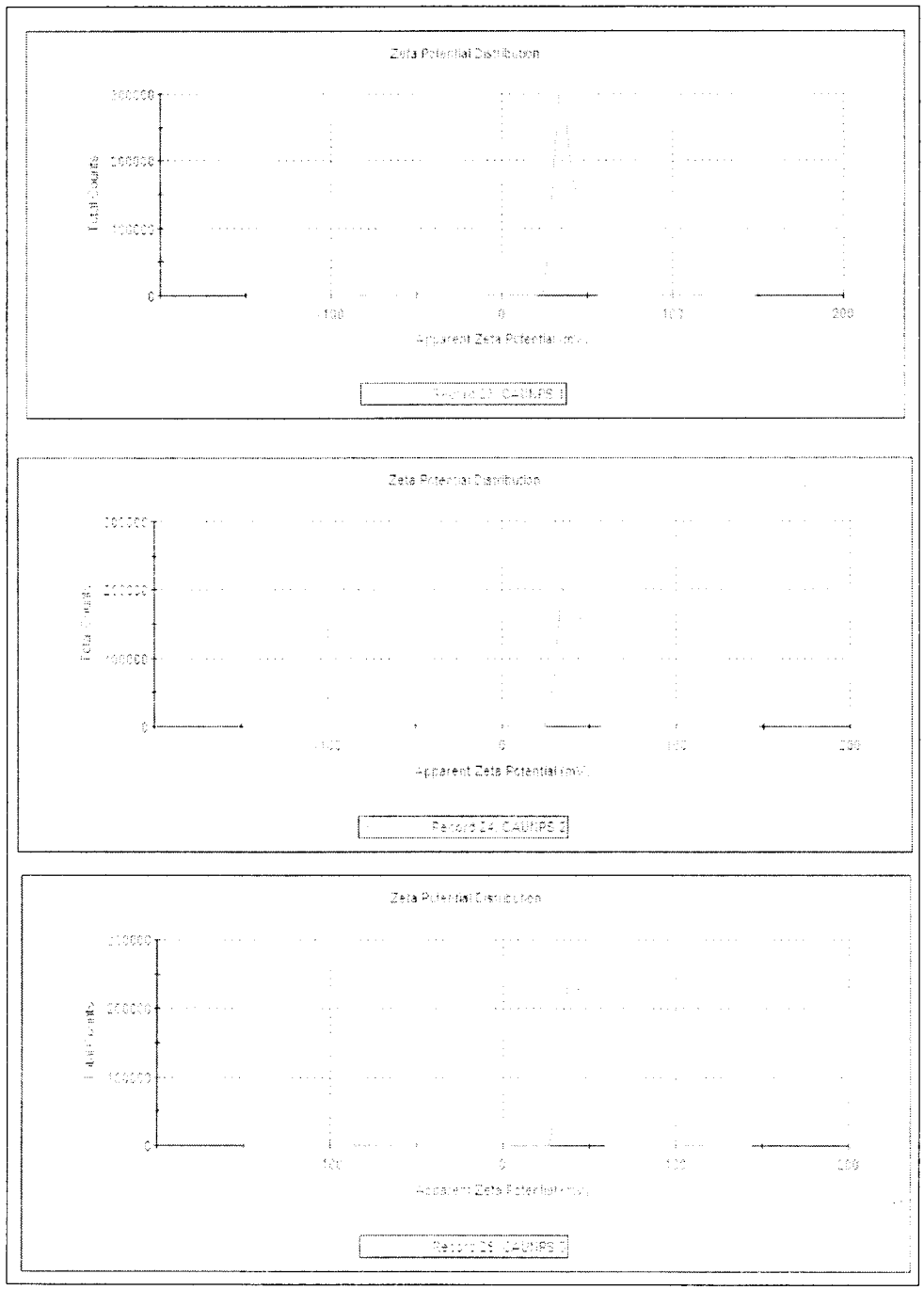

Figure 4.2 Zeta Potential of Colloidal C-AuNPs confirming the presence of high surface charges which advocates the dispersed nature of these nanoparticles.

4.2.3 Darkfield microscopy

Darkfield microscopy was done to further confirm the non-aggregated and dispersed nature of C-AuNPs. This kind of microscopy is ideal to illuminate unstained samples because in this method test sample particles appear bright and the background appears dark black. Another advantage of darkfield is it produced images with better resolutions as compared to bright field imaging. Due to these advantages, dark field analysis was done to study the scattered nature of colloidal C-AuNPs. Images obtained from dark field analysis as shown in Fig. 4.3 strengthened the fact that C-AuNPs were well dispersed, stable, and homogenous, nearly mono-dispersed, and spherical in morphology as well. Additional DF images are provided in appendix 2.

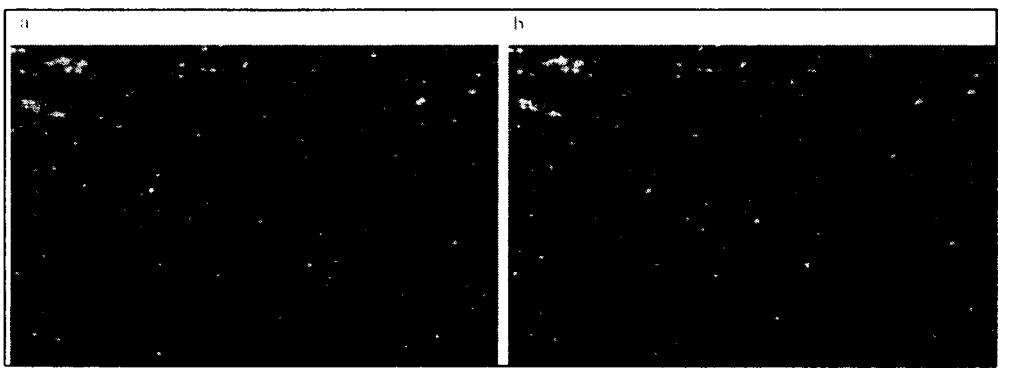

Figure 4.3 Darkfield imaging of C-AuNPs representing the dispersed nature of these nanoparticles

4.2.4 Dynamic light scattering

DLS is a simple, quick, and most prevalent scattering method to get the idea of the size of a monodisperse colloidal solution. This analysis was done to find out the particle size of the colloidal solution of C-AuNPs. In this technique speed of Brownian motion of C-AuNPs was measured which was capitalized to get the idea of the size of C-AuNPs. Fig. 4.4 represents the data obtained from the DLS analysis showing the size of C-AuNPs were 33 nm. The calculated size was the size of hydrated and dynamic particles that why the diameter obtained via DLS is called "hydrodynamic diameter. Detailed DLS diagrams are presented in appendix 3.

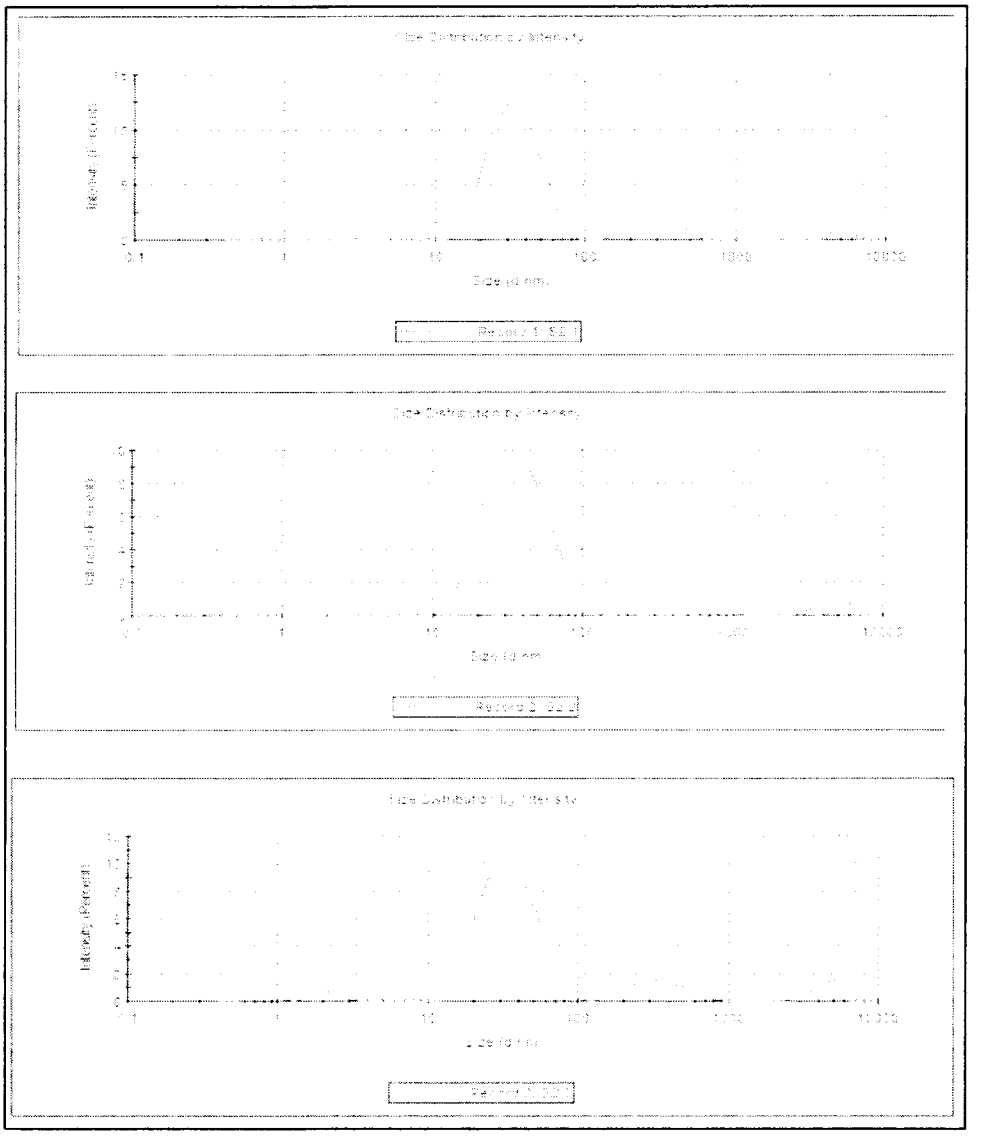

Figure 4.4 DLS of colloidal C-AuNPs showing that the average sizes of these nanoparticles are 33 nm.

4.2.5 Transmission electron microscopy

Transmission electron microscopy (TEM) was done to study the size, morphology, and size distribution of C-AuNPs. TEM measurements were used to create size distribution histograms of the C-AuNPs cores. TEM image revealed that C-AuNPs appeared approximately spherical, possessing a nearly homogenous size and with a high level of agglomeration. During the TEM sample preparation dropping and air-drying of NPs on TEM grid cause the sudden variation in the surrounding which leads

to the agglomeration of NP. The mean diameter obtained via TEM image analysis was 13.24 nm which is less than the size estimation of DLS because of the presence of cysteamine layer and associated molecules. The TEM provided only the size of the core and the capping layer was not included in diameter. The capping layer (cysteamine layer) was not visible under electron microscopy due to its very low electronic density. A few more TEM images of C-AuNPs are provided in appendix 4.

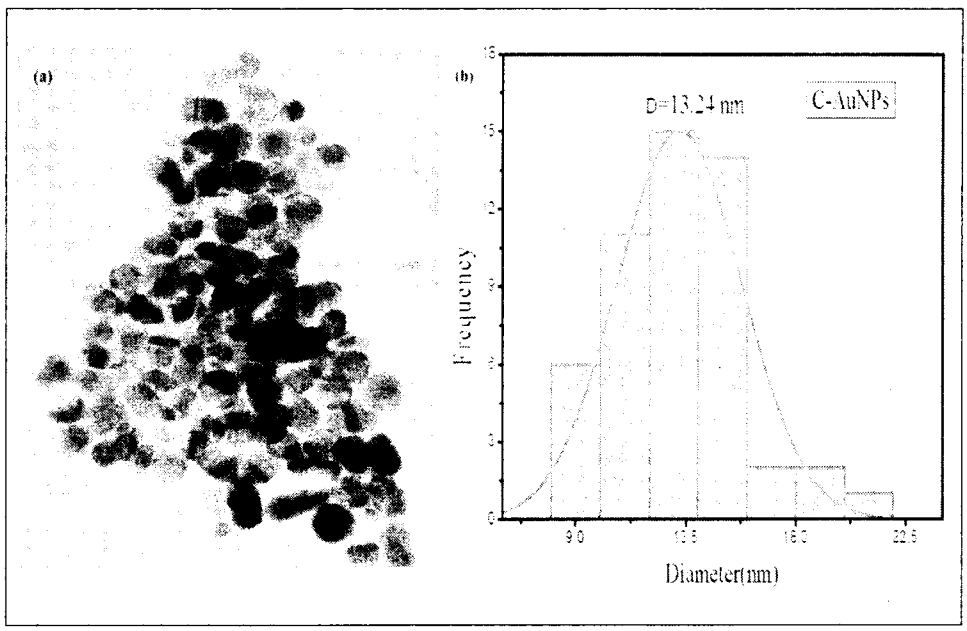

Figure 4.5 (a) TEM images depicting spherical morphology and agglomerated nature of C-AuNPs (b) Size distribution histograms for C-AuNPs denoting an average size of core C-AuNPs as 13.24 nm.

4.3 Optimization studies

Before moving to establish the assay for the sensing of the analyte with the help of the proposed colorimetric sensing system few factors need to be optimized to get the best and sensitive results with minimum concentrations of different chemicals and reagents. As this devised sensing protocol is based on two sorts of chemical reactions i.e. enzymatic hydrolysis of ACh by AChE and chromogenic reaction of TMB by C-AuNPs so all different chemical reagents, pH, and incubation time were optimized one by one.

4.3.1 Optimization of Enzymatic hydrolysis

For the optimization of enzymatic hydrolysis three factors including the pH of the buffer, incubation time, and concentration of the substrate were optimized. To calculate the ΔA to find the optimum conditions of enzymatic reaction of following conditions of the chromogenic reaction were kept constant (Sodium acetate buffer pH 4.0, TMB concentration 0.4 mmol·L^{-1}, C-AuNPs concentration 100 pM). To increase the chances of certainty each experiment was repeated three times.

4.3.1.1 Optimization of pH

As shown in Fig. 4.6, while moving from pH 7.0 to 8.4 the relative absorbance (ΔA) increased initially and maximum ΔA was observed when the Tris-HCl buffer having a pH of 7.6 was present as a reaction mixture. Further increase in pH leads to the decrease in the activity of the enzyme hence pH 7.6 was considered as the optimum pH for upcoming experiments.

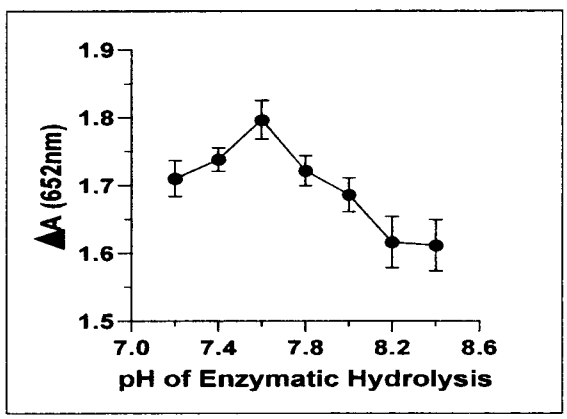

Figure 4.6 Enzymatic hydrolysis of ACh was noted to be the best at a pH of 7.6- Error bars represent the standard deviation from three replicates.

4.3.1.2 Optimization of incubation time

The ΔA at 652 nm indicates that after 20 min of incubation, the maximum product is obtained as shown in Fig. 4.7. Further extension of the incubation time did not affect the concentration of choline considerably since the peak stabilized. Hence 20 minutes was selected as the incubation time for maximum choline production.

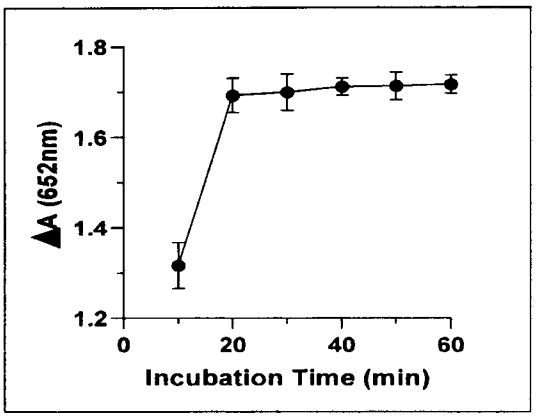

Figure 4.7 Selection of optimum incubation time- Error bars represent the standard deviation from three replicates.

4.3.1.3 Optimization of substrate concentrations

The minimum substrate concentration with the maximum product of choline was examined by selecting the range of concentrations from 2 to 10 mmol·L^{-1} of the substrate with an interval of 2 mmol·L^{-1}. A concentration of 4.0 mmol·L^{-1} of ACh was found to be the optimal concentration as shown in Fig. 4.8 and used as a standard concentration in the rest of the experiments.

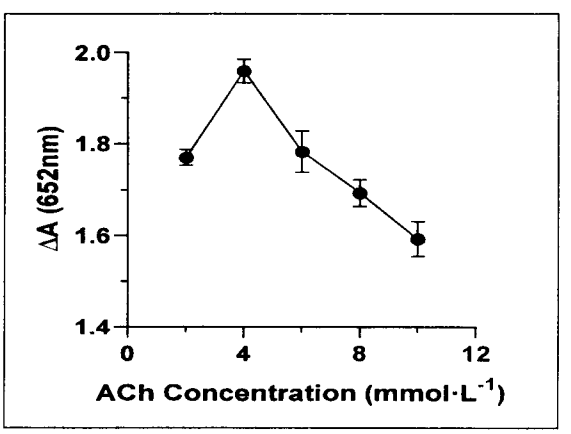

Figure 4.8 Maximum ΔA at 652 nm was obtained with a 4.0 mmol·L^{-1} concentration of ACh. Error bars represent the standard deviation from three replicates.

4.3.2 Optimization steps for the chromogenic reaction

The chromogenic reaction was conducted to assess the catalytic power of the C-AuNPs. To determine the optimum condition for the reaction, different experiments were performed to determine the optimum pH, the best concentration of TMB, and

the concentration of C-AuNPs. Sodium acetate buffer was used as the reaction medium for the chromogenic reaction. To calculate ΔA of chromogenic reaction optimization, data for enzymatic hydrolysis was also needed which was obtained by using the following concentrations AChE (2.0 $mU \cdot mL^{-1}$), ACh (4.0 $mmol \cdot L^{-1}$), incubation temp (37°C), Tris-HCl buffer (pH 7.6), incubation time (20 min).

4.3.2.1 Optimization of pH of the chromogenic reaction

It was witnessed that the reaction produced the maximum ΔA at 652 nm when the pH of the Sodium acetate buffer was 4.0 (Fig. 4.9). Hence, the 4.0 pH was employed as a standard pH for all chromogenic reaction-based experiments. To rule out the possibility of error the experiments were repeated three times.

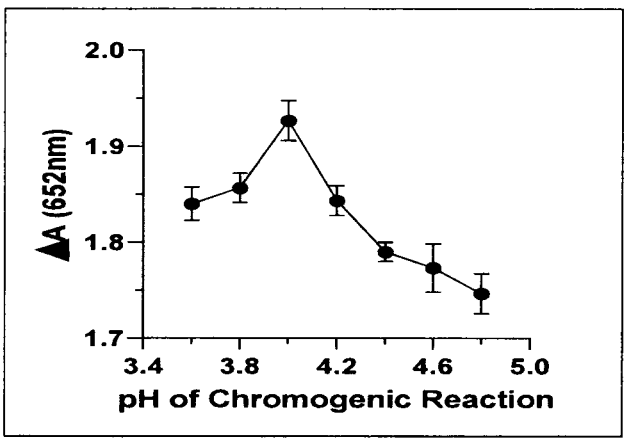

Figure 4.9 The effect of pH on chromogenic reaction. The optimum ΔA of the chromogenic reaction was at a pH of 4.0. Error bars represent the standard deviation of three replicates.

4.3.2.2 Optimization of TMB concentrations

The concentration of 0.4 $mmol \cdot L^{-1}$ provided the optimal results as represented in Fig. 4.10. A concentration lower than 0.4 $mmol \cdot L^{-1}$ was not enough to complete the oxidation of TMB, and a different chromogenic product was obtained (Di-imine formation peak). Hence, for all experiments with chromogenic reactions, 0.4 $mmol \cdot L^{-1}$ of TMB was added.

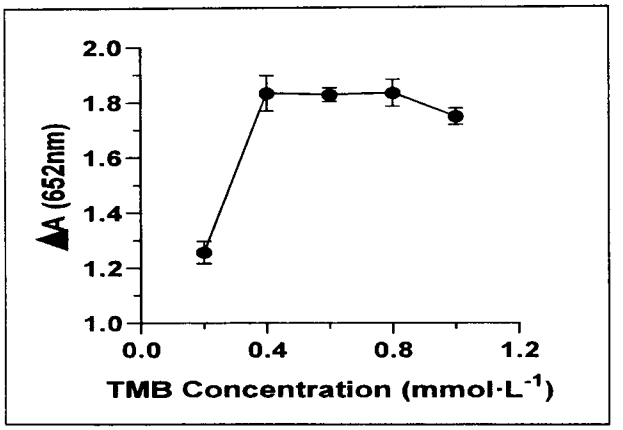

Figure 4.10 The outcome of TMB concentrations on chromogenic reaction. The maximum ΔA of the chromogenic reaction was noted at 0.4 mmol·L^{-1}. Error bars represent the standard deviation of three replicates

4.3.2.3 Optimization of concentration of C-AuNPs

It was observed that the concentration of the nanoparticles was directly linked with the oxidation potential of the nanoparticle's probes. Maximum absorbance was obtained at 100 pM further increase in the concentration did not produce any prominent increase in the value of ΔA at 652nm as represented in Fig. 4.11. So, the 100 pM concentration of C-AuNPs was found best for the oxidation of TMB under these conditions. To increase the chances of inevitability each experiment was repeated thrice.

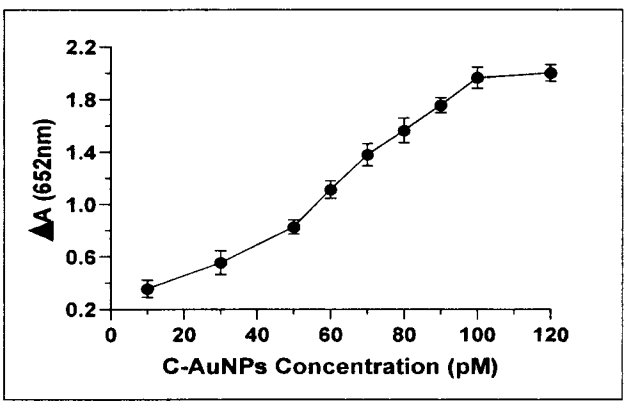

Figure 4.11 The effect of C-AuNP concentrations on chromogenic reaction. The maximum ΔA of the chromogenic reaction was observed at 100 pM concentration of C-AuNP.

4.3.3 The conclusion from the optimization practice

From above mentioned experimental results it was concluded that to get the best output from enzymatic hydrolysis of the substrate (ACh) by the enzyme (AChE) pH of Tris-HCl should be 7.6, and incubation time for 20 min at 37°C is sufficient and minimal concentration of the substrate ACh is 4.0 $mmol \cdot L^{-1}$ produced maximum output. To get the maximum colorimetric signals from chromogenic reactions, the pH of the sodium acetate buffer should be 4.0, the concentration of TMB must be 0.4 $mmol \cdot L^{-1}$ and the concentration of C-AuNPs have to be 100 pM.

So, in all the upcoming experiments which were performed to devise a sensing system for OPs above mentioned optimized concentrations and conditions were capitalized to make the sensor sensitive, economical, and cost-effective.

4.4 Instantaneous oxidation of TMB by C-AuNPs

Fig. 4.12 (a) articulates the peak of C-AuNPs with maxima at 530 nm (red spectra). UV-Vis spectra of colorless TMB is being represented by the purple color peak. However when C-AuNPs were incubated along with TMB, in existence of H_2O_2, C-AuNPs catalyzed the oxidation of the TMB at room temperature inside 10 sec of reaction. Double sharp peaks, 370 nm, and 652 nm (dark blue spectra), and extreme blue colors approved the oxidation of TMB with C-AuNPs, which established that C-AuNPs have the potential to activate an enzyme (L. Liu et al., 2019). This further endorses that C-AuNPs have a strong catalytic power to generate the colorimetric responce with TMB. This catalytic feature of C-AuNPs can be exploited for the detection of any specific analyte. The inset represents the corresponding colors of reaction mixtures. The bar chart in Fig. 4.12 (b) provides the comparison of absorbance peak at 652 nm of TMB and C-AuNPs+TMB. The peak difference of TMB and C-AuNPs+TMB advocates that the presence of C-AuNPs catalyzes the oxidation of TMB.

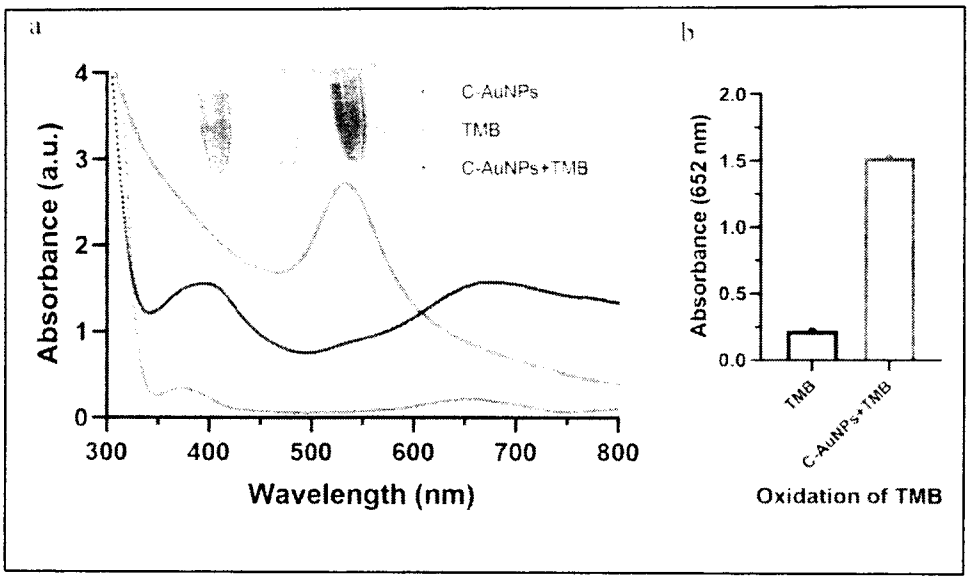

Figure 4.12 (a) The UV-Vis absorption spectra of C-AuNPs, TMB, and C-AuNPs+TMB confirm the formation of oxidized TMB admiring the enzyme-like nature of C-AuNPs. (b) Bar charts represent the absorbance peak at 652nm of TMB and C-AuNPs+TMB.

4.5 Oxidation of TMB under the different combinations of AChE and ACh.

As per the literature existence of AChE and ACh together takes to choline generation (Montali et al., 2020; Shu, Chen, & Wu, 2021; Tvorynska, Barek, & Josypcuk, 2020). To confirm the production of choline in our experimental conditions as well as to study the effect of choline presence on the oxidation of TMB different combinations of AChE and ACh were formed. The results obtained from these combinations are represented in Fig. 4.13. Results obtained supporters that the presence of AChE and ACh leads to the formation of choline because only when both of these chemicals are added to the reaction mixture obvious decrease the in the catalytic ability of C-AuNPs observed, due to the formation of choline which causes the aggregation in C-AuNPs and reduces catalytic power of C-AuNPs many times. This aggregation effect is perceived not only by the decline in the appreance of color of enzymatic product and supported by the obtained UV-Vis spectra deprived of any projecting peaks (spectrum with black color). The bar chart in Fig. 4.13 (b) also advocates that absorbance at 652 nm decreased conspicuously only when both AChE and ACh are present together in the reaction mixture.

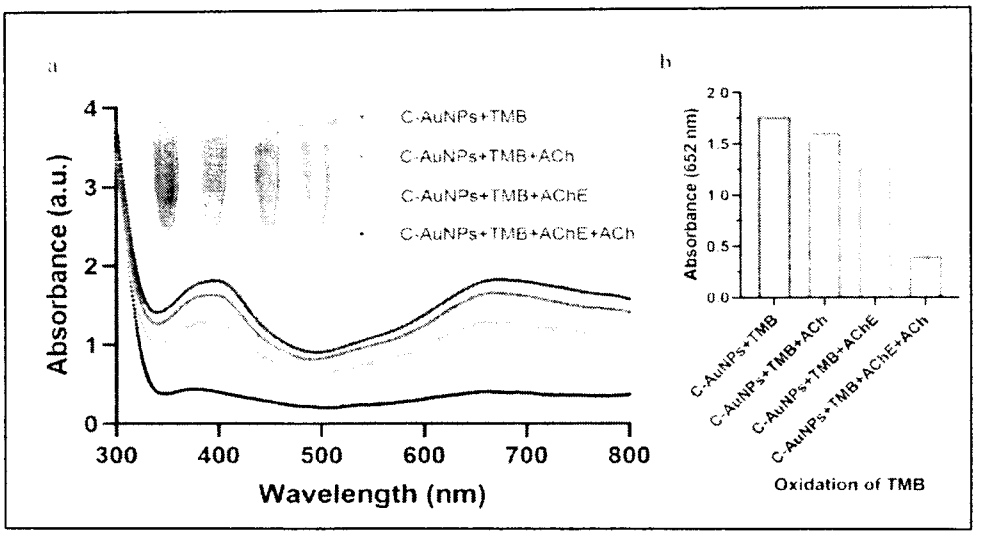

Figure 4.13 (a) UV-Vis absorption spectra confirm that the formation of choline due to AChE and ACh ultimately causes the aggregation of C-AuNPs. Inset diagram showing the corresponding colors of different reaction mixtures. (b) Bar charts representing the absorbance peak at 652nm of different combinations and expressing that absorbance decreases prominently when both substrate and enzyme are present in the reaction mixture.

4.6 Aggregation of C-AuNPs under the influence of choline.

To study the effect of choline (enzymatic product of ACh) on the nature of positively charged C-AuNPs a simple experiment was done. When C-AuNPs were added in the Tris-HCl buffer reaction mixture already containing AChE and ACh the noticeable color change of colloidal solution of C-AuNPs from wine red to light grey was observed. This color change was associated with the aggregation of in C-AuNPs. UV-Vis spectra analysis confirmed that C-AuNPs lose their mono-dispersed nature and get aggregated. Red-shift was also obvious as shown by the black spectrum of Fig. 4.14 (a) which further confirmed the aggregated state of C-AuNPs. Results obtained confirm the presence of choline is causing the aggregation of C-AuNPs. Bar chart of Fig. 4.14 (b) representing the absorbance of C-AuNPs at 530 nm decreased very much in the presence of AChE and ACh, which mean that C-AuNPs was loose its mono-dispersed nature and get aggregated due to the formation of choline.

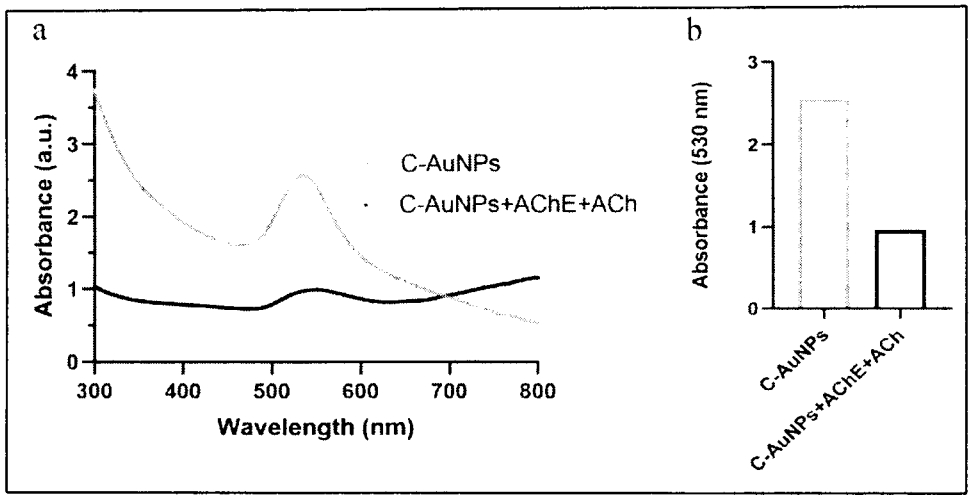

Figure 4.14 (a) Red spectrum represents the UV-Vis of C-AuNPs and black spectrum of C-AuNPs+AChE+ACh with low peak and redshift confirm that the C-AuNPs were being aggregated. (b) The bar chart represents the absorbance at 530 nm and confirms that choline presence causes the aggregation in C-AuNPs

4.7 Oxidation of TMB under the presence of choline and PE

To study the effect of PE on the production of choline and restoration of enzymatic power of C-AuNPs in the presence of PE were investigated and represented in Fig. 4.15. The black spectrum of the diagram (Fig. 4.15) indicates the loss of the catalytic power of C-AuNPs in the incidence of choline. In the presence of PE less hydrolysis of ACh due to the inefficacy of AChE which resultantly produced less concentration of choline. Less choline means a reduced aggregation of C-AuNPs which eventually produced stronger catalytic activity of C-AuNPs, and brighter colorimetric signals have been obtained. Bar chart 4.15(b) validates that the presence of PE restores the nanozymic power of C-AuNPs.

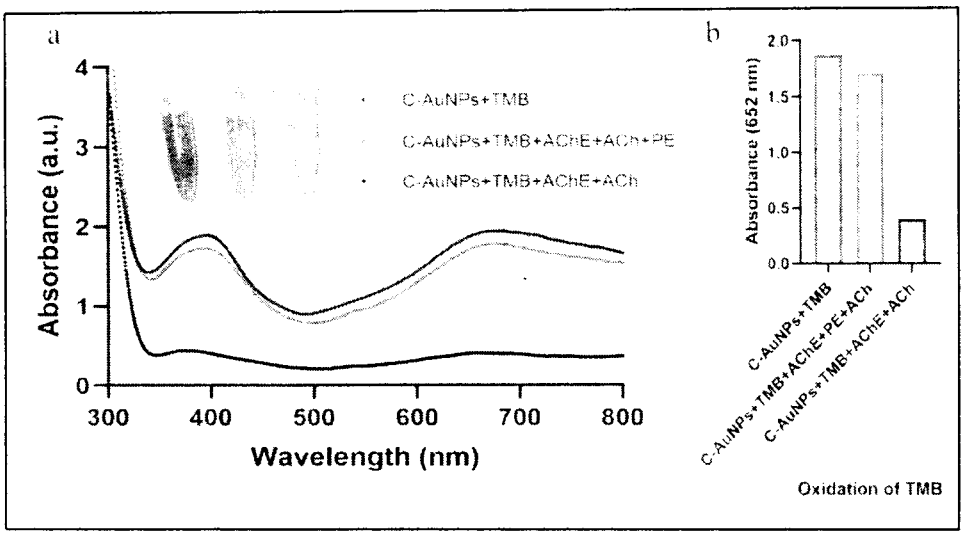

Figure 4.15. UV-Vis spectra in the presence and absence of PE. PE presence leads to the restoration in the catalytic activity of C-AuNPs (blue spectrum) (b) Bar chart demonstrates that the presence of PE restores the nanozymic power of C-AuNPs, and absorbance at 652 nm was very high when PE was present in the reaction mixture.

4.8 C-AuNPs aggregation and concentrations of PE

Results obtained from the experiment to study the effect of different concentrations of PE on the monodisperse nature of C-AuNPs advocated that an increase in the PE concentration had positive effects on the enzymatic activity of C-AuNPs. The presence of a higher concentration of PE induced more blockage of AChE and ultimately reduced choline production. Below, Fig. 4.16 (a) indicates that with the increase in the concentration of PE, the UV-Vis absorbance of increases, which suggests the decrease in the aggregation of C-AuNPs. Redshift was observed which was the indication of aggregation of C-AuNPs by the existence of choline. According to Fig. 4.16, (b) absorbance at 530 nm is higher when PE is present at 100 nM concentration as compared to when PE was added at 50 or 0 nM concentrations.

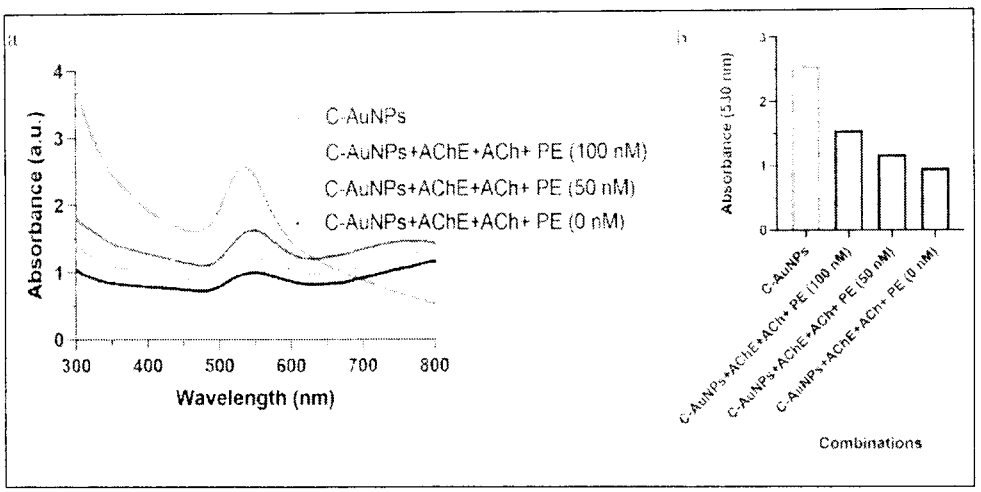

Figure 4.16 (a) The presence of a higher concentration of PE reduced the aggregation of C-AuNPs. (b) Absorbance peak at 530nm provides the comparison of aggregation effect of different concentrations of PE, representing that at 100 nM concentration of PE has to batter absorbance in comparison to lower concentrations of PE.

4.9 Concentration of C-AuNPs and oxidation of TMB

Correlation between C-AuNP concentrations and the catalytic oxidation of TMB was considered and a direct association was observed between the NPs concentrations and oxidation of TMB. The greater the concentration of C-AuNPs, the higher the absorbance (ΔA) was witnessed. Fig. 4.17 (a) illustrates a direct relationship between C-AuNPs and the oxidation of TMB. The inset diagram represents the absorbance spectra of oxidized TMB with the addition of different concentrations of C-AuNPs indicates that a higher concentration of C-AuNPs produces the brighter product with higher oxidation spectra for oxidized TMB.

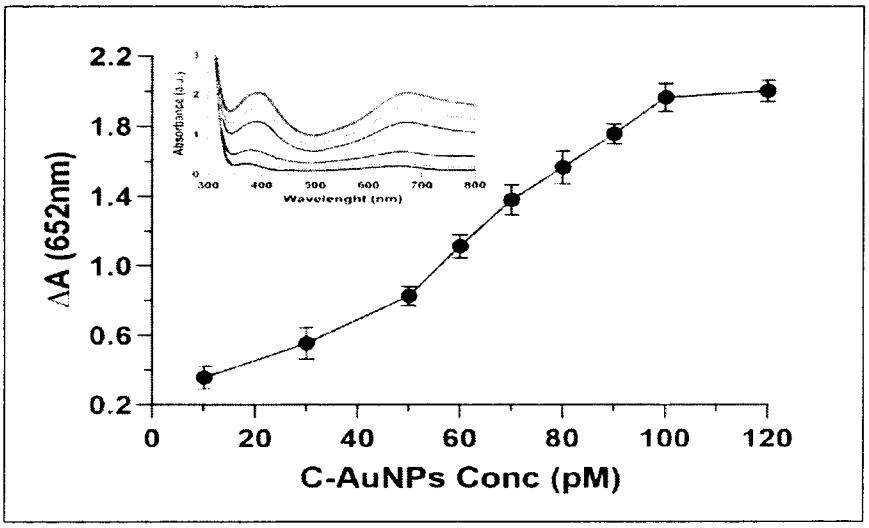

Figure 4.17 Explain the catalytic activity of C-AuNP increasing with increasing concentrations. Inset presenting the UV-Vis spectra of C-AuNPs and TMB with growing concentrations of C-AuNPs.

4.10 Detection of PE by the oxidation of TMB

To detect the presence of PE by the catalytic oxidation power of C-AuNPs different concentrations of PE were incubated with AChE. At the end of incubation time, other reagents such as ACh, C-AuNPs, and TMB were added to this reaction mixture. Consequently, a inhibited quantity of choline was produced with the increasing concentrations of PE because a regular inhibition pattern of AChE was perceived, and henceforward better oxidation of TMB by C-AuNPs was observed which is clear from the absorbance spectra of Fig. 4.18. The inset diagram represents the colorimetric variation in the oxidation product of TMB under the different concentrations of PE. From the inset Fig. 4.18, it is obvious that the C-AuNPs+TMB sensing system can differentiate the different concentrations of PE which can be witnessed by the unaided eye.

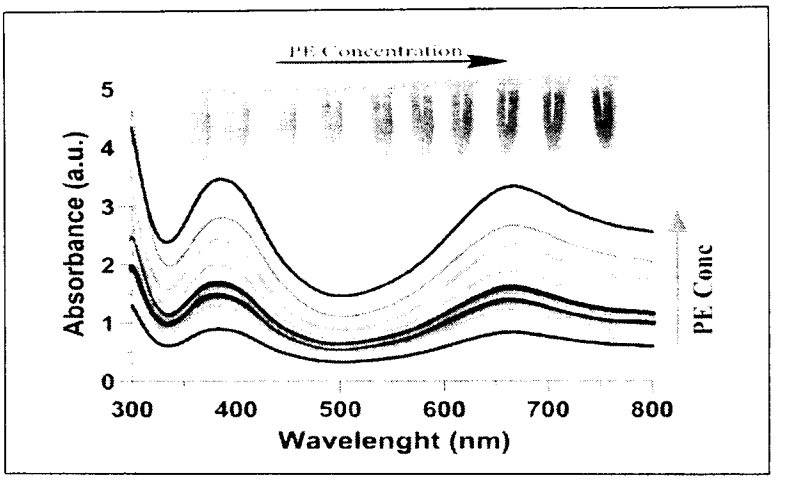

Figure 4.18 UV-Vis absorption spectra of AChE+ACh+C-AuNPs+TMB plotted with growing concentrations of PE (0-400 nM). The increase in PE concentration leads to less aggregation of C-AuNPs thus a stronger catalyzed colorimetric reaction with deeper color from oxidized TMB was observed. The inset shows the color of the corresponding reaction mixtures.

4.11 The inhibition efficiency

The inhibition efficiency (IE%) of AChE was measureable in the tested range between 20-400 nM concentrations as represented in Fig. 4.19. The inhibitor displayed a linear correlation in the range between 40-320 nM, which is in covenant with the recently reported methods (Sun et al., 2018; Yan et al., 2017). The limit of detection of the C-AuNPs+TMB assay is 20 nM, which is superior than numerous earlier reports (Lan et al., 2012; X. Li et al., 2018; P. Wang et al., 2016; Yan, Li, Wang, et al., 2015). The IE (%) was calculated for different concentrations, and it was noted that with an increase in the concentration of the PE, a more and higher decrease in the activity of AChE was observed. The 400 nM concentration of PE resulted in a 65% reduction in the activity of AChE.

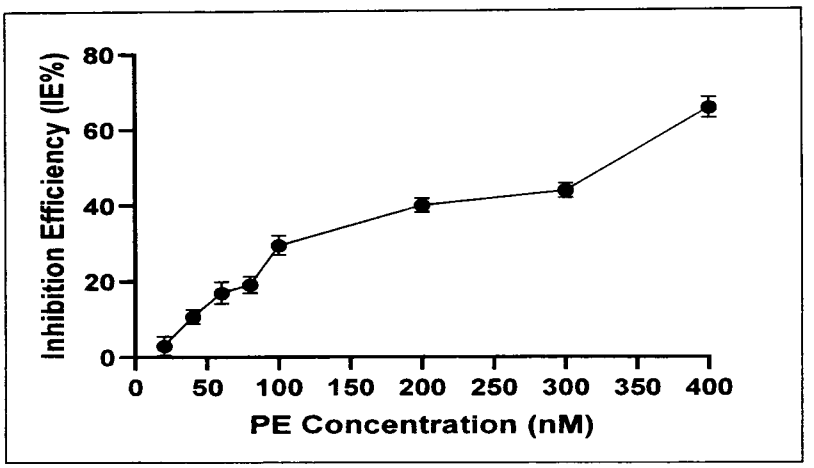

Figure 4.19 Inhibition efficiency of PE on AChE activity. The inhibition of AChE enhanced with increasing concentrations of PE.

4.12 Selectivity assay

The C-AuNPs+TMB biosensing system was devised to detect the presence of OP toxins from the environmental samples, so it was probable that the sample may have diverse kinds of toxins and chemicals which may lead to falling results. So, to check the selectivity of the proposed assay it was necessary to check the cross-reactivity of the proposed assay. The graph made with the help of data which is obtained from this experiment is shown in Fig. 4.20 confirms that none of these chemicals induce the blockage in the activity of AChE and no one reduced the hydrolysis of ACh as to the level of PE. None of these toxic compounds convinced the equivalent colorimetric response up to the extent of PE. These outcomes designated that the probe is accurate and specific enough to monitor the PE selectively with high precision and reliability.

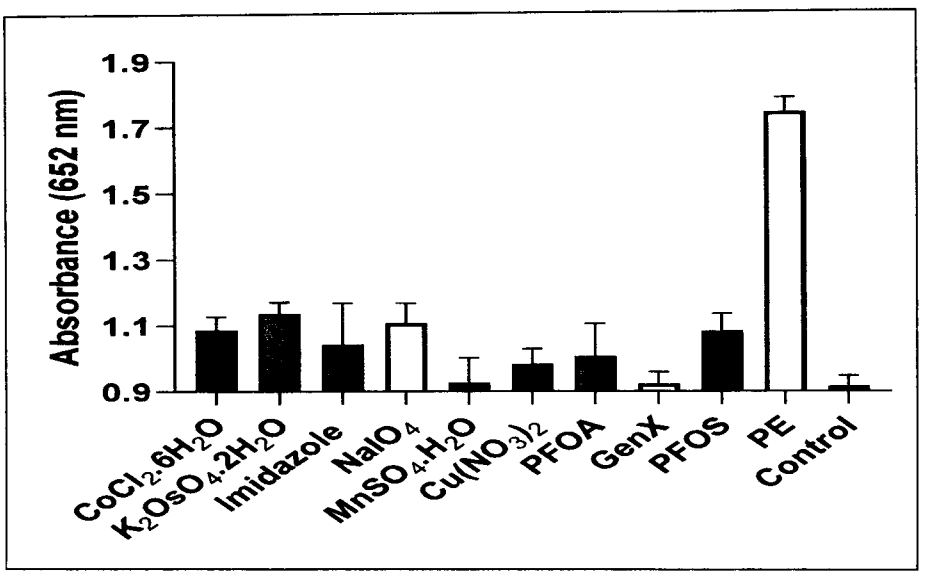

Figure 4.20 The selectivity assay of the developed sensing system towards PE, oncogenic compounds, and other contaminants at a wavelength of 652 nm, advocating high selectivity of the C-AuNPs+TMB system.

Discussion

Discussions

In advanced agricultural practices, various mediators and enhancers including monoculture farming, use of inorganic fertilizer, improvement of irrigation systems, pest control by the help of chemicals, and genetic manipulation of crop plants have been applied extensively to increase the per hector production of agricultural products. Out of these practices use of chemical agents such as pesticides (insecticides, herbicides, bactericides, fungicides, etc.) is frequent to protect the crops from the damages caused by the pest. Uses of organophosphate (OP) based pesticides are very common all over the world (Adeyinka et al., 2018; Ballantyne & Marrs, 2017; Eskenazi et al., 2014; P. Singh & Prasad, 2018; Yadav et al., 2017). The presence of very small quantities of OPs can induce ecological risk and even irreversible damage to living beings, due to the neurotoxic natures of OPs which is well documented in the literature (Aroniadou et al., 2020; Y. Chen, 2012; Figueiredo et al., 2018; Guignet & Lein, 2019; Pereira et al., 2014; Richardson et al., 2019; Tsai & Lein, 2021). Therefore, rapid, real-time, sensitive, and selective monitoring of these pesticides are essentials to control it's over usage and protect the natural environment from their lethal effects.

Different conventional analytical methods (Bastiaensen et al., 2018; Bazrafshan et al., 2017; Farajzadeh et al., 2016; Ottavio et al., 2017) and biosensing systems (Cui et al., 2018; Y. Li, Zhao, Shi, Han, & Xiao, 2017; Nagabooshanam et al., 2020; P. Zhang et al., 2019) have been reported to keep a check on the concentration of these OPs compounds in different sources including water, soil, and food samples. Among these biosensing systems, colorimetric-based sensing protocols provide a detection system that does not need any analytical device, and readouts can be observed by the naked eye (Cha et al., 2020; Qi, Chen, Xiu, & Hou, 2020; L. Wang et al., 2020). To take the advantage of colorimetric biosensing system a novel C-AuNPs+TMB based biosensor is devised. The proposed detection system of OP reported in this dissertation is the explanation of an enzyme-based colorimetric method that exploited the nanozyme characteristics of cysteamine capped gold nanoparticles (C-AuNPs).

To get the proposed objectives of this dissertation the nanomaterial should have enzyme-mimic features and be able to produce some definite colorimetric response

with a chromogenic agent. Additionally, the nanomaterial should respond differently in functional and non-functional states of AChE. To search for a nanomaterial that holds these characteristics preliminary experiments were performed. Different nanomaterials such as citrate-AgNPs (Fang et al., 2005), borohydride-AgNP (Van et al.,2012), Gold-Chitosan nano-composites (H. Huang et al., 2005) were synthesized by adopting reported protocols. But none of these nanomaterials were able to produce the required results. Then negatively charged AuNPs were synthesized with the help of the method elaborated by (Fahimi-Kashani & Hormozi-Nezhad, 2016). This citrate capped AuNPs can differentiate between functional and non-functional AChE as they get aggregated when AChE was fully functional and remain in mono-dispersed form when AChE is in a non-functional state. But these AuNPs could not have enough nanozymic features and could not produce sufficient colorimetric variations with tested chromogens.

After that more digging of literature was done and it was found that positively charged MnO_2 nanosheets have the nanozymic features as they can catalyze the oxidation of TMB. So, with this in mind positively charged cysteamine capped AuNPs were synthesized by adopting a reported method (S. Ren et al., 2015). Initial experiments indicate that these C-AuNPs have required potentials that can be exploited for the development of a biosensor for the monitoring of neurotoxin with acceptable sensitivity and selectivity. So, C-AuNPs were carefully chosen for the development of a detection system for the monitoring of OPs.

Characterization of nanomaterial is the prime step after the synthesis of the nanostructures. Numerous techniques have been applied to characterize the size, morphology, crystal structure, surface charge, and other physical properties of nanoparticles. Every characterization technique has diverse strengths and limitations so the adaptation of a suitable technique to get enough information of the nanoparticle is a complicated choice. To get the full spectrum of characterization often multiple characterization approaches are applied altogether (Mourdikoudis et al., 2018). The main parameters for the characterization of C-AuNPs were size, shape, degree of aggregation, and the surface charge has been comprehensively inspected as the first step after the synthesis C-AuNPs.

UV–Vis spectroscopy is one of the most imperative and commonly applied easy, fast and sensitive methods for confirming the successful formation of the metal nanoparticles (Martinez et al., 2012). A qualitative theory on the shape and size allocation of nanoparticles can be achieved from the position, width, and shape of the SPR band obtained by UV-Vis (X. Huang & El-Sayed, 2010). A single narrow SPR band indicates the spherical monodisperse nanoparticles, although broadband indicates the wide distribution of particle sizes. The surface plasmon resonance (SPR) obtained by UV-Vis indicates that the maximum absorbance is at 530 nm. The interaction of collective oscillation of electrons presents on the surface of C-AuNPs with electromagnetic radiation results in the SPR absorption peak at 530 nm (Doyen, Bartik, & Bruylants, 2013; Ganapuram et al., 2015) This well-defined SPR wavelength position in this range indicates the spherical nature of C-AuNPs (S. Li et al., 2017; Sobczak-Kupiec et al., 2011).

These results agree with the previous studies where synthesized spherical AuNPs were synthesis by adopting different chemical and biological methods (Ganapuram et al., 2015; Sobczak-Kupiec et al., 2011). The observed SPR peak at 530 nm recommends that the average size of the synthesized spherical nanoparticles is lesser than 40 nm (S. Li et al., 2017; S. Rahman, 2016). While analyzing the structural changes in four different states and structures (primary particles, agglomerated particles, aggregates particles, and agglomerated aggregates) of AuNPs reported that by using UV-Vis spectra different structures of nanoparticles can be differentiated and UV-Vis spectra is a cheap and quick approach to monitor the formation of different AuNP structures (Keene & Tyner, 2011). UV-vis data is further capitalized to determine the concentration of these C-AuNPs with the help of the method elaborated by (Haiss et al., 2007). The concentration found was 7.15×10^{10} nanoparticles·mL^{-1} which is the agreement with the results mentioned previously (S. Rahman, 2016).

In colloidal solutions, the electrokinetic system is termed as zeta potential (ζ). To find out the potential difference between the dispersion medium and stationary layer of the medium attached to the C-AuNPs zeta potential (ZP) analysis was done. It was done to find out the charge-based stability, surface charge, and aggregation state of C-AuNPs. Higher ZP values, either positive or negative, are necessary to ensure stability

and avoid aggregation of particles. The positive or negative sign value signifies whether the positive or negative forces on the surface of the particle are dominant. ZP values greater than 30 mV indicate the monodisperse nature of nanoparticles and the highly charged particles incline to repel each other (Mourdikoudis et al., 2018). The ZP values lower than 5 mV indicate nanomaterials are poly-dispersed and in aggregated form (Mourdikoudis et al., 2018). As the C-AuNPs capitalized here have the ZP value greater than 30 mV (+39.4 ± 2.05 mV) because of the presence of the NH^{3+} group of cysteamine. The presence of this high positive surface charge provides enough electrostatic repulsion among the C-AuNPs which eventually provides the stability to these NPs against aggregation (S. Ren, Li, & Zhang, 2013). So, from the above discussion, it is established that due to the high electrostatic repulsion among these charged C-AuNPs, these nanoparticles are stable and remain to disperse and a mono-dispersed particle, resisted aggregation, and have negligible tendencies to agglomerate.

To further confirm that the mono-disperse nature of C-AuNPs; Darkfield (DF) imaging was performed. It is an optical method with excessive potential in diverse disciplines including biological and nano-biotechnology because it permits identification and quantitative determination of precise components. Optical methods are applied widely because these methods provide direct and reliable observation but rely on the resolution of applied optical systems (Verebes et al., 2013). In bright field imaging objects that can absorb light against a non-absorbing background are studied effectively. But darkfield imaging microscopy considers only the incoming reflected light from the sample (Xiao & Yeung, 2014). So, dark field imaging produces high contrast results for low contrast samples (H. Hu et al., 2010). Different nanoparticles can be differentiated with the help of DF microscopy because this microscopy produces images of a different color for the differently capped AuNPs (Zamora-Perez et al., 2018). The same color red bright dots in DF images of C-AuNPs (Fig.3.3) indicate that only one kind of material is present in my samples. The DF microscopy is ideal to study C-AuNPs because its applications are better for the unstained samples. The DF samples under study appear brightly lit against the dark background. Special kinds of condensers are present in this microscope which scatters the light and light gets reflected off from the specimen at a certain angle.

After the development of the darkfield immersion microscope, initially, it was used to study the single metal particle and estimated the size of these metal particles. Later the method was further developed and successfully applied for the structural analysis of diverse systems (M. Hu et al., 2008). As darkfield can be applied to study diverse materials (Soft and hard matters) so its usage has increased in the research of biological and materials sciences. The intensity of scattering light was being used to obtain the images of the particles so primarily it was hard to locate the extremely small-sized particle but with the application of sensitive absorption techniques, successful imaging of smaller particle have been achieved (Berciaud et al., 2006; Boyer et al., 2002). The thermal lensing detection method was applied to study the spherical gold nanoparticles having the size down to 5.0 nm (Berciaud et al., 2005; Lasne et al., 2006). The hyperspectral darkfield was applied for imaging and characterization of AuNPs at a single-particle level (Patskovsky et al., 2015). AuNPs are strongly polarized so C-AuNPs were good material to study by polarization microscopy.

ZP and DF results established the fact that the colloidal solution of C-AuNPs is well dispersed and non-aggregated form, to get the idea of the size of these colloidal NPs, DLS was done. DLS is a simple and quick measurement that is ideal for the size measurement of colloidal nanoparticles and a very effective method to measure the particle size in the range of approximately 1nm to 10 μm. The information obtained from the fluctuation of scattered light imprints the idea about the particle sizes in the sample. It is a cheap and quick way to measure the functional size of nanoparticles including any opsonization (Keene & Tyner, 2011). In this technique, random movement (Brownian motion) of the suspended C-AuNPs was measured with the help of variation in light scattering. Brownian motion of smaller-sized nanomaterials was much higher than the larger size nanoparticle, so the speed of the motion also acts as an indicator for the size distribution. It is a temperature-dependent process because the viscosity of liquids depends on temperature, viscous liquids retards the Brownian motion.

The Brownian motion of the particle not only depends on the core size of the particles but also on the capping agents. So, the diameter obtained with the help of DLS was

the diameter of particles including the capping agent. That way diameter obtained by DLS is greater than the diameter obtained with microscopy (Malvern, 2012). The mean size of nanomaterials obtained by DLS was about 20% greater than the obtained size of the same particle from TEM. DLS not only provides the data for size distribution also provides the information for the aggregation state of the nanomaterials (Souza et al., 2016).

As DLS analysis was performed in colloidal solution and when nanoparticles are dispersed in water they may get aggregated which leads to the change in the size and surface properties may also alter. As a result, the size obtained via the DLS method may be much higher than the actual size obtained via TEM. Size distribution is also altered in DLS measurements (Manaia et al., 2017). Secondly, the polymer layer is present as a capping agent which appears as a part of diameter in DLS. That is why DLS diameter is greater than TEM diameter. This layer is not detectable in the imaging of TEM because of the low density of the polymer layer. But recant TEM microscopes are capable enough and can differentiate the polymer layer present on the sample if images are clean of artifact and aberrations. The size of DLS includes the core, capping agent, and associated water molecules (Diegoli et al., 2008). TEM only provides the size of core nanoparticles and did not include the size of the capping agent and associated molecules (solvent layer). Due to these reasons the size of dried core C-AuNPs was only 13.24 nm as shown in Fig. 4.5 was much less than the size of nanoparticles in colloidal solutions (33 nm). The difference among the size difference between DLS and TEM results has already been reported (Alexander et al., 2013).

TEM is an electron microscopic technique which is complemented DLS measurements. It is extensively and reliably applied to measure the primary size of nanoparticles (Hondow et al., 2012; Z. Ji et al., 2010; Orts-Gil et al., 2011). It is an excellent tool for the evaluating and characterization of nanomaterial to acquire a quantitative measurement including particle shape, morphology, and size distribution of individual nanoparticle and superstructures (aggregates and agglomerates) because its ultrahigh resolution reaches about 0.07nm whereas the resolution of modern SEM is about 2 nm (Souza et al., 2016).

General requirements of electron microscopy including ultrahigh vacuum and tinny samples make the microscopy hard to achieve method. Besides that, the main issue and the drawback associated with TEM is a sample preparation method for TEM imaging. Typically drop-cast method was adopted for the sample preparation of TEM which induces agglomeration in the sample of nanoparticles (Jiwen Zheng, 2014). During this method, an aliquot of nanoparticle solution is being dropped and then air-dried on the TEM grid (Dutta et al., 2007; Hondow et al., 2012). The characteristics features of NP depend upon the surface chemistry of NP, these characteristics may be altered due to the self-clustering of NP by the result of aggregation and agglomeration. Alterations in the environment of NPs frequently lead, to the formation of aggregates and agglomerates (Keene & Tyner, 2011). This self-association of NP leads to the altered in the surface area of the individual particle so the chemistry of mono-dispersed particles is different from the aggregated NPs (Coccini et al., 2010; Guarise et al., 2005).

Aggregation/aggregate involves permanent changes as the new bonds generated among the two or more interacting NP are non-reversible which leads to the variation in size and morphology of individual particles. On the other hand, when the bond formations are reversible new clusters of NP are called agglomeration/ agglomerate as a result the shape and size of the individual NP remains unchanged (Keene & Tyner, 2011). This is a non-permanent change so-called as just rearrangement of individual NP (Nakaso et al.,2002). Agglomeration of C-AuNPs was clear from Fig. 4.5 (a) but as it a non-permanent change so the size and chemical properties of C-AuNPs were not being disturbed by this agglomeration. The C-AuNPs are overlapping with each other rendering the assembly of the ploy-dispersed NPs represents a large network of small particles which is in agreement with the mono-dispersed NPs shown in TEM scans presented recently (A. Shah et al., 2021). As sample preparation for TEM analysis was done by the drop-casting method, so mono-dispersed NPs are getting interconnected contributing to agglomeration. Evaporation of water from the sample leads to the unexpected agglomeration of the sample on the TEM grid due to surface tension during the air-drying step, though it is a temporary clustering (Nakaso et al., 2002; Jiwen Zheng, 2014), Since these bond formations are reversible, the shape and size of the individual AuNPs remain unchanged (Keene & Tyner, 2011). According to

the histogram Fig. 4.5, (b) the average size of these NPs are only 13.24 nm which shows the application potential of these miniature sizes C-AuNPs since smaller NPs have strong and better activity compared to large size AuNPs (Chang et al., 2019; D. Liu et al., 2014; Turner et al., 2008).

It is the practice of the research community to find optimal working and experimental conditions to get the best outcomes with minimal inputs, before moving toward core experiments. Different research groups consider the optimization of many factors including concentrations of reagents, pH of buffer solutions, and incubation milieus as preliminary experiments for the development of a successful colorimetric assay (F. Wang et al., 2017; Yan et al., 2017). Likewise, to make the C-AuNPs+TMB sensing system more efficient, highly sensitive with minimal cost different factors that is directly and indirectly involved in this sensing platform was optimized one by one.

The pH of the reaction medium is the fundamental aspect of such kinds of colorimetric sensing platforms because it directly affects the efficacy of the sensing system. The variation in the pH alters the expected outcomes that why the pH of the enzymatic reaction was optimized as a first step and found that at alkaline pH (7.0) the C-AuNPs+TMB sensing system produced the best results as shown in Fig. 4.2. Yan and his colleagues selected PBS buffer as a reaction medium and found that the initial increase in pH from 6.0 to 8.5 produced an obvious increase in outputs but further increase in pH induces retarding effects so pH 8.5 is selected as an optimum pH (Yan et al., 2017). As different buffer (PBS) was capitalized as reaction mediums and different nanomaterials were being utilized they got optimum results at slightly basic pH as compared to our finding where at alkaline pH maximum output was obtained. Similarly, PBS buffer at pH 7.4 was found best for the hydrolysis of ATCh (Han & Wang, 2019).

To study the effects of incubation time on the activity of AChE optimization of incubation time was considered by the research groups. It was reported that 30 min incubation time is enough to convert substrate into product further incubation time did not affect significantly (El Alami et al., 2020). In the same way in the C-AuNPs+TMB system, it was found that 20 min incubation time produced the

maximum activity of AChE after that no such increase in the product was found indicating that 20 min incubation is enough as shown in Fig 4.7. Substrate concentration was another factor that was optimized to get the best results from the enzymatic reaction. In one study acetylthiocholine (ATCh) was utilized as a substrate and found that maximum results were obtained at 5.0 $mmol \cdot L^{-1}$ concentration of ATCh (Yan et al., 2017). But here as we cast off different substrates (ACh) and found that 4.0 $mmol \cdot L^{-1}$ of ACh produced maximum ΔA at 652 nm.

The C-AuNPs+TMB sensing system mainly depends on two kinds of reactions e.g. enzymatic reactions and chromogenic reactions so in the same way, a few factors that can influence the output of chromogenic reactions were studied one by one and superlative concentrations and experimental conditions were selected. Acidic pH suites for the TMB oxidation so the reaction medium of lower pH was considered for the optimum output from a chromogenic reaction. Sodium acetate buffer (SAB) was used as a reaction buffer and found that at the 4.0 pH chromogenic reaction produced the best results. The same buffer with pH ranging from 2.5 to 6.0 was applied and reported that TMB was being oxidized maximally at a pH of 4.0, pH lower or higher than 4.0 reduced the output (Sun et al., 2018). It is also reported that C-AuNPs give maximum peroxidase activity (TMB oxidation) at pH 4.0 (Mohamad et al., 2019). At this acidic pH, the C-AuNPs surface has more NH^{3+} groups because in an acidic medium more protons exist. Liang et al. 2013 also selected the best pH for the development of a sensor for OP detection by utilizing TMB as a chromogen and capitalized acetate buffer (pH 5.0). OPs are unstable at higher pH and the half-life of the OP compounds is better at lower pH (Liang et al., 2013). Correspondingly, it was reported that change in the concentration of TMB did not affect the output of the chromogenic reaction of the MnO_2+TMB system (Sun et al., 2018), but in the C-AuNPs+TMB sensing system, the output was being varied by the change in the concentration of TMB. The difference in the chemical nature of both nanoparticles may be the reason for the variance.

The concentrations of nanomaterials were also considered for optimization and reported that a higher concentration of nanomaterials produces better sensing signals (Sun et al., 2018; Yan et al., 2017). A direct connection was perceived between the

NPs concentrations and oxidation of TMB. Higher the concentration of C-AuNPs catalyzed the higher oxidation of TMB, so an appropriate concentration of nanoparticles should be present in the sensing system to get the prominent signals which can be observed with the unaided eye. The variation in the peroxidase-like activity of AuNPs in the existence of different biomolecules (ATP and ADP) and ions (phosphate, sulfate, and carbonate anions) were analyzed and reported that the higher concentration of AuNPs leads to the higher oxidation of TMB. The concentration of AuNPs was applied as a factor to get higher oxidation of TMB (J. Shah et al., 2015). Graphene conjugated-Gold nanoparticles (AuNPs-GO) were applied for the sensing of uric acid and found that a higher concentration of AuNP-GO would increase the number of binding sites which in turn increase the oxidation of TMB (Sanjay et al., 2016). The outcome of the concentrations of nanomaterials on the oxidation of TMB is being also considered and reported that in comparison to low concentration high concentration of nanomaterials has better catalytic power (Sun et al., 2018). A higher concentration of nanomaterial catalyzed more oxidation of TMB and a more obvious, clear, and dark blue product was obtained. Higher oxidation was observed when a higher concentration of nanosheets was applied to catalyze the oxidation of TMB (F. Wang et al., 2017; Yan et al., 2017). So, the higher concentration of C-AuNPs catalysis the oxidation of TMB in a better way and brighter color product with higher peaks at 652 nm was observed during the development of a biosensing system for the OPs.

After optimization of different factors of enzymatic and chromogenic reaction, the peroxidase-like activity of C-AuNPs was established by capitalizing TMB as a typical peroxidase substrate (Cho & Irudayaraj, 2013). The peroxidase-like activity of C-AuNPs was analyzed by incubating C-AuNPs with TMB in presence of H_2O_2. Results obtained as shown in the Fig. 4.8 confirmed that TMB was being oxidized within 10 sec at room temp without any other prerequisites. This prompt oxidation of TMB confirms the peroxidase-like nature of C-AuNPs. The peroxidase-like activity of positively charged AuNPs is being observed and showed that the positively charged AuNPs have strong nature to catalyze the oxidation of TMB at room temp as compared to citrate capped AuNPs having citrate molecules as a capping agent (Jv et al., 2010). This variation in the peroxidase-like activity of positively and negatively charged AuNPs is only due to the properties of

capping agents. The presence of different capping agents alters the surface chemistry of AuNPs which leads to cause variation in the electron transfer process (Mohamad et al., 2019). This timeless peroxidase activity of C-AuNPs without any sophisticated need confirms the potential of the C-AuNPs+TMB system for the development of a quick monitoring assay. C-AuNPs exploited for the detection of OP have enzyme mimic features to catalyze the oxidation of TMB and possess the peroxidase-like activity. Cysteamine-capped nanoparticles have been utilized for colorimetric detection (Bhattacharjee et al., 2014; S. Ren et al., 2015).

To examine the effects of choline on the C-AuNPs+TMB system the possible combinations of the substrate (ACh) and enzyme (AChE) were made to rule out the false-negative results and to confirm that the choline production only inducing aggregation in C-AuNPs. The addition of ACh in AChE solution leads to the formation of positively charged choline and the presence of this positive choline causes the aggregation of C-AuNPs (El Alami et al., 2020). The results reported in chapter 04 section 4.5 demonstrate that choline is successfully produced when both substrate (ACh) and the enzyme (AChE) are present together in the reaction mixture. After all, C-AuNPs are not performing peroxidase activity because C-AuNPs get aggregated due to the presence of choline. The aggregation of C-AuNPs in the presence of choline has already been described (El Alami et al., 2020). Deprotonation of cysteamine get occur due to the influence of pH which is the main reason behind the aggregation of these NPs. Capping agents (amine groups) of C-AuNPs are being deprotonated at alkaline pH (Yujie Ma et al., 2013). An acidic medium carries an excess number of protons but in an alkaline solution absence of protons leads to the deprotonation of NH^{3+} (amine group) (Mohamad et al., 2019). The positively charged choline behaved as a bridge among deprotonated C-AuNPs and leads to the aggregation of these NPs. The aggregated state of these NPs loses its catalytic action and is incapable to catalyze the oxidization of TMB. Depending upon the pH of the medium cysteamine exists in three ionic forms: the positively charged form (cys+), the zwitterionic form (cys-ZW), and the negatively charged form (cys-) (Atallah et al., 2020). It has been reported that when AChE is present along with its substrate and the enzymatic product, it behaves adversely on the TMB oxidation and very low peak at 652 obtained (Y. Wu et al., 2019). The change in the color of colloidal solution of C-AuNPs and redshift in the absorption peak in the UV-spectra due

to this aggregation is reported earlier (Ghosh & Pal, 2007; Rosi & Mirkin, 2005) due to the variation in the plasma coupling between the nanoparticles (Wen-Wen et al., 2014). This is concluded that to produce choline both substrate and enzyme should be present with all other required conditions and the presence of choline inducing aggregation in C-AuNPs.

It is well documented that the presence of OP pesticides leads to the malfunctioning of AChE (El Alami et al., 2020; S. H. Lee et al., 2015). Irretrievable inhibition of AChE has previously been documented in the existence of OPs (Guo et al., 2015; X. Meng et al., 2015). The formation of a covalent bond with the active site (phosphorylate serine residues) of AChE by these toxic chemicals converts the enzyme into a non-functioning molecule (Colovic et al., 2013). PE was applied as a neurotoxin in the presence of AChE and reported that the presence of PE leads to the inactivity of the enzyme (D. Sharma et al., 2021). Likewise, to detect the presence of OPs toxin, PE was introduced to intrude the enzymatic activity of AChE and the presence of PE was detected with the help of the C-AuNPs+TMB system. The incidence of PE in the reaction mixture decrease the hydrolysis of ACh, less hydrolysis means lesser choline, and the presence of lesser choline will reduce the aggregation in C-AuNPs, resultantly C-AuNPs remained catalytically active and showed peroxidase-like activity. So, PE presence reduced the enzymatic activity of AChE, and eventually C-AuNPs+TMB system produces brighter colorimetric signals to detect PE.

As mentioned that PE has an inhibitory effect on the catalytic power of AChE, higher concentrations of PE induce more retarding effects on the activity of AChE. Step by step increase in the concentration of PE, a continuing inhibition array of AChE was observed as shown in Fig.4.18 which indicates the more malfunctioning of AChE. This inactivity of AChE reduces the production of ACh subsequently, a repressed quantity of choline was formed which leads to greater oxidation of TMB along with an evident blue color (W. Ren et al., 2019). Irreversible inhibition of AChE has been described earlier due to the existence of neurotoxins (Guo et al., 2015; D. N. Kumar et al., 2018; X. Meng et al., 2015). The establishment of a covalent bond with the active site (phosphorylate serine residues) of AChE by these poisonous compounds alters the enzyme into a non-functioning particle (Colovic et al., 2013). Increasing

concentration of paraoxon induced more inability in the functioning of AChE, less enzymatic product lead to increase absorbance intensity of the sensing system (Han & Wang, 2019). The presence of different concentrations of neostigmine (a member of OP) induces different effects on the functionality of AChE and absorbance at 652 increases continuously with the increase in the concentration of the OPs (Sun et al., 2018). Paraoxon was applied as a candidate OP and reported that with the addition of paraoxon in the AChE-MnO_2-TMB system, the enzyme hydrolysis is significantly retarded and an increase in absorbance intensity is observed with higher concentrations of paraoxon (Yan et al., 2017). Colorimetric variation in the oxidation product of TMB under the different concentrations of PE in this proposed C-AuNPs+TMB sensing system advocates that different concentrations of PE can be differentiated by the unaided eye.

Sensing systems are devised to detect the analyte from the samples which may have different chemicals and possible coexisting substances which can act like target analyte leads to false results. A colorimetric sensing system to detect the presence of six individual pesticides including carbaryl, paraoxon, parathion, malathion, diazinon, and chlorpyrifos was developed and to cross-check the selectivity of the assay metal ions, anions, amino acids, sugar, and vitamins were applied (Bordbar et al., 2020). Samples may probably have different types of chemicals which can mimic the role of OPs and false colorimetric signals can be produced so sensing systems were cross-checked with similar kinds of compounds to make sure to avoid the unreliability of the results (L. Lin et al., 2020). Similarly, several research groups conducted the selectivity assay for the proposed sensing systems to make sure that their devices can produce the required results and detect the target analyte present in complex samples (Han & Wang, 2019; M. Zheng et al., 2018; Y. Zhu et al., 2015).

As the assay was elaborated in this dissertation was devised to detect the presence of OP toxins from the environmental samples so it was likely that the sample may have diverse kinds of toxins and chemicals which may lead to fall results. So, to check the selectivity of the proposed assay it was necessary to check the cross-reactivity of the proposed assay. Some of the prospective chemical agents and environmental pollutants were tested for the cross-reactivity of the proposed system. It is found that

none of these filthy and toxic substances produced the equivalent colorimetric response up to the level of PE. So it was concluded that the C-AuNPs+TMB sensing assay is specific plentiful to sense the PE with extraordinary correctness, precision, trustworthiness and reliability.

The limit of detection (LOD) is the lowest concretions or the quantity of analyte which can be detected with reliable certainty with the help of any analytical sensing method. The limit of detection should be as low as possible which reflects the sensitivity of the sensing system. Different techniques and strategies including aggregation and decomposition of nanoparticles, application of nanozymes, fluorescence on-off systems, ligand-receptor interactions, and addition of photonic structures have been adopted by the research groups to make the sensing and analytical system more sensitive and accurate to respond to the minute concentration of an analyte (Diaz et al., 2017; Loiseau et al., 2019; Y. Zhou, Huang, & He, 2018).

The C-AuNPs+TMB bio-sensing system reported here for the sensing of OP toxins has enough sensitivity and can respond to the 20nM (5.8 $ng \cdot mL^{-1}$) concentration of the OP compounds which are better than several previous reports (Lan et al., 2012; X. Li et al., 2018; P. Wang et al., 2016; Yan, Li, Wang, et al., 2015). By paralleling this study with already described approaches, the proposed sensing system elaborated in this work has 180 folds superior sensitivity compared to the MPH enzyme-based biosensor (Lan et al., 2012). Similarly, our sensing system is 18 times better sensitivity than reported by (Selvolini et al., 2018). While comparing with the quantum dot-based detection system of OP (Yan et al., 2015) our results are 3 times better. Also, our C-AuNP+TMB system has better sensing than the reports of (Jin et al., 2019; Kundu et al., 2019; X.L. Yin et al., 2021). The sensitivity achieved in our system is analogous to the sensitivity of Fe_3O_4 imprinted polymers-based sensing methodology (S. Xu et al., 2014). This is the vibrant indication of the better and reliable sensitivity of the C-AuNP+TMB assay (Guo et al., 2015; X. Meng et al., 2015). As per the Codex Alimentarius (FAO-WHO) database (Alimentarius, 2020) extreme residual limit for parathion in spices and fruits must not surpass 200 $ng \cdot mL^{-1}$ (0.2 $mg \cdot kg^{-1}$). The sensing assay reported in our study have potential to identify

parathion (PE) as low as 5.8 $ng \cdot mL^{-1}$ (20 nM), which supporters for the great sensitivity of this methodology.

The LOD of classical analytical methods is comparable (S. Xu et al., 2014) and better (Okada et al., 2019; Z.-L. Xu et al., 2012) than our proposed system; however, these methods are less robust and expensive. The electrochemical sensing approaches (Dong et al., 2019; X. Sun et al., 2017) have additional steps to follow long protocols and need high temperatures for hours to successfully synthesize nanomaterials. The protocol of gold nanoclusters-anchored MnO_2 composite also needs 4-5 hours to complete the synthesis in addition to other steps of the protocol (Yan et al., 2019). Compared to nanozyme based biosensing (Yan et al., 2017) which capitalized the MnO_2 sheets as nanozyme, the synthesis of MnO_2 is complex and needs heating at 90 °C for an additional 15 min followed by MnO_2+TMB based detection, which needed more prolonged incubations. Contrarily, our protocol involves the simple synthesis of C-AuNPs, which is easy to follow, and all steps occur at room temperature. Our protocol requires 85-95 min, which includes synthesis of particles and sensing of the analytes. So we can say that in terms of simplicity, economics, easiness of procedure, and robustness of the protocol, the C-AuNPs+TMB sensing is also better than all these reports.

Besides the LOD linear range is another parameter that reflects the efficacy of a sensing assay. It is the output signal ranges that are the linear function of input signals. It is the range of maximum and minimum output signals which showed the direct relation with inputs signals. The broad range singing devices are considered more effective and consider better sensing systems in comparison with the sensing devices which have a narrow linear range. The sensing system reported by (Ton et al., 2013) has the linear range of 0.5–25 $ng \cdot mL^{-1}$ and (Khaksarinejad et al., 2015) which reported that the sensing system for paraoxon has the linear range of 2.75-68.8 $ng \cdot mL^{-1}$ but C-AuNPs+TMB have a much wider linear range 11.6-92.8 $ng \cdot mL^{-1}$ (40-320 nM) which is in agreement with the previously described methods (Sun et al., 2018; Yan et al., 2017). Similarly, the linear range of our reported system is wider than the linear range reported by (Ozer et al., 2020; Soysal, 2019; Ton et al., 2013). All these facts are clear evidence that the colorimetric assay reported here is a simple

non-instrument-based approach that is more sensitive and was highly selective in detecting OPs. All this indicates this sensing system is better than several existing reports.

Conclusion

A simple, sensitive, and easy to perform biosensing assay, based upon cysteamine capped gold nanoparticles (C-AuNPs) as nanozyme and acetylcholinesterase inhibition by parathion ethyl (PE) was developed. The assay accomplishes the detection requirements for on-field and quick visual monitoring of OPs with high, precision, sensitivity and reproducibility. C-AuNPs have straightforward synthesis protocols as well as possess more significant and substantial catalytic power (peroxidase activity). The C-AuNPs+TMB assay requires only 35-40 minutes to be performed including both incubations. The C-AuNPs were utilized to catalyze the oxidization of colorless TMB into a blue-colored product instantly for sensing PE with admirable specificity. The LOD of the proposed system is fine below the supreme contaminant level recommended by the FAO-WHO. The most important characteristic of the development method is that the assay not only provides direct visualization of PE presence with the naked eye but also delivers evidence of the concentration of PE which is indicated by the darkness of color signals. This visual monitoring makes the method more adaptable than other analytical techniques which depend on advanced instrumentations. This colorimetric monitoring system can be employed for a variety of applications to detect PE in environmental and food processing applications such as tab water, nectars, milk products, and vegetables for quality control, and safety purposes. So we can say that in terms of simplicity, sensitivity, economics, easiness of procedure, and robustness of the protocol, the C-AuNPs+TMB sensing system is straightforward, easy, robust, and quick, which advocates the novelty of the protocol.

References

References

Adeyinka, A., Muco, E., & Pierre, L. (2018). Organophosphates. *StatPearls Publishing, Treasure Island (FL),, PMID: 29763035.*

Aguirre, C. M., Kaspar, T. R., Radloff, C., & Halas, N. J. (2003). CTAB mediated reshaping of metallodielectric nanoparticles. *Nano Letters, 3*(12), 1707-1711.

Akanda, R., Hasan, M., Ema, U. H., & Haque, M. A. (2021). Optimization of Spondias mombin peel extract mediated synthesis of palladium nanoparticles as nanozyme exhibits potent multienzyme activity. *Journal of the Iranian Chemical Society*, 1-9.

Alexander, C. M., Dabrowiak, J. C., & Goodisman, J. (2013). Gravitational sedimentation of gold nanoparticles. *Journal of colloid interface science, 396*, 53-62.

Alimentarius, C. (2020). International Food Standards. Retrieved from http://www.fao.org/fao-who-codexalimentarius/codex-texts/dbs/pestres/pesticide-detail/en/?p_id=58

Alle, M., Park, S. C., Bandi, R., Lee, S.-H., & Kim, J.-C. (2021). Rapid in-situ growth of gold nanoparticles on cationic cellulose nanofibrils: Recyclable nanozyme for the colorimetric glucose detection. *Carbohydrate Polymers, 253*, 117239.

Andreescu, S., & Marty, J.-L. (2006). Twenty years research in cholinesterase biosensors: from basic research to practical applications. *Biomolecular engineering, 23*(1), 1-15.

Arduini, F., Forchielli, M., Amine, A., Neagu, D., Cacciotti, I., Nanni, F., Palleschi, G. (2015). Screen-printed biosensor modified with carbon black nanoparticles for the determination of paraoxon based on the inhibition of butyrylcholinesterase. *Microchimica Acta, 182*(3), 643-651.

Arias, P. G., Martinez-Perez-Cejuela, H., Combes, A., Pichon, V., Pereira, E., Herrero-Martinez, J. M., & Bravo, M. (2020). Selective solid-phase extraction of organophosphorus pesticides and their oxon-derivatives from water samples using molecularly imprinted polymer followed by high-performance liquid chromatography with UV detection. *Journal of Chromatography A, 1626*, 461346.

Aroniadou-Anderjaska, V., Figueiredo, T. H., Apland, J. P., & Braga, M. F. (2020). Targeting the glutamatergic system to counteract organophosphate poisoning: A novel therapeutic strategy. *Neurobiology of disease, 133*, 104406.

Atallah, C., Charcosset, C., & Greige-Gerges, H. (2020). Challenges for cysteamine stabilization, quantification, and biological effects improvement. *Journal of Pharmaceutical Analysis*.

Bala, R., Sharma, R. K., & Wangoo, N. (2016). Development of gold nanoparticles-based aptasensor for the colorimetric detection of organophosphorus pesticide phorate. *Analytical and bioanalytical chemistry, 408*(1), 333-338.

Balderacchi, M., Benoit, P., Cambier, P., Eklo, O. M., Gargini, A., Gemitzi, A., Predaa, E. (2013). Groundwater pollution and quality monitoring approaches at the European level. *Critical reviews in environmental science technology, 43*(4), 323-408.

Ballantyne, B., & Marrs, T. C. (2017). *Clinical and experimental toxicology of organophosphates and carbamates*.

Barizuddin, S., Bok, S., & Gangopadhyay, S. (2016). Plasmonic sensors for disease detection-a review. *Journal of Nanomedicine and Nanotechnology, 7*(3), 1000373.

Bassi, A. S. (2009). Biosensors, Environmental. *Encyclopedia of Industrial Biotechnology: Bioprocess, Bioseparation, and Cell Technology*, 1-15.

Bastiaensen, M., Xu, F., Been, F., Van den Eede, N., & Covaci, A. (2018). Simultaneous determination of 14 urinary biomarkers of exposure to organophosphate flame retardants and plasticizers by LC-MS/MS. *Analytical and Bioanalytical Chemistry, 410*(30), 7871-7880.

Bazrafshan, A., Ghaedi, M., Rafiee, Z., Hajati, S., & Ostovan, A. (2017). Nano-sized molecularly imprinted polymer for selective ultrasound-assisted microextraction of pesticide Carbaryl from water samples: Spectrophotometric determination. *Journal of colloid interface science, 498*, 313-322.

Benito-Peña, E., Valdés, M. G., Glahn-Martínez, B., & Moreno-Bondi, M. C. (2016). Fluorescence based fiber optic and planar waveguide biosensors. A review. *Analytica chimica acta, 943*, 17-40.

Berciaud, S., Cognet, L., Tamarat, P., & Lounis, B. (2005). Observation of intrinsic size effects in the optical response of individual gold nanoparticles. *Nano Letters, 5*(3), 515-518.

Berciaud, S., Lasne, D., Blab, G. A., Cognet, L., & Lounis, B. (2006). Photothermal heterodyne imaging of individual metallic nanoparticles: Theory versus experiment. *Physical Review B, 73*(4), 045424.

Bhattacharjee, Y., Chakraborty, A., & Engineering. (2014). Label-free cysteamine-capped silver nanoparticle-based colorimetric assay for Hg (II) detection in water with subnanomolar exactitude. *ACS Sustainable Chemistry & Engineering, 2*(9), 2149-2154.

Bordbar, M. M., Nguyen, T. A., Arduini, F., & Bagheri, H. (2020). A paper-based colorimetric sensor array for discrimination and simultaneous determination of organophosphate and carbamate pesticides in tap water, apple juice, and rice. *Microchimica Acta, 187*(11), 1-13.

Borghei, Y. S., Hosseini, M., & Ganjali, M. R. J. S. (2018). Oxidase-like catalytic activity of Cys-AuNCs upon visible light irradiation and its application for visual miRNA detection. *Sensors and Actuators B: Chemical, 273*, 1618-1626.

Boyer, D., Tamarat, P., Maali, A., Lounis, B., & Orrit, M. (2002). Photothermal imaging of nanometer-sized metal particles among scatterers. *Science, 297*(5584), 1160-1163.

Brust, M., Walker, M., Bethell, D., Schiffrin, D. J., & Whyman, R. (1994). Synthesis of thiol-derivatised gold nanoparticles in a two-phase liquid–liquid system. *Journal of the Chemical Society, Chemical Communications*(7), 801-802.

Bui, M.-P. N., & Abbas, A. (2015). Simple and rapid colorimetric detection of p-nitrophenyl substituent organophosphorous nerve agents. *Sensors and Actuators B: Chemical, 207*, 370-374.

Busbee, B. D., Obare, S. O., & Murphy, C. J. (2003). An improved synthesis of high-aspect-ratio gold nanorods. *Advanced Materials, 15*(5), 414-416.

Buzea, C., Pacheco, I. I., & Robbie, K. (2007). Nanomaterials and nanoparticles: sources and toxicity. *Biointerphases, 2*(4), MR17-MR71.

Caballero-Diaz, E., Benitez-Martinez, S., & Valcarcel, M. (2017). Rapid and simple nanosensor by combination of graphene quantum dots and enzymatic inhibition mechanisms. *Sensors and Actuators B: Chemical, 240*, 90-99.

Cacciatore, L. C., Nemirovsky, S. I., Guerrero, N. R. V., & Cochón, A. C. (2015). Azinphos-methyl and chlorpyrifos, alone or in a binary mixture, produce oxidative stress and lipid peroxidation in the freshwater gastropod Planorbarius corneus. *Aquatic Toxicology, 167*, 12-19.

Campas, M., Prieto-Simon, B., & Marty, J.L. (2009). *A review of the use of genetically engineered enzymes in electrochemical biosensors.* Paper presented at the Seminars in cell & developmental biology.

Cao, X., Hogan, A., & Moore, E. (2019). Rapid Separation of Organophosphate Pesticides using Micellar Electrokinetic Chromatography and Short-end Injection. *Journal of forensic sciences, 64*(4), 1213-1220.

Carullo, P., Cetrangolo, G. P., Mandrich, L., Manco, G., & Febbraio, F. (2015). Fluorescence spectroscopy approaches for the development of a real-time organophosphate detection system using an enzymatic sensor. *Sensors, 15*(2), 3932-3951.

Cha, B. S., Lee, E. S., Kim, S., Kim, J. M., Hwang, S. H., Oh, S. S., & Park, K. S. (2020). Simple colorimetric detection of organophosphorus pesticides using naturally occurring extracellular vesicles. *Microchemical journal, 158*, 105130.

Chai, F., Wang, C., Wang, T., Li, L., & Su, Z. (2010). Colorimetric detection of Pb2+ using glutathione functionalized gold nanoparticles. *ACS applied materials & interfaces, 2*(5), 1466-1470.

Chang, C.-C., Chen, C.-P., Wu, T.-H., Yang, C.-H., Lin, C.-W., & Chen, C.-Y. (2019). Gold nanoparticle-based colorimetric strategies for chemical and biological sensing applications. *Nanomaterials, 9*(6), 861.

Chen, W., Li, S., Wang, J., Sun, K., & Si, Y. (2019). Metal and metal-oxide nanozymes: bioenzymatic characteristics, catalytic mechanism, and eco-environmental applications. *Nanoscale, 11*(34), 15783-15793.

Chen, Y. (2012). Organophosphate-induced brain damage: mechanisms, neuropsychiatric and neurological consequences, and potential therapeutic strategies. *Neurotoxicology, 33*(3), 391-400.

Chinen, A. B., Guan, C. M., Ferrer, J. R., Barnaby, S. N., Merkel, T. J., & Mirkin, C. A. (2015). Nanoparticle probes for the detection of cancer biomarkers, cells, and tissues by fluorescence. *Chemical reviews, 115*(19), 10530-10574.

Cho, I.-H., & Irudayaraj, J. (2013). Lateral-flow enzyme immunoconcentration for rapid detection of Listeria monocytogenes. *Analytical and bioanalytical chemistry, 405*(10), 3313-3319.

Clark Jr, L. C., & Lyons, C. (1962). Electrode systems for continuous monitoring in cardiovascular surgery. *Annals of the New York Academy of sciences, 102*(1), 29-45.

Cobley, C. M., Chen, J., Cho, E. C., Wang, L. V., & Xia, Y. (2011). Gold nanostructures: a class of multifunctional materials for biomedical applications. *Chemical Society Reviews, 40*(1), 44-56.

Coccini, T., Roda, E., Sarigiannis, D., Mustarelli, P., Quartarone, E., Profumo, A., & Manzo, L. (2010). Effects of water-soluble functionalized multi-walled carbon nanotubes examined by different cytotoxicity methods in human astrocyte D384 and lung A549 cells. *Toxicology, 269*(1), 41-53.

Colovic, M. B., Krstic, D. Z., Lazarevic-Pasti, T. D., Bondzic, A. M., & Vasic, V. M. (2013). Acetylcholinesterase inhibitors: pharmacology and toxicology. *Current neuropharmacology, 11*(3), 315-335.

Cormode, D. P., Gao, L., & Koo, H. (2018). Emerging biomedical applications of enzyme-like catalytic nanomaterials. *Trends in biotechnology, 36*(1), 15-29.

Cui, H.F., Wu, W.W., Li, M.-M., Song, X., Lv, Y., & Zhang, T.T. (2018). A highly stable acetylcholinesterase biosensor based on chitosan-TiO2-graphene nanocomposites for detection of organophosphate pesticides. *Biosensors and Bioelectronics, 99*, 223-229.

Deng, H.H., Lin, X.L., Liu, Y.H., Li, K.L., Zhuang, Q.-Q., Peng, H.-P., Chen, W. (2017). Chitosan-stabilized platinum nanoparticles as effective oxidase mimics for colorimetric detection of acid phosphatase. *Nanoscale, 9*(29), 10292-10300.

Diaz-Resendiz, K., Ortiz-Lazareno, P., Covantes-Rosales, C., Trujillo-Lepe, A., Toledo-Ibarra, G., Ventura-Ramon, G., & Giron-Perez, M. (2019). Effect of diazinon, an organophosphate pesticide, on signal transduction and death induction in mononuclear cells of Nile tilapia fish (Oreochromis niloticus). *Fish & shellfish immunology, 89*, 12-17.

Diaz, Y. J., Page, Z. A., Knight, A. S., Treat, N. J., Hemmer, J. R., Hawker, C. J., & Read de Alaniz, J. (2017). A versatile and highly selective colorimetric sensor for the detection of amines. *Chemistry–A European Journal, 23*(15), 3562-3566.

Diegoli, S., Manciulea, A. L., Begum, S., Jones, I. P., Lead, J. R., & Preece, J. A. (2008). Interaction between manufactured gold nanoparticles and naturally occurring organic macromolecules. *Science of the Total Environment, 402*(1), 51-61.

Dissanayake, N. M., Arachchilage, J. S., Samuels, T. A., & Obare, S. O. (2019). Highly sensitive plasmonic metal nanoparticle-based sensors for the detection of organophosphorus pesticides. *Talanta, 200*, 218-227.

Dong, P., Jiang, B., & Zheng, J. (2019). A novel acetylcholinesterase biosensor based on gold nanoparticles obtained by electroless plating on three-dimensional graphene for detecting organophosphorus pesticides in water and vegetable samples. *Analytical Methods, 11*(18), 2428-2434.

Doyen, M., Bartik, K., & Bruylants, G. (2013). UV–Vis and NMR study of the formation of gold nanoparticles by citrate reduction: Observation of gold–citrate aggregates. *Journal of colloid interface science, 399*, 1-5.

Dutta, D., Sundaram, S. K., Teeguarden, J. G., Riley, B. J., Fifield, L. S., Jacobs, J. M.,Weber, T. J. (2007). Adsorbed proteins influence the biological activity and molecular targeting of nanomaterials. *Toxicological Sciences, 100*(1), 303-315.

Dvir, H., Silman, I., Harel, M., Rosenberry, T. L., & Sussman, J. L. (2010). Acetylcholinesterase: from 3D structure to function. *Chemico-biological interactions, 187*(1-3), 10-22.

Dykman, L., & Khlebtsov, N. (2011). Gold nanoparticles in biology and medicine: recent advances and prospects. *Acta Naturae, 3*(2 (9)).

Eddleston, M., Buckley, N. A., Eyer, P., & Dawson, A. H. (2008). Management of acute organophosphorus pesticide poisoning. *The Lancet, 371*(9612), 597-607.

El Alami, A., Lagarde, F., Huo, Q., Zheng, T., Baitoul, M., & Daniel, P. (2020). Acetylcholine and acetylcholinesterase inhibitors detection using gold nanoparticles coupled with dynamic light scattering. *Sensors International, 1*, 100007.

Ensafi, A. A. (2019). An introduction to sensors and biosensors. In *Electrochemical Biosensors* (pp. 1-10): Elsevier.

Ensafi, A. A., & Kazemzadeh, A. (1999). Optical pH sensor based on chemical modification of polymer film. *Microchemical journal, 63*(3), 381-388.

Erathodiyil, N., & Ying, J. Y. (2011). Functionalization of inorganic nanoparticles for bioimaging applications. *Accounts of Chemical Research, 44*(10), 925-935.

Eskenazi, B., Kogut, K., Huen, K., Harley, K. G., Bouchard, M., Bradman, A., Holland, N. (2014). Organophosphate pesticide exposure, PON1, and neurodevelopment in school-age children from the CHAMACOS study. *Environmental research, 134*, 149-157.

Faghiri, F., Hajjami, M., & Ghorbani, F. (2021). Development of a sensing system based on coupling magnetic solid phase extraction and colorimetric detection for determination of organophosphorus pesticides in fruit extract and environmental sample. *Sensors Actuators B: Chemical*, 130157.

Fahimi-Kashani, N., & Hormozi-Nezhad, M. R. (2016). Gold-nanoparticle-based colorimetric sensor array for discrimination of organophosphate pesticides. *Analytical Chemistry, 88*(16), 8099-8106.

Fang, J., Zhong, C., & Mu, R. (2005). The study of deposited silver particulate films by simple method for efficient SERS. *Chemical Physics Letters, 401*(1-3), 271-275.

Faraday, M. (1857). X. The Bakerian Lecture. Experimental relations of gold (and other metals) to light. *Philosophical Transactions of the Royal Society of London*(147), 145-181.

Farajzadeh, M. A., Mogaddam, M. R. A., Aghdam, S. R., Nouri, N., & Bamorrowat, M. (2016). Application of elevated temperature-dispersive liquid-liquid microextraction for determination of organophosphorus pesticides residues in

aqueous samples followed by gas chromatography-flame ionization detection. *Food Chemistry, 212*, 198-204.

Feng, J., Huang, P., Shi, S., Deng, K.-Y., & Wu, F.-Y. (2017). Colorimetric detection of glutathione in cells based on peroxidase-like activity of gold nanoclusters: a promising powerful tool for identifying cancer cells. *Analytica Chimica Acta, 967*, 64-69.

Feynman, R. (2018). There's plenty of room at the bottom. In *Feynman and computation* (pp. 63-76): CRC Press.

Figueiredo, T. H., Apland, J. P., Braga, M. F., & Marini, A. M. (2018). Acute and long-term consequences of exposure to organophosphate nerve agents in humans. *Epilepsia, 59*, 92-99.

Frens, G. (1973). Controlled nucleation for the regulation of the particle size in monodisperse gold suspensions. *Nature physical science, 241*(105), 20-22.

Fu, Q., Zhang, C., Xie, J., Li, Z., Qu, L., Cai, X., Lin, Y. (2019). Ambient light sensor based colorimetric dipstick reader for rapid monitoring organophosphate pesticides on a smart phone. *Analytica Chimica Acta, 1092*, 126-131.

Funari, R., Della Ventura, B., Schiavo, L., Esposito, R., Altucci, C., & Velotta, R. (2013). Detection of parathion pesticide by quartz crystal microbalance functionalized with UV-activated antibodies. *Analytical Chemistry, 85*(13), 6392-6397.

Gadogbe, M., Ansar, S. M., He, G., Collier, W. E., Rodriguez, J., Liu, D., Zhang, D. (2013). Determination of colloidal gold nanoparticle surface areas, concentrations, and sizes through quantitative ligand adsorption. *Analytical and Bioanalytical Chemistry, 405*(1), 413-422.

Ganapuram, B. R., Alle, M., Dadigala, R., Dasari, A., Maragoni, V., & Guttena, V. (2015). Catalytic reduction of methylene blue and Congo red dyes using green synthesized gold nanoparticles capped by salmalia malabarica gum. *International Nano Letters, 5*(4), 215-222.

Gao, L., Fan, K., & Yan, X. (2020). Iron oxide nanozyme: A multifunctional enzyme mimetics for biomedical application. *Nanozymology*, 105-140.

Gao, L., Zhuang, J., Nie, L., Zhang, J., Zhang, Y., Gu, N., Perrett, S. (2007). Intrinsic peroxidase-like activity of ferromagnetic nanoparticles. *Nature nanotechnology, 2*(9), 577-583.

Ghosh, S. K., & Pal, T. (2007). Interparticle coupling effect on the surface plasmon resonance of gold nanoparticles: from theory to applications. *Chemical reviews, 107*(11), 4797-4862.

Golchin, K., Golchin, J., Ghaderi, S., Alidadiani, N., Eslamkhah, S., Eslamkhah, M., . . . Akbarzadeh, A. (2018). Gold nanoparticles applications: from artificial enzyme till drug delivery. *Artificial cells, nanomedicine and biotechnology, 46*(2), 250-254.

Gomez-Arribas, L. N., Benito-Pena, E., Hurtado-Sanchez, M. d. C., & Moreno-Bondi, M. C. (2018). Biosensing based on nanoparticles for food allergens detection. *Sensors, 18*(4), 1087.

Greaves, A. K., & Letcher, R. J. (2017). A review of organophosphate esters in the environment from biological effects to distribution and fate. *Bulletin of environmental contamination toxicology, 98*(1), 2-7.

Gu, H., Huang, Q., Zhang, J., Li, W., & Fu, Y. J. C. (2020). Heparin as a bifunctional biotemplate for Pt nanocluster with exclusively peroxidase mimicking activity at near-neutral pH. *Colloids Surfaces A: Physicochemical Engineering Aspects, 606*, 125455.

Guarise, C., Pasquato, L., & Scrimin, P. (2005). Reversible aggregation/deaggregation of gold nanoparticles induced by a cleavable dithiol linker. *Langmuir, 21*(12), 5537-5541.

Guignet, M., & Lein, P. J. (2019). Neuroinflammation in organophosphate-induced neurotoxicity. In *Advances in neurotoxicology* (Vol. 3, pp. 35-79): Elsevier.

Guo, J., Wong, J. X., Cui, C., Li, X., & Yu, H.Z. (2015). A smartphone-readable barcode assay for the detection and quantitation of pesticide residues. *Analyst, 140*(16), 5518-5525.

Gupta, M., & Lee, H.I.J. S. (2017). A dual responsive molecular probe for the efficient and selective detection of nerve agent mimics and copper (II) ions with controllable detection time. *Sensors and Actuators B: Chemical, 242*, 977-982.

Haiss, W., Thanh, N. T., Aveyard, J., & Fernig, D. G. (2007). Determination of size and concentration of gold nanoparticles from UV-Vis spectra. *Analytical Chemistry, 79*(11), 4215-4221.

Halamek, J., Přibyl, J., Makower, A., Skladal, P., & Scheller, F. (2005). Sensitive detection of organophosphates in river water by means of a piezoelectric biosensor. *Analytical and Bioanalytical Chemistry, 382*(8), 1904-1911.

Han, T., & Wang, G. (2019). Peroxidase-like activity of acetylcholine-based colorimetric detection of acetylcholinesterase activity and an organophosphorus inhibitor. *Journal of Materials Chemistry B, 7*(16), 2613-2618.

He, S.B., Yang, L., Lin, X.L., Chen, L.M., Peng, H.P., Deng, H.H., Chen, W. (2020). Heparin-platinum nanozymes with enhanced oxidase-like activity for the colorimetric sensing of isoniazid. *Talanta, 211*, 120707.

He, W., Zhou, Y.T., Wamer, W. G., Hu, X., Wu, X., Zheng, Z.,Yin, J.-J. (2013). Intrinsic catalytic activity of Au nanoparticles with respect to hydrogen peroxide decomposition and superoxide scavenging. *Biomaterials, 34*(3), 765-773.

Hemalatha, D., Amala, A., Rangasamy, B., Nataraj, B., & Ramesh, M. (2016). Sublethal toxicity of quinalphos on oxidative stress and antioxidant responses in a freshwater fish Cyprinus carpio. *Environmental toxicology, 31*(11), 1399-1406.

Herizchi, R., Abbasi, E., Milani, M., & Akbarzadeh, A. J. A. C., nanomedicine,. (2016). Current methods for synthesis of gold nanoparticles. *Artificial cells, nanomedicine and biotechnology, 44*(2), 596-602.

Homberger, M., & Simon, U. (2010). On the application potential of gold nanoparticles in nanoelectronics and biomedicine. *Philosophical Transactions of the Royal Society A: Mathematical, Physical and Engineering Sciences, 368*(1915), 1405-1453.

Hondow, N., Brydson, R., Wang, P., Holton, M. D., Brown, M. R., Rees, P.,Brown, A. (2012). Quantitative characterization of nanoparticle agglomeration within biological media. *Journal of Nanoparticle Research, 14*(7), 1-15.

Hu, H., Ma, C., & Liu, Z. (2010). Plasmonic dark field microscopy. *Applied Physics Letters, 96*(11), 113107.

Hu, L., Liao, H., Feng, L., Wang, M., & Fu, W. (2018). Accelerating the peroxidase-like activity of gold nanoclusters at neutral pH for colorimetric detection of heparin and heparinase activity. *Analytical Chemistry, 90*(10), 6247-6252.

Hu, M., Novo, C., Funston, A., Wang, H., Staleva, H., Zou, S.,Hartland, G. V. (2008). Dark-field microscopy studies of single metal nanoparticles: understanding the factors that influence the linewidth of the localized surface plasmon resonance. *Journal of Materials Chemistry B, 18*(17), 1949-1960.

Huang, H., Yuan, Q., & Yang, X. J. J. O. C. (2005). Morphology study of gold–chitosan nanocomposites. *Journal of colloid interface science, 282*(1), 26-31.

Huang, X., & El-Sayed, M. A. (2010). Gold nanoparticles: Optical properties and implementations in cancer diagnosis and photothermal therapy. *Journal of advanced research, 1*(1), 13-28.

Huang, X., Jain, P. K., El-Sayed, I. H., & El-Sayed, M. A. (2007). Gold nanoparticles: interesting optical properties and recent applications in cancer diagnostics and therapy. *Future Medicine*, 681-693.

Huang, Y., Ren, J., & Qu, X. (2019). Nanozymes: classification, catalytic mechanisms, activity regulation, and applications. *Chemical reviews, 119*(6), 4357-4412.

Hulla, J., Sahu, S., & Hayes, A. (2015). Nanotechnology: History and future. *Human & experimental toxicology, 34*(12), 1318-1321.

Iijima, S. (1991). Helical microtubules of graphitic carbon. *Nature, 354*(6348), 56-58.

Iijima, S., & Ichihashi, T. (1993). Single-shell carbon nanotubes of 1-nm diameter. *Nature, 363*(6430), 603-605.

Ji, X., Song, X., Li, J., Bai, Y., Yang, W., & Peng, X. (2007). Size control of gold nanocrystals in citrate reduction: the third role of citrate. *Journal of the American Chemical Society, 129*(45), 13939-13948.

Ji, Z., Jin, X., George, S., Xia, T., Meng, H., Wang, X.,Godwin, H. (2010). Dispersion and stability optimization of TiO2 nanoparticles in cell culture media. *Environmental science & technology, 44*(19), 7309-7314.

Jiang, T., Song, Y., Wei, T., Li, H., Du, D., Zhu, M.J., & Lin, Y. (2016). Sensitive detection of Escherichia coli O157: H7 using Pt–Au bimetal nanoparticles with peroxidase-like amplification. *Biosensors and Bioelectronics, 77*, 687-694.

Jiang, X., Sun, C., Guo, Y., Nie, G., & Xu, L. (2015). Peroxidase-like activity of apoferritin paired gold clusters for glucose detection. *Biosensors and Bioelectronics, 64*, 165-170.

Jin, R., Kong, D., Yan, X., Zhao, X., Li, H., Liu, F.,Lu, G. (2019). Integrating target-responsive hydrogels with smartphone for on-site ppb-level quantitation of organophosphate pesticides. *ACS Applied Materials & Interfaces, 11*(31), 27605-27614.

Jv, Y., Li, B., & Cao, R. (2010). Positively-charged gold nanoparticles as peroxidiase mimic and their application in hydrogen peroxide and glucose detection. *Chemical Communications, 46*(42), 8017-8019.

Kaur, N., & Prabhakar, N. (2017). Current scenario in organophosphates detection using electrochemical biosensors. *TrAC Trends in Analytical Chemistry, 92*, 62-85.

Kaushal, J., Khatri, M., & Arya, S. K. (2021). A treatise on Organophosphate pesticide pollution: Current strategies and advancements in their environmental degradation and elimination. *Ecotoxicology and Environmental Safety, 207*, 111483.

Keene, A. M., & Tyner, K. M. (2011). Analytical characterization of gold nanoparticle primary particles, aggregates, agglomerates, and agglomerated aggregates. *Journal of Nanoparticle Research, 13*(8), 3465-3481.

Khaksarinejad, R., Mohsenifar, A., Rahmani-Cherati, T., Karami, R., & Tabatabaei, M. (2015). An organophosphorus hydrolase-based biosensor for direct detection of paraoxon using silica-coated magnetic nanoparticles. *Applied biochemistry and biotechnology, 176*(2), 359-371.

Khaled, E., Hassan, H., Mohamed, G. G., Ragab, F. A., & Seleim, A. E. A. (2010). Disposable potentiometric sensors for monitoring cholinesterase activity. *Talanta, 83*(2), 357-363.

Kim, F., Connor, S., Song, H., Kuykendall, T., & Yang, P. (2004). Platonic gold nanocrystals. *Angewandte Chemie International Edition, 43*(28), 3673-3677.

Kim, N., Park, I.-S., & Kim, D.-K. (2007). High-sensitivity detection for model organophosphorus and carbamate pesticide with quartz crystal microbalance-precipitation sensor. *Biosensors and Bioelectronics, 22*(8), 1593-1599.

Korram, J., Dewangan, L., Karbhal, I., Nagwanshi, R., Vaishanav, S. K., Ghosh, K. K., & Satnami, M. L. (2020). CdTe QD-based inhibition and reactivation assay of acetylcholinesterase for the detection of organophosphorus pesticides. *RSC Advances, 10*(41), 24190-24202.

Kosarac, I., Kubwabo, C., & Foster, W. G. (2016). Quantitative determination of nine urinary metabolites of organophosphate flame retardants using solid phase extraction and ultra performance liquid chromatography coupled to tandem mass spectrometry (UPLC-MS/MS). *Journal of Chromatography B, 1014*, 24-30.

Kotov, N. A. (2010). Inorganic nanoparticles as protein mimics. *Science, 330*(6001), 188-189.

Kroto, H. W., Heath, J. R., O'Brien, S. C., Curl, R. F., & Smalley, R. E. (1985). C 60: buckminsterfullerene. *Nature, 318*(6042), 162-163.

Kumar, D. N., Satija, J., Chandrasekaran, N., & Mukherjee, A. (2018). Acetylcholinesterase-based inhibition screening through in situ synthesis of gold nanoparticles: Application for detection of nerve agent simulant. *Journal of Molecular Liquids, 249*, 623-628.

Kumar, P., Kim, K.-H., & Deep, A. (2015). Recent advancements in sensing techniques based on functional materials for organophosphate pesticides. *Biosensors and Bioelectronics, 70*, 469-481.

Kumar, P. S., Pastoriza-Santos, I., Rodriguez-Gonzalez, B., De Abajo, F. J. G., & Liz-Marzan, L. M. (2007). High-yield synthesis and optical response of gold nanostars. *Nanotechnology, 19*(1), 015606.

Kumar, S., Ahlawat, W., Kumar, R., & Dilbaghi, N. (2015). Graphene, carbon nanotubes, zinc oxide and gold as elite nanomaterials for fabrication of biosensors for healthcare. *Biosensors and Bioelectronics, 70*, 498-503.

Kumar, S., Bhushan, P., & Bhattacharya, S. (2016). Development of a paper-based analytical device for colorimetric detection of uric acid using gold nanoparticles graphene oxide (AuNPs–GO) conjugates. *Analytical Methods, 8*(38), 6965-6973.

Kumar, S., Kaushik, G., & Villarreal-Chiu, J. F. (2016). Scenario of organophosphate pollution and toxicity in India: A review. *Environmental Science & Pollution Research, 23*(10), 9480-9491.

Kumar, V., Bano, D., Singh, D. K., Mohan, S., Singh, V. K., & Hasan, S. H. (2018). Size-dependent synthesis of gold nanoparticles and their peroxidase-like activity for the colorimetric detection of glutathione from human blood serum. *ACS Sustainable Chemistry & Engineering, 6*(6), 7662-7675.

Kumar, V., Upadhay, N., Wasit, A., Singh, S., & Kaur, P. (2013). Spectroscopic methods for the detection of organophosphate pesticides–a preview. *Current World Environment, 8*(2), 313.

Kundu, S., Saha, S., & Sahoo, P. (2019). Rapid and selective visual detection of DCNP (nerve gas mimic) in sea water and soil with a simple paper strip. *Results in Chemistry, 1*, 100014.

Lakshmaiah, G. (2016). Acute lethal and chronic sublethal toxic stress induced alterations in lactate dehydrogenase activity of phorate intoxicated freshwater fish Cyprinus carpio. *International Journal of Fisheries and Aquatic Studies, 4*(3), 685-689.

Lan, W., Chen, G., Cui, F., Tan, F., Liu, R., & Yushupujiang, M. (2012). Development of a novel optical biosensor for detection of organophoshorus pesticides based on methyl parathion hydrolase immobilized by metal-chelate affinity. *Sensors, 12*(7), 8477-8490.

Lasne, D., Blab, G. A., Berciaud, S., Heine, M., Groc, L., Choquet, D., Lounis, B. (2006). Single nanoparticle photothermal tracking (SNaPT) of 5-nm gold beads in live cells. *Biophysical journal, 91*(12), 4598-4604.

Lee, C.W., Su, H., Lee, R.H., Lin, Y.P., Tsai, Y.D., Wu, D.C., & Shiea, J. (2018). Point-of-care identification of organophosphates in gastric juice by ambient mass spectrometry in emergency settings. *Clinica Chimica Acta, 485*, 288-297.

Lee, G.H., & Choi, K.C. (2020). Adverse effects of pesticides on the functions of immune system. *Comparative Biochemistry and Physiology Part C: Toxicology &Pharmacology, 235*, 108789.

Lee, S. H., Kim, Y. H., Kwon, D. H., Cha, D. J., & Kim, J. H. (2015). Mutation and duplication of arthropod acetylcholinesterase: implications for pesticide resistance and tolerance. *Pesticide biochemistry & physiology, 120*, 118-124.

Li, C., Li, D., Wan, G., Xu, J., & Hou, W. (2011). Facile synthesis of concentrated gold nanoparticles with low size-distribution in water: temperature and pH controls. *Nanoscale research letters, 6*(1), 1-10.

Li, H., Yan, X., Lu, G., & Su, X. (2018). Carbon dot-based bioplatform for dual colorimetric and fluorometric sensing of organophosphate pesticides. *Sensors & Actuators B: Chemical, 260*, 563-570.

Li, Q., Dou, X., Zhang, L., Zhao, X., Luo, J., & Yang, M. (2019). Oriented assembly of surface plasmon resonance biosensor through staphylococcal protein A for the chlorpyrifos detection. *Analytical and Bioanalytical Chemistry, 411*(23), 6057-6066.

Li, S., Pang, E., Gao, C., Chang, Q., Hu, S., & Li, N. (2020). Cerium-mediated photooxidation for tuning pH-dependent oxidase-like activity. *Chemical Engineering Journal, 397*, 125471.

Li, S., Wei, T., Ren, G., Chai, F., Wu, H., & Qu, F. (2017). Gold nanoparticles based colorimetric probe for Cr (III) and Cr (VI) detection. *Colloids Surfaces A: Physicochemical Engineering Aspects, 535*, 215-224.

Li, X., Cui, H., & Zeng, Z. (2018). A simple colorimetric and fluorescent sensor to detect organophosphate pesticides based on adenosine triphosphate-modified gold nanoparticles. *Sensors, 18*(12), 4302.

Li, X., Wang, L., Du, D., Ni, L., Pan, J., & Niu, X. (2019). Emerging applications of nanozymes in environmental analysis: opportunities and trends. *TrAC Trends in Analytical Chemistry*, 115653.

Li, Y., Zhao, R., Shi, L., Han, G., & Xiao, Y. (2017). Acetylcholinesterase biosensor based on electrochemically inducing 3D graphene oxide network/multi-walled carbon nanotube composites for detection of pesticides. *RSC Advances, 7*(84), 53570-53577.

Liang, M., Fan, K., Pan, Y., Jiang, H., Wang, F., Yang, D.,Yang, L. (2013). Fe3O4 magnetic nanoparticle peroxidase mimetic-based colorimetric assay for the rapid detection of organophosphorus pesticide and nerve agent. *Analytical Chemistry, 85*(1), 308-312.

Liang, M., & Yan, X. (2019). Nanozymes: from new concepts, mechanisms, and standards to applications. *Accounts of chemical research, 52*(8), 2190-2200.

Lien, C.W., Tseng, Y.T., Huang, C.C., & Chang, H.T. (2014). Logic control of enzyme-like gold nanoparticles for selective detection of lead and mercury ions. *Analytical chemistry, 86*(4), 2065-2072.

Lin, L., Ma, H., Yang, C., Chen, W., Zeng, S., & Hu, Y. (2020). A colorimetric sensing platform based on self-assembled 3D porous CeGONR nanozymes for label-free visual detection of organophosphate pesticides. *Materials Advances, 1*(8), 2789-2796.

Lin, T. J., Huang, K. T., & Liu, C. Y. (2006). Determination of organophosphorous pesticides by a novel biosensor based on localized surface plasmon resonance. *Biosensors and Bioelectronics, 22*(4), 513-518.

Lin, Z., Zhang, X., Liu, S., Zheng, L., Bu, Y., Deng, H.,Chen, W. (2020). Colorimetric acid phosphatase sensor based on MoO3 nanozyme. *Analytica Chimica Acta, 1105*, 162-168.

Liu, B., Huang, Z., & Liu, J. (2016). Boosting the oxidase mimicking activity of nanoceria by fluoride capping: rivaling protein enzymes and ultrasensitive F− detection. *Nanoscale, 8*(28), 13562-13567.

Liu, C. P., Wu, T. H., Lin, Y. L., Liu, C. Y., Wang, S., & Lin, S. Y. (2016). Tailoring Enzyme-Like Activities of Gold Nanoclusters by Polymeric Tertiary Amines for Protecting Neurons Against Oxidative Stress. *Small, 12*(30), 4127-4135.

Liu, D., Yang, J., Wang, H.-F., Wang, Z., Huang, X., Wang, Z.,Chen, X. (2014). Glucose oxidase-catalyzed growth of gold nanoparticles enables quantitative detection of attomolar cancer biomarkers. *Analytical Chemistry, 86*(12), 5800-5806.

Liu, L., Du, J., Liu, W.E., Guo, Y., Wu, G., Qi, W., & Lu, X. (2019). Enhanced His@ AuNCs oxidase-like activity by reduced graphene oxide and its application for

colorimetric and electrochemical detection of nitrite. *Analytical and bioanalytical chemistry, 411*(10), 2189-2200.

Liu, X., Gao, Y., Chandrawati, R., & Hosta-Rigau, L. (2019). Therapeutic applications of multifunctional nanozymes. *Nanoscale, 11*(44), 21046-21060.

Liu, X., Zhou, Y., Liu, J., & Xia, H. (2021). The intrinsic enzyme mimetic activity of platinum oxide for biosensing of glucose. *Spectrochimica Acta Part A: Molecular and Biomolecular Spectroscopy, 248*, 119280.

Liu, Y., Lin, X., Ji, X., Hao, Z., & Tao, Z. (2020). Smartphone-based enzyme-free fluorescence sensing of organophosphate DDVP. *Microchimica Acta, 187*(7), 1-8.

Liu, Y., Wu, H., Li, M., Yin, J.-J., & Nie, Z. (2014). pH dependent catalytic activities of platinum nanoparticles with respect to the decomposition of hydrogen peroxide and scavenging of superoxide and singlet oxygen. *Nanoscale, 6*(20), 11904-11910.

Lohse, S. E., & Murphy, C. J. (2012). Applications of colloidal inorganic nanoparticles: from medicine to energy. *Journal of the American Chemical Society, 134*(38), 15607-15620.

Loiseau, A., Zhang, L., Hu, D., Salmain, M., Mazouzi, Y., Flack, R., (2019). Core–shell gold/silver nanoparticles for localized surface Plasmon resonance-based naked-eye toxin biosensing. *ACS Applied Materials and Interfaces, 11*(50), 46462-46471.

Lopez-Garcia, M., Romero-Gonzalez, R., & Frenich, A. G. (2019). Monitoring of organophosphate and pyrethroid metabolites in human urine samples by an automated method (TurboFlow™) coupled to ultra-high performance liquid chromatography-Orbitrap mass spectrometry. *Journal of pharmaceutical & biomedical analysis, 173*, 31-39.

Lou, T., Chen, L., Zhang, C., Kang, Q., You, H., Shen, D., & Chen, L. (2012). A simple and sensitive colorimetric method for detection of mercury ions based on anti-aggregation of gold nanoparticles. *Analytical Methods, 4*(2), 488-491.

Lu, X., Tuan, H.-Y., Korgel, B. A., & Xia, Y. (2008). Facile synthesis of gold nanoparticles with narrow size distribution by using AuCl or AuBr as the precursor. *Chemistry–A European Journal, 14*(5), 1584.

Ma, Y., Jiang, H., Shen, C., Hou, C., Huo, D., Wu, H., & Yang, M. (2017). Detection of carbendazim residues with a colorimetric sensor based on gold nanoparticles. *Journal of Applied Spectroscopy, 84*(3), 460-465.

Ma, Y., Jiang, L., Mei, Y., Song, R., Tian, D., & Huang, H. (2013). Colorimetric sensing strategy for mercury (II) and melamine utilizing cysteamine-modified gold nanoparticles. *Analyst, 138*(18), 5338-5343.

Mahajan, R., & Chatterjee, S. (2018). A simple HPLC–DAD method for simultaneous detection of two organophosphates, profenofos and fenthion, and validation by soil microcosm experiment. *Environmental monitoring assessment, 190*(6), 1-8.

Mahmudunnabi, R. G., Farhana, F. Z., Kashaninejad, N., Firoz, S. H., Shim, Y.-B., & Shiddiky, M. J. (2020). Nanozyme-based electrochemical biosensors for disease biomarker detection. *Analyst, 145*(13), 4398-4420.

Makower, A., Halamek, J., Skladal, P., Kernchen, F., & Scheller, F. W. (2003). New principle of direct real-time monitoring of the interaction of cholinesterase and its inhibitors by piezolectric biosensor. *Biosensors and Bioelectronics, 18*(11), 1329-1337.

Malaikozhundan, B., Vaseeharan, B., Vijayakumar, S., Pandiselvi, K., Kalanjiam, M. A. R., Murugan, K., & Benelli, G. (2017). Biological therapeutics of Pongamia pinnata coated zinc oxide nanoparticles against clinically important pathogenic bacteria, fungi and MCF-7 breast cancer cells. *Microbial pathogenesis, 104*, 268-277.

Manaia, E. B., Abucafy, M. P., Chiari-Andreo, B. G., Silva, B. L., Junior, J. A. O., & Chiavacci, L. A. (2017). Physicochemical characterization of drug nanocarriers. *International journal of nanomedicine, 12*, 4991.

Manea, F., Houillon, F. B., Pasquato, L., & Scrimin, P. (2004). Nanozymes: Gold-nanoparticle-based transphosphorylation catalysts. *Angewandte Chemie International Edition, 43*(45), 6165-6169.

Marrazza, G. (2014). Piezoelectric biosensors for organophosphate and carbamate pesticides: a review. *Biosensors, 4*(3), 301-317.

Martinez, J., Chequer, N., Gonzalez, J., & Cordova, T. (2012). Alternative methodology for gold nanoparticles diameter characterization using PCA

technique and UV-VIS spectrophotometry. *Nanoscience and Nanotechnology, 2*(6), 184-189.

Mauriz, E., Calle, A., Manclus, J., Montoya, A., Escuela, A., Sendra, J., & Lechuga, L. M. (2006). Single and multi-analyte surface plasmon resonance assays for simultaneous detection of cholinesterase inhibiting pesticides. *Sensors and Actuators B: Chemical, 118*(1-2), 399-407.

Meng, X., Schultz, C. W., Cui, C., Li, X., & Yu, H.Z. (2015). On-site chip-based colorimetric quantitation of organophosphorus pesticides using an office scanner. *Sensors and Actuators B: Chemical, 215*, 577-583.

Meng, Y., Zhao, K., Zhang, Z., Gao, P., Yuan, J., Cai, T., He, D. (2020). Effects of crystal structure on the activity of MnO_2 nanorods oxidase mimics. *Nano Research, 13*(3), 14.

Millstone, J. E., Park, S., Shuford, K. L., Qin, L., Schatz, G. C., & Mirkin, C. A. (2005). Observation of a quadrupole plasmon mode for a colloidal solution of gold nanoprisms. *Journal of the American Chemical Society, 127*(15), 5312-5313.

Mohamad, A., Teo, H., Keasberry, N. A., & Ahmed, M. U. (2019). Recent developments in colorimetric immunoassays using nanozymes and plasmonic nanoparticles. *Critical reviews in biotechnology, 39*(1), 50-66.

Montali, L., Calabretta, M. M., Lopreside, A., D'Elia, M., Guardigli, M., & Michelini, E. (2020). Multienzyme chemiluminescent foldable biosensor for on-site detection of acetylcholinesterase inhibitors. *Biosensors and Bioelectronics, 162*, 112232.

Mourdikoudis, S., Pallares, R. M., & Thanh, N. T. (2018). Characterization techniques for nanoparticles: comparison and complementarity upon studying nanoparticle properties. *Nanoscale, 10*(27), 12871-12934.

Muhammad, G., Rashid, I., & Firyal, S. (2017). Practical aspects of treatment of organophosphate and carbamate insecticide poisoning in animals. *Matrix Science Pharma, 1*(1), 10-11.

Mulla, S. I., Ameen, F., Talwar, M. P., Eqani, S. A., Bharagava, R. N., Saxena, G., Ninnekar, H. Z. (2020). Organophosphate pesticides: impact on environment,

toxicity, and their degradation. In *Bioremediation of industrial waste for environmental safety* (pp. 265-290).

Musarurwa, H., & Tavengwa, N. T. (2020). Supramolecular solvent-based micro-extraction of pesticides in food and environmental samples. *Talanta*, 121515.

Nagabooshanam, S., John, A. T., Wadhwa, S., Mathur, A., Krishnamurthy, S., & Bharadwaj, L. M. (2020). Electro-deposited nano-webbed structures based on polyaniline/multi walled carbon nanotubes for enzymatic detection of organophosphates. *Food chemistry, 323*, 126784.

Nakaso, K., Shimada, M., Okuyama, K., & Deppert, K. (2002). Evaluation of the change in the morphology of gold nanoparticles during sintering. *Journal of Aerosol Science, 33*(7), 1061-1074.

Ngumbi, P. K., Mugo, S. W., & Ngaruiya, J. M. (2018). Determination of gold nanoparticles sizes via surface plasmon resonance. *IOSR Journal of Applied Chemistry, 11*, 25–29.

Nirala, N. R., & Prakash, R. (2018). One step synthesis of AuNPs@ MoS2-QDs composite as a robust peroxidase-mimetic for instant unaided eye detection of glucose in serum, saliva and tear. *Sensors & Actuators B: Chemical, 263*, 109-119.

Niu, X., He, Y., Pan, J., Li, X., Qiu, F., Yan, Y.,Lan, M. (2016). Uncapped nanobranch-based CuS clews used as an efficient peroxidase mimic enable the visual detection of hydrogen peroxide and glucose with fast response. *Analytica chimica acta, 947*, 42-49.

O Brien, R. D. (2016). *Toxic phosphorus esters: Chemistry, metabolism, and biological effects*: Elsevier.

Okada, E., Coggan, T., Anumol, T., Clarke, B., & Allinson, G. (2019). A simple and rapid direct injection method for the determination of glyphosate and AMPA in environmental water samples. *Analytical and Bioanalytical Chemistry, 411*(3), 715-724.

Orts-Gil, G., Natte, K., Drescher, D., Bresch, H., Mantion, A., Kneipp, J., & Osterle, W. (2011). Characterisation of silica nanoparticles prior to in vitro studies: from primary particles to agglomerates. *Journal of Nanoparticle Research, 13*(4), 1593-1604.

Ottavio, F. d., Pelle, F. d., Montesano, C., Scarpone, R., Escarpa, A., Compagnone, D., & Sergi, M. (2017). Determination of pesticides in wheat flour using microextraction on packed sorbent coupled to ultra-high performance liquid chromatography and tandem mass spectrometry. *Food Analytical Methods, 10*(6), 1699-1708.

Ouyang, Q., Wang, L., Ahmad, W., Rong, Y., Li, H., Hu, Y., & Chen, Q. (2021). A highly sensitive detection of carbendazim pesticide in food based on the upconversion-MnO_2 luminescent resonance energy transfer biosensor. *Food Chemistry, 349*, 129157.

Ovalle, M., Stoytcheva, M., Zlatev, R., & Valdez, B. (2009). Electrochemical study of rat brain acetylcholinesterase inhibition by chlorofos: Kinetic aspects and analytical applications. *Electrochimica Acta, 55*(2), 516-520.

Ozer, E. T., Osman, B., & Parlak, B. (2020). An experimental design approach for the solid phase extraction of some organophosphorus pesticides from water samples with polymeric microbeads. *Microchemical journal, 154*, 104537.

Ozkutuk, E. B., Diltemiz, S. E., Ozalp, E., Say, R., & Ersoz, A. (2013). Ligand exchange based paraoxon imprinted QCM sensor. *Materials Science & Engineering: C, 33*(2), 938-942.

Pandey, I., Sonawane, A., & Bhansali, S. (2020). *Novel Imprinted Metallic Nanozymes Based Nanosensor with Fast Catalytic Activity and Specificity for Cortisol.* Paper presented at the ECS Meeting Abstracts.

Patskovsky, S., Bergeron, E., & Meunier, M. (2015). Hyperspectral darkfield microscopy of PEGylated gold nanoparticles targeting CD44-expressing cancer cells. *Journal of biophotonics, 8*(1-2), 162-167.

Pereira, E. F., Aracava, Y., DeTolla, L. J., Beecham, E. J., Basinger, G. W., Wakayama, E. J., & Albuquerque, E. X. (2014). Animal models that best reproduce the clinical manifestations of human intoxication with organophosphorus compounds. *Journal of Pharmacology Experimental Therapeutics, 350*(2), 313-321.

Perera, S. D., & Dulmini, A. T. (2020). Chemical nature of pesticide. *The Tri-Annual Publication of the Institute of Chemistry Ceylon, 37*, 45-49.

Pilolli, R., Monaci, L., & Visconti, A. (2013). Advances in biosensor development based on integrating nanotechnology and applied to food-allergen management. *TrAC Trends in Analytical Chemistry, 47*, 12-26.

Pinkas, A., Turgeman, G., Tayeb, S., & Yanai, J. (2015). An avian model for ascertaining the mechanisms of organophosphate neuroteratogenicity and its therapy with mesenchymal stem cell transplantation. *Neurotoxicology & teratology, 50*, 73-81.

Pogacnik, L., & Franko, M. (2003). Detection of organophosphate and carbamate pesticides in vegetable samples by a photothermal biosensor. *Biosensors and Bioelectronics, 18*(1), 1-9.

Popovtzer, R., Agrawal, A., Kotov, N. A., Popovtzer, A., Balter, J., Carey, T. E., & Kopelman, R. (2008). Targeted gold nanoparticles enable molecular CT imaging of cancer. *Nano Letters, 8*(12), 4593-4596.

Pundir, C., & Malik, A. J. (2019). Bio-sensing of organophosphorus pesticides: A review. *Biosensors and Bioelectronics, 140*, 111348.

Pundir, C. S., & Chauhan, N. (2012). Acetylcholinesterase inhibition-based biosensors for pesticide determination: A review. *Analytical Biochemistry, 429*(1), 19-31.

Qi, Y., Chen, Y., Xiu, F.R., & Hou, J. J. (2020). An aptamer-based colorimetric sensing of acetamiprid in environmental samples: Convenience, sensitivity and practicability. *Sensors & Actuators B: Chemical, 304*, 127359.

Quinn, D. M. (1987). Acetylcholinesterase: enzyme structure, reaction dynamics, and virtual transition states. *Chemical reviews, 87*(5), 955-979.

Rahman, M. S., Islam, S. M., Haque, A., & Shahjahan, M. (2020). Toxicity of the organophosphate insecticide sumithion to embryo and larvae of zebrafish. *Toxicology reports, 7*, 317-323.

Rahman, S. (2016). Size and concentration analysis of gold nanoparticles with ultraviolet-visible spectroscopy. *Undergraduate Journal of Mathematical Modeling: One+ Two, 7*(1), 2.

Rajangam, B., Daniel, D. K., & Krastanov, A. I. (2018). Progress in enzyme inhibition based detection of pesticides. *Engineering in Life Sciences, 18*(1), 4-19.

Rassaei, L., Marken, F., Sillanpää, M., Amiri, M., Cirtiu, C. M., & Sillanpää, M. (2011). Nanoparticles in electrochemical sensors for environmental monitoring. *TrAC Trends in Analytical Chemistry, 30*(11), 1704-1715.

Ren, S., Li, B., & Zhang, L. (2013). Visual detection of hexokinase activity and inhibition with positively charged gold nanoparticles as colorimetric probes. *Analyst, 138*(11), 3142-3145.

Ren, S., Zhou, F., Xu, C., & Li, B. (2015). Simple method for visual detection of glutathione S-transferase activity and inhibition using cysteamine-capped gold nanoparticles as colorimetric probes. *Gold Bulletin, 48*(3), 147-152.

Ren, W., Mohammed, S. I., Wereley, S., & Irudayaraj, J. (2019). Magnetic focus lateral flow sensor for detection of cervical cancer biomarkers. *Analytical chemistry, 91*(4), 2876-2884.

Renneberg, R., Pfeiffer, D., Lisdat, F., Wilson, G., Wollenberger, U., Ligler, F., & Turner, A. P. (2007). Frieder Scheller and the short history of biosensors. In *Biosensing for the 21st Century* (pp. 1-18).

Reuveni, T., Motiei, M., Romman, Z., Popovtzer, A., & Popovtzer, R. (2011). Targeted gold nanoparticles enable molecular CT imaging of cancer: an in vivo study. *International journal of nanomedicine, 6*, 2859.

Reybier, K., Zairi, S., Jaffrezic-Renault, N., & Fahys, B. (2002). The use of polyethyleneimine for fabrication of potentiometric cholinesterase biosensors. *Talanta, 56*(6), 1015-1020.

Richardson, J. R., Fitsanakis, V., Westerink, R. H., & Kanthasamy, A. G. (2019). Neurotoxicity of pesticides. *Acta neuropathologica, 138*(3), 343-362.

Rodriguez-Mozaz, S., de Alda, M. J. L., Marco, M.-P., & Barcelo, D. (2005). Biosensors for environmental monitoring: A global perspective. *Talanta, 65*(2), 291-297.

Rosch, A., Beck, B., Hollender, J., & Singer, H. (2019). Picogram per liter quantification of pyrethroid and organophosphate insecticides in surface waters: a result of large enrichment with liquid–liquid extraction and gas chromatography coupled to mass spectrometry using atmospheric pressure chemical ionization. *Analytical and Bioanalytical Chemistry, 411*(14), 3151-3164.

Rosi, N. L., & Mirkin, C. A. (2005). Nanostructures in biodiagnostics. *Chemical reviews, 105*(4), 1547-1562.

Saha, K., Agasti, S. S., Kim, C., Li, X., & Rotello, V. M. (2012). Gold nanoparticles in chemical and biological sensing. *Chemical reviews, 112*(5), 2739-2779.

Sajanlal, P. R., Sreeprasad, T. S., Samal, A. K., & Pradeep, T. (2011). Anisotropic nanomaterials: structure, growth, assembly, and functions. *Nano reviews, 2*(1), 5883.

Santoni, G., de Sousa, J., de la Mora, E., Dias, J., Jean, L., Sussman, J. L.,Weik, M. (2018). Structure-based optimization of nonquaternary reactivators of acetylcholinesterase inhibited by organophosphorus nerve agents. *Journal of medicinal chemistry, 61*(17), 7630-7639.

Sapsford, K. E., Algar, W. R., Berti, L., Gemmill, K. B., Casey, B. J., Oh, E., Medintz, I. L. (2013). Functionalizing nanoparticles with biological molecules: developing chemistries that facilitate nanotechnology. *Chemical reviews, 113*(3), 1904-2074.

Saratale, R. G., Saratale, G. D., Shin, H. S., Jacob, J. M., Pugazhendhi, A., Bhaisare, M., & Kumar, G. (2018). New insights on the green synthesis of metallic nanoparticles using plant and waste biomaterials: current knowledge, their agricultural and environmental applications. *Environmental Science and Pollution Research, 25*(11), 10164-10183.

Selvolini, G., Bajan, I., Hosu, O., Cristea, C., Sandulescu, R., & Marrazza, G. (2018). DNA-based sensor for the detection of an organophosphorus pesticide: Profenofos. *Sensors, 18*(7), 2035.

Shah, A., Tauseef, I., Ali, M. B., Yameen, M. A., Mezni, A., Hedfi, A.,Haq, S. (2021). In-Vitro and In-Vivo Tolerance and Therapeutic Investigations of Phyto-Fabricated Iron Oxide Nanoparticles against Selected Pathogens. *Toxics, 9*(5), 105.

Shah, J., Purohit, R., Singh, R., Karakoti, A. S., & Singh, S. (2015). ATP-enhanced peroxidase-like activity of gold nanoparticles. *Journal of colloid interface science, 456*, 100-107.

Sharma, C., Shukla, N., & Bansal, G. (2020). Selected blood parameters altered by different doses of pesticide Malathion in albino rat (Rattus-norvegicus). *Environment Conservation Journal, 21*(3), 93-103.

Sharma, D., Wangoo, N., & Sharma, R. K. (2021). Sensing platform for pico-molar level detection of ethyl parathion using Au-Ag nanoclusters based enzymatic strategy. *Talanta, 221*, 121267.

Shimada, H., Kiyozumi, Y., Koga, Y., Ogata, Y., Katsuda, Y., Kitamura, Y., Ihara, T. (2019). A novel cholinesterase assay for the evaluation of neurotoxin poisoning based on the electron-transfer promotion effect of thiocholine on an Au electrode. *Sensors and Actuators B: Chemical, 298*, 126893.

Shu, H. C., Chen, Y. S., & Wu, N. P. (2021). Analysis of pesticides based on immobilized housefly head acetylcholinesterase reactor with choline oxidase and horseradish peroxidase carbon paste electrode. *Journal of the Chinese Chemical Society, 68*(2), 306-314.

Sidhu, G. K., Singh, S., Kumar, V., Dhanjal, D. S., Datta, S., & Singh, J. (2019). Toxicity, monitoring and biodegradation of organophosphate pesticides: a review. *Critical reviews in environmental science technology, 49*(13), 1135-1187.

Silva Adaya, D., Aguirre-Cruz, L., Guevara, J., & Ortiz-Islas, E. (2017). Nanobiomaterials' applications in neurodegenerative diseases. *Journal of biomaterials applications, 31*(7), 953-984.

Singh, P., & Prasad, S. M. (2018). Antioxidant enzyme responses to the oxidative stress due to chlorpyrifos, dimethoate and dieldrin stress in palak (Spinacia oleracea L.) and their toxicity alleviation by soil amendments in tropical croplands. *Science of the Total Environment, 630*, 839-848.

Singh, S. (2019a). Emerging Trends in Nanotechnology: Nanozymes, Imaging Probes and Biosensors and Nanocarriers. *Current drug metabolism, 20*(6), 414-415.

Singh, S. (2019b). Nanomaterials exhibiting enzyme-like properties (Nanozymes): Current advances and future perspectives. *Frontiers in Chemistry, 7*, 46.

Sobczak-Kupiec, A., Malina, D., Zimowska, M., & Wzorek, Z. (2011). Characterization of gold nanoparticles for various medical application. *Digest Journal of Nanomaterials and Biostructures, 6*(2), 803-808.

Song, W., Zhao, B., Wang, C., Ozaki, Y., & Lu, X. (2019). Functional nanomaterials with unique enzyme-like characteristics for sensing applications. *Journal of Materials Chemistry B, 7*(6), 850-875.

Songa, E. A., Arotiba, O. A., Owino, J. H., Jahed, N., Baker, P. G., & Iwuoha, E. I. (2009). Electrochemical detection of glyphosate herbicide using horseradish peroxidase immobilized on sulfonated polymer matrix. *Bioelectrochemistry, 75*(2), 117-123.

Songa, E. A., & Okonkwo, J. O. (2016). Recent approaches to improving selectivity and sensitivity of enzyme-based biosensors for organophosphorus pesticides: A review. *Talanta, 155*, 289-304.

Souza, T. G., Ciminelli, V. S., & Mohallem, N. D. (2016). *A comparison of TEM and DLS methods to characterize size distribution of ceramic nanoparticles.* Paper presented at the Journal of physics: conference series.

Soysal, M. (2019). Voltammetric determination of fenitrothion based on pencil graphite electrode modified with poly (Purpald®). *Chemical Papers, 73*(7), 1785-1794.

Srivastav, A. K., Srivastava, S., Srivastav, S. K., & Suzuki, N. (2017). Acute toxicity of an organophosphate insecticide chlorpyrifos to an anuran, Rana cyanophlyctis. *Iranian Journal of Toxicology, 11*(2), 45-49.

Subburaj, A., Jawahar, P., Jayakumar, N., Srinivasan, A., & Ahilan, B. (2018). Histopathological investigations in liver and kidney of the fish, Oreochromis mossambicus (Tilapia) exposed to acute Malathion (EC 50%) toxicity. *Journal of Experimental Zoology, India, 21*(1), 77-81.

Sulaiman, I. C., Chieng, B., Osman, M., Ong, K., Rashid, J., Yunus, W. W., Mohamad, A. (2020). A review on colorimetric methods for determination of organophosphate pesticides using gold and silver nanoparticles. *Microchimica Acta, 187*(2), 1-22.

Sun, L., Xu, W., Peng, T., Chen, H., Ren, L., Tan, H., Fu, Z. (2016). Developmental exposure of zebrafish larvae to organophosphate flame retardants causes neurotoxicity. *Neurotoxicology & teratology, 55*, 16-22.

Sun, X., Gao, C., Zhang, L., Yan, M., Yu, J., & Ge, S. (2017). Photoelectrochemical sensor based on molecularly imprinted film modified hierarchical branched

titanium dioxide nanorods for chlorpyrifos detection. *Sensors and Actuators B: Chemical, 251*, 1-8.

Sun, Y., Tan, H., & Li, Y. (2018). A colorimetric assay for acetylcholinesterase activity and inhibitor screening based on the thiocholine-induced inhibition of the oxidative power of MnO_2 nanosheets on 3, 3′, 5, 5′-tetramethylbenzidine. *Microchimica Acta, 185*(10), 1-8.

Teranishi, T. (2003). Fabrication and electronic properties of gold nanoparticle superlattices. *Comptes Rendus Chimie, 6*(8-10), 979-987.

Thepudom, T., Lertvachirapaiboon, C., Shinbo, K., Kato, K., Kaneko, F., Kerdcharoen, T., & Baba, A. (2018). Surface plasmon resonance-enhanced photoelectrochemical sensor for detection of an organophosphate pesticide chlorpyrifos. *MRS Communications, 8*(1), 107-112.

Thompson, D. T. (2007). Using gold nanoparticles for catalysis. *Nano Today, 2*(4), 40-43.

Tiwari, N., Asthana, A., & Upadhyay, K. (2013). Kinetic-spectrophotometric determination of methyl parathion in water and vegetable samples. *Spectrochimica Acta Part A: Molecular and Biomolecular Spectroscopy, 101*, 54-58.

Ton, X. A., Tse Sum Bui, B., Resmini, M., Bonomi, P., Dika, I., Soppera, O., & Haupt, K. (2013). A Versatile Fiber-Optic Fluorescence Sensor Based on Molecularly Imprinted Microstructures Polymerized in Situ. *Angewandte Chemie - International Edition, 125*(32), 8475-8479.

Touloupakis, E., Boutopoulos, C., Buonasera, K., Zergioti, I., & Giardi, M. T. (2012). A photosynthetic biosensor with enhanced electron transfer generation realized by laser printing technology. *Analytical and Bioanalytical Chemistry, 402*(10), 3237-3244.

Tretter, T. (2006). Conceptualizing nanoscale. *The Science Teacher, 73*(9), 50.

Tsai, Y. H., & Lein, P. J. (2021). Mechanisms of Organophosphate Neurotoxicity. *Current Opinion in Toxicology, 26*, 49-60.

Tseng, M.H., Hu, C.C., & Chiu, T.C. (2019). A fluorescence turn-on probe for sensing thiodicarb using rhodamine B functionalized gold nanoparticles. *Dyes and Pigments, 171*, 107674.

Turkevich, J., Stevenson, P. C., & Hillier, J. (1951). A study of the nucleation and growth processes in the synthesis of colloidal gold. *Discussions of the Faraday Society, 11*, 55-75.

Turner, M., Golovko, V. B., Vaughan, O. P., Abdulkin, P., Berenguer-Murcia, A., Tikhov, M. S.,Lambert, R. M. (2008). Selective oxidation with dioxygen by gold nanoparticle catalysts derived from 55-atom clusters. *Nature, 454*(7207), 981-983.

Tvorynska, S., Barek, J., & Josypcuk, B. (2020). Acetylcholinesterase-choline oxidase-based mini-reactors coupled with silver solid amalgam electrode for amperometric detection of acetylcholine in flow injection analysis. *Journal of Electroanalytical Chemistry, 860*, 113883.

Tyagi, H., Kushwaha, A., Kumar, A., & Aslam, M. (2016). A facile pH controlled citrate-based reduction method for gold nanoparticle synthesis at room temperature. *Nanoscale research letters, 11*(1), 1-11.

Van Dong, P., Ha, C. H., & Kasbohm, J. (2012). Chemical synthesis and antibacterial activity of novel-shaped silver nanoparticles. *International Nano Letters, 2*(1), 1-9.

Verebes, G. S., Melchiorre, M., Garcia-Leis, A., Ferreri. C., Marzetti, C., & Torreggiani, A. (2013). Hyperspectral enhanced dark field microscopy for imaging blood cells. *Journal of biophotonics, 6*(11-12), 960-967.

Vikesland, P. J. (2018). Nanosensors for water quality monitoring. *Nature nanotechnology, 13*(8), 651-660.

Wang, A., Cockburn, M., Ly, T. T., Bronstein, J. M., & Ritz, B. (2014). The association between ambient exposure to organophosphates and Parkinson's disease risk. *Occupational and environmental medicine, 71*(4), 275-281.

Wang, C., Liu, C., Luo, J., Tian, Y., & Zhou, N. (2016). Direct electrochemical detection of kanamycin based on peroxidase-like activity of gold nanoparticles. *Analytica Chimica Acta, 936*, 75-82.

Wang, F., Lu, Y., Jing, W., He, L., Gao, X., & Liu, Y. (2017). Lab-on-nanoparticle as a multidimensional device for colorimetric discrimination of proteins. *Microchimica Acta, 184*(9), 3265-3271.

Wang, G.L., Jin, L.Y., Dong, Y.M., Wu, X.M., & Li, Z.J. (2015). Intrinsic enzyme mimicking activity of gold nanoclusters upon visible light triggering and its application for colorimetric trypsin detection. *Biosensors and Bioelectronics, 64*, 523-529.

Wang, L., Hu, Z., Wu, S., Pan, J., Xu, X., & Niu, X. (2020). A peroxidase-mimicking Zr-based MOF colorimetric sensing array to quantify and discriminate phosphorylated proteins. *Analytica Chimica Acta, 1121*, 26-34.

Wang, M., Su, K., Cao, J., She, Y., Abd El-Aty, A., Hacımuftuoglu, A.,Lao, S. (2019). "Off-On" non-enzymatic sensor for malathion detection based on fluorescence resonance energy transfer between β-cyclodextrin@ Ag and fluorescent probe. *Talanta, 192*, 295-300.

Wang, P., Wan, Y., Ali, A., Deng, S., Su, Y., Fan, C., & Yang, S. (2016). Aptamer-wrapped gold nanoparticles for the colorimetric detection of omethoate. *Science China Chemistry, 59*(2), 237-242.

Wang, R., Tang, J., Xie, Z., Mi, W., Chen, Y., Wolschke, H., Ebinghaus, R. (2015). Occurrence and spatial distribution of organophosphate ester flame retardants and plasticizers in 40 rivers draining into the Bohai Sea, north China. *Environmental Pollution, 198*, 172-178.

Wani, A. A., Dar, A. A., Jan, I., Sofi, K. A., Sofi, J. A., & Dar, I. H. J. (2019). Method validation and simultaneous quantification of eight organochlorines/organophosphates in apple by gas chromatography. *Journal of the Science of Food & Agriculture, 99*(7), 3687-3692.

Weerathunge, P., Behera, B. K., Zihara, S., Singh, M., Prasad, S. N., Hashmi, S., Ramanathan, R. (2019). Dynamic interactions between peroxidase-mimic silver NanoZymes and chlorpyrifos-specific aptamers enable highly-specific pesticide sensing in river water. *Analytica chimica acta, 1083*, 157-165.

Wei, H., & Wang, E. (2013). Nanomaterials with enzyme-like characteristics (nanozymes): next-generation artificial enzymes. *Chemical Society Reviews, 42*(14), 6060-6093.

Wen-Wen, C., Yong-Ming, G., Zheng, W.-S., Xianyu, Y.L., Zhuo, W., & Jiang, X.Y. (2014). Recent progress of colorimetric assays based on gold nanoparticles for biomolecules. *Chinese Journal of Analytical Chemistry, 42*(3), 307-314.

Whitesides, G. M. (2003). The'right'size in nanobiotechnology. *Nature biotechnology, 21*(10), 1161-1165.

Willets, K. A., & Van Duyne, R. P. (2007). Localized surface plasmon resonance spectroscopy and sensing. *Annual Review of Physical Chemistry, 58*, 267-297.

Wu, J., Wang, X., Wang, Q., Lou, Z., Li, S., Zhu, Y.,Wei, H. (2019). Nanomaterials with enzyme-like characteristics (nanozymes): next-generation artificial enzymes (II). *Chemical Society Reviews, 48*(4), 1004-1076.

Wu, M., Deng, H., Fan, Y., Hu, Y., Guo, Y., & Xie, L. (2018). Rapid colorimetric detection of cartap residues by AgNP sensor with magnetic molecularly imprinted microspheres as recognition elements. *Molecules, 23*(6), 1443.

Wu, S., Li, D., Wang, J., Zhao, Y., Dong, S., & Wang, X. (2017). Gold nanoparticles dissolution based colorimetric method for highly sensitive detection of organophosphate pesticides. *Sensors and Actuators B: Chemical, 238*, 427-433.

Wu, X., Song, Y., Yan, X., Zhu, C., Ma, Y., Du, D., & Lin, Y. (2017). Carbon quantum dots as fluorescence resonance energy transfer sensors for organophosphate pesticides determination. *Biosensors and Bioelectronics, 94*, 292-297.

Wu, Y., Chen, Y., Li, Y., Huang, J., Yu, H., & Wang, Z. (2018). Accelerating peroxidase-like activity of gold nanozymes using purine derivatives and its application for monitoring of occult blood in urine. *Sensors & Actuators B: Chemical, 270*, 443-451.

Wu, Y., Jiao, L., Luo, X., Xu, W., Wei, X., Wang, H.,Du, D. (2019). Oxidase-Like Fe-N-C single-atom nanozymes for the detection of acetylcholinesterase activity. *Small, 15*(43), 1903108.

Xia, F., Zuo, X., Yang, R., Xiao, Y., Kang, D., Vallee-Belisle, A.,Heeger, A. J. (2010). Colorimetric detection of DNA, small molecules, proteins, and ions using unmodified gold nanoparticles and conjugated polyelectrolytes. *Proceedings of the National Academy of Sciences, 107*(24), 10837-10841.

Xia, Y., Xiong, Y., Lim, B., & Skrabalak, S. E. (2009). Shape-controlled synthesis of metal nanocrystals: simple chemistry meets complex physics? *Angewandte Chemie International Edition, 48*(1), 60-103.

Xiao, L., & Yeung, E. S. (2014). Optical imaging of individual plasmonic nanoparticles in biological samples. *Annual Review of Analytical Chemistry, 7*, 89-111.

Xiong, S., Deng, Y., Zhou, Y., Gong, D., Xu, Y., Yang, L., Luo, A. (2018). Current progress in biosensors for organophosphorus pesticides based on enzyme functionalized nanostructures: a review. *Analytical Methods, 10*(46), 5468-5479.

Xu, S., Guo, C., Li, Y., Yu, Z., Wei, C., & Tang, Y. (2014). Methyl parathion imprinted polymer nanoshell coated on the magnetic nanocore for selective recognition and fast adsorption and separation in soils. *Journal of hazardous materials, 264*, 34-41.

Xu, Z.L., Deng, H., Deng, X.F., Yang, J.Y., Jiang, Y.M., Zeng, D.P.,Wang, H. (2012). Monitoring of organophosphorus pesticides in vegetables using monoclonal antibody-based direct competitive ELISA followed by HPLC–MS/MS. *Food Chemistry, 131*(4), 1569-1576.

Yadav, I. C., Devi, N. L., Zhong, G., Li, J., Zhang, G., & Covaci, A. (2017). Occurrence and fate of organophosphate ester flame retardants and plasticizers in indoor air and dust of Nepal: implication for human exposure. *Environmental Pollution, 229*, 668-678.

Yan, X., Kong, D., Jin, R., Zhao, X., Li, H., Liu, F.,Lu, G. (2019). Fluorometric and colorimetric analysis of carbamate pesticide via enzyme-triggered decomposition of Gold nanoclusters-anchored MnO_2 nanocomposite. *Sensors and Actuators B: Chemical, 290*, 640-647.

Yan, X., Li, H., Han, X., & Su, X. (2015). A ratiometric fluorescent quantum dots based biosensor for organophosphorus pesticides detection by inner-filter effect. *Biosensors and Bioelectronics, 74*, 277-283.

Yan, X., Li, H., Wang, X., & Su, X. (2015). A novel fluorescence probing strategy for the determination of parathion-methyl. *Talanta, 131*, 88-94.

Yan, X., Song, Y., Wu, X., Zhu, C., Su, X., Du, D., & Lin, Y. (2017). Oxidase-mimicking activity of ultrathin MnO_2 nanosheets in colorimetric assay of acetylcholinesterase activity. *Nanoscale, 9*(6), 2317-2323.

Yan, X., Song, Y., Zhu, C., Li, H., Du, D., Su, X., & Lin, Y. (2018). MnO_2 nanosheet-carbon dots sensing platform for sensitive detection of organophosphorus pesticides. *Analytical Chemistry, 90*(4), 2618-2624.

Yanez-Sedeno, P., Agui, L., Villalonga, R., & Pingarron, J. (2014). Biosensors in forensic analysis. A review. *Analytica Chimica Acta, 823*, 1-19.

Yang, T., & Duncan, T. V. (2021). Challenges and potential solutions for nanosensors intended for use with foods. *Nature nanotechnology, 16*(3), 251-265.

Yanga Liu, X. (2018). Remote activation of nanoparticulate biomimetic activity by light triggered pH-jump. *Chemical Communications, 54*(62), 8641-8644.

Yin, H., Huang, X., Ma, W., Xu, L., Zhu, S., Kuang, H., & Xu, C. (2014). Ligation Chain Reaction based gold nanoparticle assembly for ultrasensitive DNA detection. *Biosensors and Bioelectronics, 52*, 8-12.

Yin, X.L., Liu, Y. Q., Gu, H.W., Zhang, Q., Zhang, Z. W., Li, H., Zhou, Y. (2021). Multicolor enzyme-linked immunosorbent sensor for sensitive detection of organophosphorus pesticides based on TMB2+-mediated etching of gold nanorods. *Microchemical journal, 168*, 106411.

Ying, X., Xu, X., Hu, M.J., Zhu, Z.W., Min, J., & Shi, J.H. (2009). Determination of Thirteen Organophosphate Pesticides Residue in Chinese Chive by Capillary Gas Chromatography [J]. *Journal of Instrumental Analysis, 10.*

You, J.G., Liu, Y.W., Lu, C.Y., Tseng, W.L., & Yu, C.J. (2017). Colorimetric assay of heparin in plasma based on the inhibition of oxidase-like activity of citrate-capped platinum nanoparticles. *Biosensors and Bioelectronics, 92*, 442-448.

Yu, D., Blankert, B., Vire, J. C., & Kauffmann, J. M. (2005). Biosensors in drug discovery and drug analysis. *Analytical letters, 38*(11), 1687-1701.

Yuan, X., Chen, S., Li, S., Liu, Q., Kou, M., Xu, T.,Zhang, M. (2019). Enzymatic reaction modulation of G-quadruplex formation for the sensitive homogeneous fluorescence sensing of cholinesterase and organophosphate pesticides. *Analytical Methods, 11*(7), 980-988.

Zamora-Perez, P., Tsoutsi, D., Xu, R., & Rivera-Gil, P. (2018). Hyperspectral-enhanced dark field microscopy for single and collective nanoparticle characterization in biological environments. *Materials Advances, 11*(2), 243.

Zeng, Y., Zhu, Z., Du, D., & Lin, Y. (2016). Nanomaterial-based electrochemical biosensors for food safety. *Journal of Electroanalytical Chemistry, 781*, 147-154.

Zhan, Y., Zeng, Y., Li, L., Guo, L., Luo, F., Qiu, B., Lin, Z. (2019). Cu2+-modified boron nitride nanosheets-supported subnanometer gold nanoparticles: an oxidase-mimicking nanoenzyme with unexpected oxidation properties. *Analytical Chemistry, 92*(1), 1236-1244.

Zhang, D., Chen, Z., Omar, H., Deng, L., & Khashab, N. M. (2015). Colorimetric peroxidase mimetic assay for uranyl detection in sea water. *ACS applied materials & interfaces, 7*(8), 4589-4594.

Zhang, H., & Yang, K.L. (2020). In situ formation and immobilization of gold nanoparticles on polydimethylsiloxane (PDMS) exhibiting catalase-mimetic activity. *Chemical Communications, 56*(47), 6416-6419.

Zhang, M., Liu, Y.Q., & Ye, B.C. (2011). Colorimetric assay for sulfate using positively-charged gold nanoparticles and its application for real-time monitoring of redox process. *Analyst, 136*(21), 4558-4562.

Zhang, P., Sun, T., Rong, S., Zeng, D., Yu, H., Zhang, Z.,Pan, H. (2019). A sensitive amperometric AChE-biosensor for organophosphate pesticides detection based on conjugated polymer and Ag-rGO-NH_2 nanocomposite. *Bioelectrochemistry, 127*, 163-170.

Zhang, S.X., Xue, S.F., Deng, J., Zhang, M., Shi, G., & Zhou, T. (2016). Polyacrylic acid-coated cerium oxide nanoparticles: an oxidase mimic applied for colorimetric assay to organophosphorus pesticides. *Biosensors and Bioelectronics, 85*, 457-463.

Zhang, Y., Chu, W., Foroushani, A. D., Wang, H., Li, D., Liu, J.Yang, W. (2014). New gold nanostructures for sensor applications: a review. *Materials, 7*(7), 5169-5201.

Zhao, G., Zhou, B., Wang, X., Shen, J., & Zhao, B. (2021). Detection of organophosphorus pesticides by nanogold/mercaptomethamidophos multi-residue electrochemical biosensor. *Food Chemistry, 354*, 129511.

Zhao, Q., Yan, H., Liu, P., Yao, Y., Wu, Y., Zhang, J., Chang, J. (2016). An ultra-sensitive and colorimetric sensor for copper and iron based on glutathione-functionalized gold nanoclusters. *Analytica Chimica Acta, 948*, 73-79.

Zheng, J. (2014). Improving Sample Preparation Methods to Assess Nanoparticle Agglomeration using TEM. *Microscopy and Microanalysis, 20*(S3), 1236-1237.

Zheng, J., Zhang, H., Qu, J., Zhu, Q., & Chen, X. (2013). Visual detection of glyphosate in environmental water samples using cysteamine-stabilized gold nanoparticles as colorimetric probe. *Analytical Methods, 5*(4), 917-924.

Zheng, M., Wang, Y., Wang, C., Wei, W., Ma, S., Sun, X., & He, J. (2018). Silver nanoparticles-based colorimetric array for the detection of Thiophanate-methyl. *Spectrochimica Acta Part A: Molecular & Biomolecular Spectroscopy, 198*, 315-321.

Zhou, W., Hu, K., Kwee, S., Tang, L., Wang, Z., Xia, J., & Li, X. (2020). Gold nanoparticle aggregation-induced quantitative photothermal biosensing using a thermometer: a simple and universal biosensing platform. *Analytical Chemistry, 92*(3), 2739-2747.

Zhou, X., Wang, C., Wu, L., Wei, W., & Liu, S. (2021). An OliGreen-responsive fluorescence sensor for sensitive detection of organophosphorus pesticide based on its specific selectivity towards T-Hg2+-T DNA structure. *Spectrochimica Acta Part A: Molecular & Biomolecular Spectroscopy, 247*, 119155.

Zhou, Y., Huang, W., & He, Y. (2018). pH-Induced silver nanoprism etching-based multichannel colorimetric sensor array for ultrasensitive discrimination of thiols. *Sensors & Actuators B: Chemical, 270*, 187-191.

Zhu, S., Zeng, M., Guo, W., Feng, G., & Wu, H. J. (2019). Catalase-mimetic gold nanoparticles inhibit the antagonistic action of Lactobacillus gasseri toward foodborne enteric pathogens in associative cultures. *Journal of Environmental Science Health, Part C, 37*(2), 55-66.

Zhu, Y., Cai, Y., Zhu, Y., Zheng, L., Ding, J., Quan, Y.,Qi, B. (2015). Highly sensitive colorimetric sensor for Hg^{2+} detection based on cationic polymer/DNA interaction. *Biosensors and Bioelectronics, 69*, 174-178.

Appendices

APPENDIX 1: Zeta Potential Analysis of C-AuNPs

		Mean (mV)	Area (%)	St Dev (mV)
	Peak 1:	37.4	100.0	5.97
Zeta Deviation (mV): 5.97	Peak 2:	0.00	0.0	0.00
Conductivity (mS/cm): 1.12	Peak 3:	0.00	0.0	0.00

Result quality :

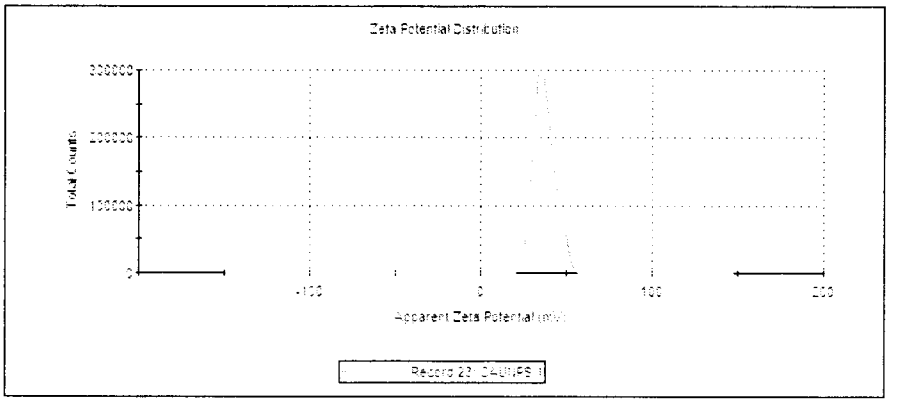

		Mean (mV)	Area (%)	St Dev (mV)
	Peak 1:	41.8	100.0	6.01
Zeta Deviation (mV): 6.01	Peak 2:	0.00	0.0	0.00
Conductivity (mS/cm): 1.23	Peak 3:	0.00	0.0	0.00

Result quality :

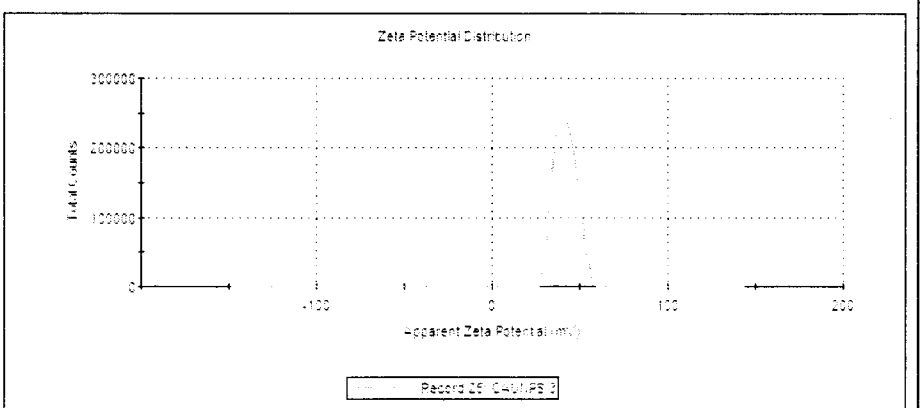

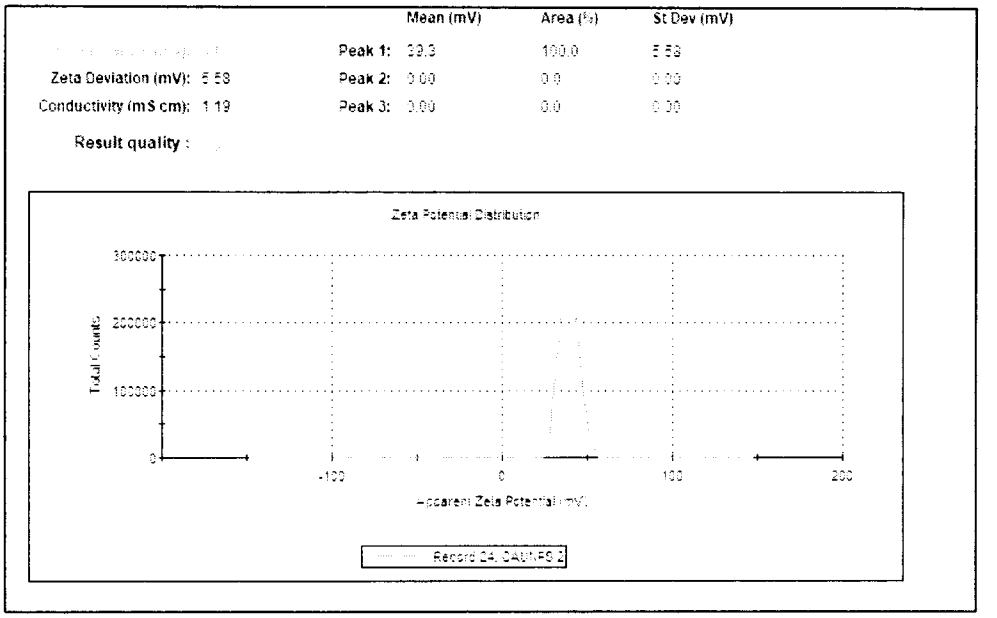

APPENDIX 2: Dark field imagging of C-AuNPs

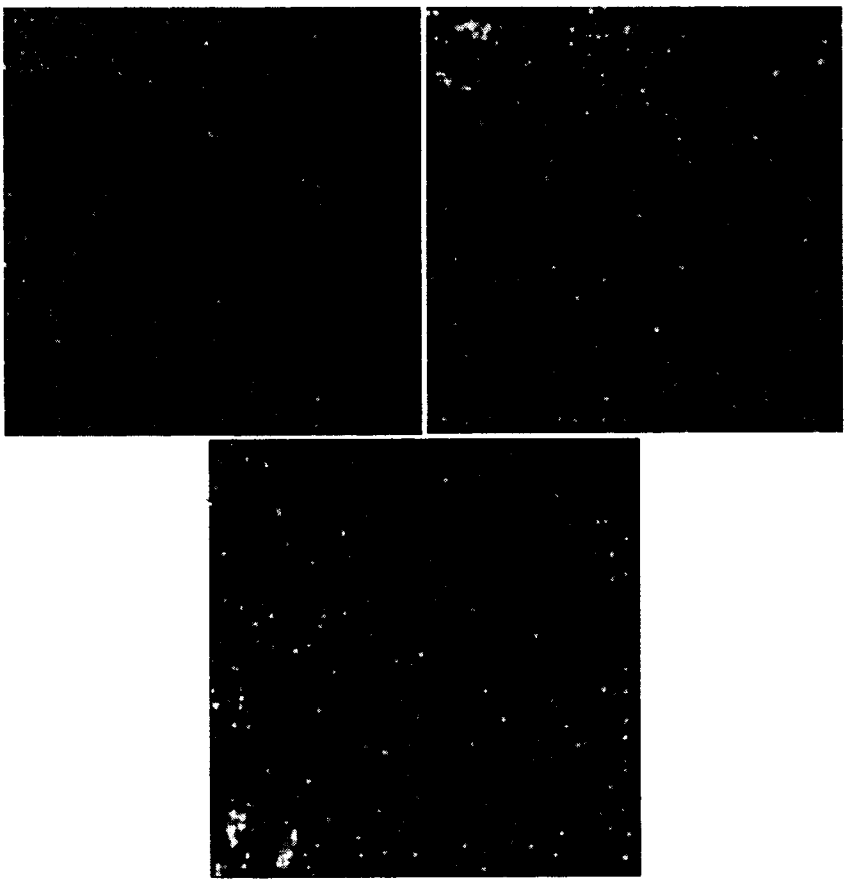

APPENDIX 3: Dynaminc Light Scattering of C-AuNPs

		Size (d.nm):	% Intensity:	St Dev (d.nm):
	Peak 1:	35.04	82.1	12.53
	Peak 2:	299.9	13.8	87.00
Intercept: 0.872	Peak 3:	5169	4.2	491.0

Result quality :

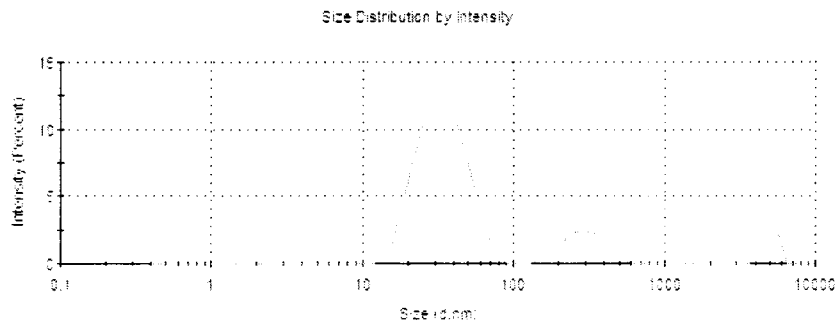

		Size (d.nm):	% Intensity:	St Dev (d.nm):
	Peak 1:	39.25	84.2	16.74
	Peak 2:	444.4	11.1	175.7
Intercept: 0.872	Peak 3:	4620	4.7	824.8

Result quality :

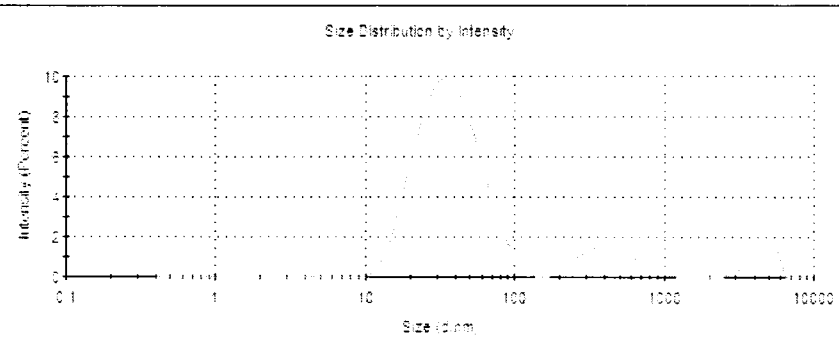

		Size (d.nm):	% Intensity:	St Dev (d.nm):
	Peak 1:	36.69	77.0	15.30
	Peak 2:	347.0	11.2	133.9
Intercept: 0.868	Peak 3:	4559	5.6	956.9

Result quality :

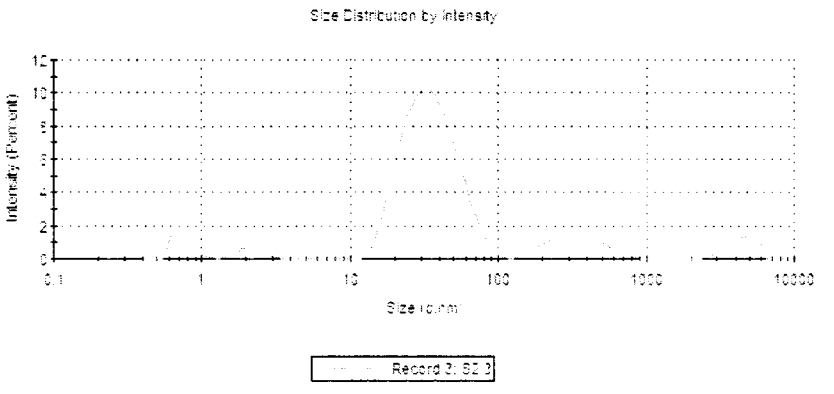

APPENDIX 4: TEM Images of C-AuNPs

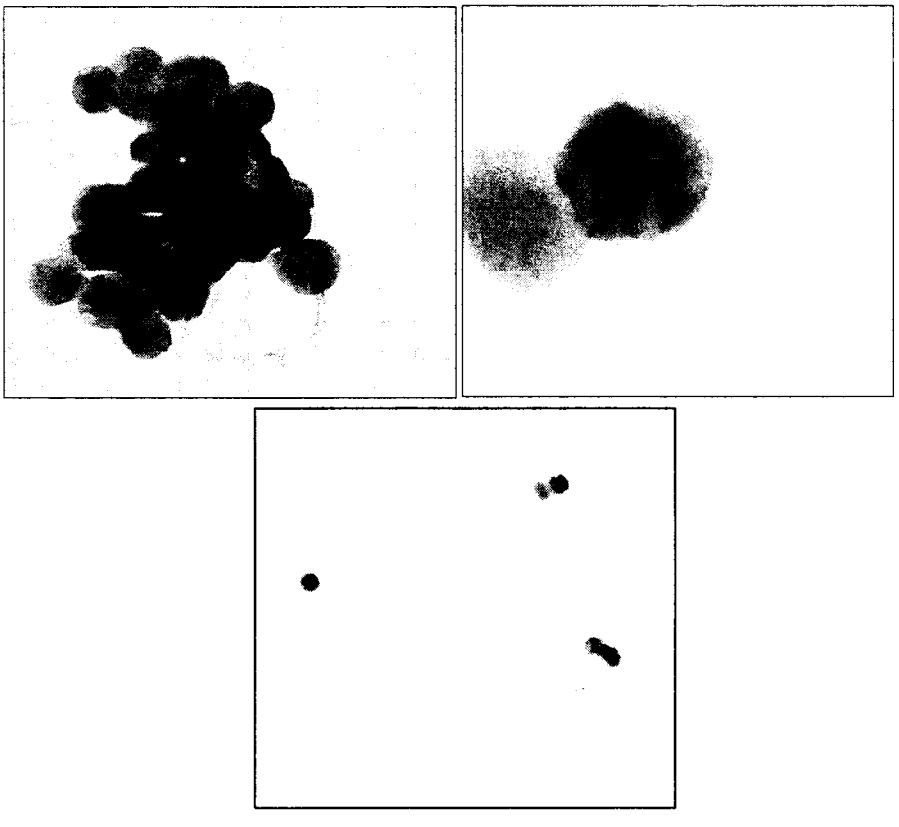

sensors

MDPI

Article

Colorimetric Detection of Organophosphate Pesticides Based on Acetylcholinesterase and Cysteamine Capped Gold Nanoparticles as Nanozyme

Muhammad Musaddiq Shah [1,2,3], Wen Ren [2,3], Joseph Irudayaraj [2,3,4], Abdulrahim A. Sajini [5], Muhammad Ishtiaq Ali [6] and Bashir Ahmad [1,*]

1 Department of Biological Sciences, International Islamic University, Islamabad 44000, Pakistan; musaddiq.phdbt74@iiu.edu.pk
2 Department of Bioengineering, The University of Illinois at Urbana-Champaign, Urbana, IL 61801, USA; wenren@illinois.edu (W.R.); jirudaya@illinois.edu (J.I.)
3 Biomedical Research Center, Mills Breast Cancer Institute, Carle Foundation Hospital, Urbana, IL 61801, USA
4 Micro and Nanotechnology Laboratory, The University of Illinois at Urbana-Champaign, Urbana, IL 61801, USA
5 Department of Biomedical Engineering, The Khalifa University, Abu Dhabi 127788, United Arab Emirates; abdulrahim.sajini@ku.ac.ae
6 Department of Microbiology, Quaid-i-Azam University, Islamabad 45320, Pakistan; ishimrl@qau.edu.pk
* Correspondence: bashir.ahmad@iiu.edu.pk

Citation: Shah, M.M.; Ren, W.; Irudayaraj, J.; Sajini, A.A.; Ali, M.I.; Ahmad, B. Colorimetric Detection of Organophosphate Pesticides Based on Acetylcholinesterase and Cysteamine Capped Gold Nanoparticles as Nanozyme. *Sensors* **2021**, *21*, 8050. https://doi.org/10.3390/s21238050

Academic Editor: Pedro Viana Baptista

Received: 12 October 2021
Accepted: 18 November 2021
Published: 2 December 2021

Abstract: Organophosphates (OPs) are neurotoxic agents also used as pesticides that can permanently block the active site of the acetylcholinesterase (AChE). A robust and sensitive detection system of OPs utilising the enzyme mimic potential of the cysteamine capped gold nanoparticles (C-AuNPs) was developed. The detection assay was performed by stepwise addition of AChE, parathion ethyl (PE)-a candidate OP, acetylcholine chloride (ACh), C-AuNPs, and 3, 3′, 5, 5′-tetramethylbenzidine (TMB) in the buffer solution. The whole sensing protocol completes in 30–40 min, including both incubations. The Transmission Electron Microscopy (TEM) results indicated that the NPs are spherical and have an average size of 13.24 nm. The monomers of C-AuNPs exhibited intense catalytic activity (nanozyme) for the oxidization of TMB, revealed by the production of instant blue colour and confirmed by a sharp peak at 652 nm. The proposed biosensor's detection limit and linear ranges were 5.8 ng·mL^{-1} and 11.6–92.8 ng·mL^{-1}, respectively, for PE. The results strongly advocate that the suggested facile colorimetric biosensor may provide an excellent platform for on-site monitoring of OPs.

Keywords: acetylcholinesterase inhibitors; pesticide intoxication; colorimetric biosensor; neurotoxin; nanozyme; parathion ethyl

1. Introduction

Organophosphates (OPs) are commonly used as chemical warfare agents and pesticides in developing countries due to their low cost, wide availability, and high potency [1,2]. Due to their inclusive efficacy as insecticides (methyl parathion, chlorpyrifos), herbicides (glyphosate, diuron), nematicide (carbofuran, carbaryl), and fungicides (imazalil, thiabendazole); the OP pesticides have extensively been applied in agricultural pest control. The residues of the OPs, which have a long persistence in the natural environment, pose a severe threat to terrestrial and aquatic animals [3]. Even low-dose exposures of OPs for a long time can induce adversative health effects on fauna [4]. According to the U.S. Environmental Protection Agency, OPs are highly toxic and categorized as the most toxic "Class 1" compound [5,6]. The presence of OPs leads to the malfunctioning of the central and peripheral nervous system by blocking the active site of AChE (EC 3.1.1.7), a prime functioning enzyme of the nervous system and the neurotransmitters. The enzyme controls